ANALYSIS OF THE EFFECTS OF ACID GAS INJECTION IN THE RETLAW MANNVILLE Y POOL

Report Submitted to

Natural Resources Canada

Ressources naturelles Canada

By

Stefan Bachu, Ph.D., P. Eng.,
Alberta Geological Survey
Energy Resources Conservation Board

Mehran Pooladi-Darvish, Ph.D., P. Eng.
Sophie Theys
Fekete Associates Inc.

ERCB Energy Resources Conservation Board | AGS Alberta Geological Survey

Fekete Associates Inc.

Shahin Dashtgard, Ph.D., P. Geo.
Osprey Geological Inc.

February 2008

Executive Summary

This report describes work undertaken by the Alberta Geological Survey (AGS) of the Alberta Energy and Utilities Board (ERCB) in collaboration with Fekete Associates Inc. and with financial support from Natural Resources Canada (NRCan) to understand the behavior of the Retlaw Mannville Y Pool in southern Alberta, where injected acid gas broke through at producing wells, as an analogue for future large-scale operations of CO_2 geological storage in gas reservoirs. Acid-gas (96% CO_2 and 1.7% H_2S, with hydrocarbon gases for the balance) has been injected in this pool since August 2004. At the start of acid gas injection two gas wells were still producing at an approximate distance of about 1500 and 2100 m from the injection well, respectively. In March 2005, the closest well showed an increase in CO_2 concentration, and the well was shut-in because of high CO_2 concentrations (more than 80%). Breakthrough of CO_2 into the second well was observed in May 2005. Acid gas concentration in this well was at 80% as of December 2006. By this time the rate of recycling was about 11% of the injected rate. The objective of this study was to study the acid gas injection and its breakthrough in the producing wells using numerical simulations based on history matching.

Initially, history-matching of the Retlaw Mannville Y Pool was not possible because of a mismatch between the volumes of initial gas in place as determined from geology and rock properties, and produced gas to date. History matching and forecast were obtained after ERCB revised the geological maps of the Retlaw Mannville Y pool. Both black oil and compositional models were created to first history match the total gas and oil produced and then forecast gas production and reservoir pressure based on 3 scenarios: (i) forecast assuming all operating conditions as of December 2006 to be maintained until 2038, (ii) forecast assuming that no acid gas injection ever occurred, and (iii) forecast assuming that all producers are shut-in in January 2008 while acid gas injection is maintained at its same operating conditions.

The mechanism of displacement of the in-situ-gas by the acid gas and their mixing were studied using both black-oil and compositional models. Because acid gas is heavier than natural gas at in-situ initial reservoir conditions, a commonly held belief is that the heavier acid gas, if injected at the bottom of the dipping structure that forms a reservoir, will accumulate there and will not mix with the natural gas still present in the reservoir. Furthermore, it has been suggested that the acid gas accumulating at the bottom of the reservoir will push natural gas towards the top of the reservoir and towards the updip producing wells, thus enhancing gas recovery. The study of the acid gas injection in the Retlaw Mannville Y gas reservoir study showed that, in depleted reservoirs, acid gas is typically in gaseous phase, with a small density difference with the is-situ gas. Furthermore, the spread of the acid gas in the reservoir and its breakthrough at producing wells is enhanced by the hydrodynamic forces between injection and production wells that create preferential flow paths. Thus, rather than accumulating at the bottom of the reservoir, the injected acid gas will spread and mix with the resident natural gas, ultimately being produced at producing wells. Also, any additional gas produced from the Retlaw Mannville Y pool will be mostly acid gas, as confirmed by the observed and simulated concentrations of CO_2 and H_2S.

Table of Contents

List of Figures

List of Tables

1 Background

Several acid gas injection operations in Alberta have experienced unique reservoir behavior such as pressuring or acid gas breakthrough at offsetting wells. The Retlaw acid-gas injection operation into the Mannville Y pool in southern Alberta (Figure 1.1) is such a site, where CO_2 broke through at a well that was producing from the same reservoir. In an attempt to better understand reservoir behavior, a study was initiated by the Alberta Geological Survey (AGS) of the Alberta Energy and Utilities Board (ERCB), with financial support from Natural Resources Canada (NRCan) and in collaboration with Fekete Associates Inc. and the University of Calgary. This report presents the results of this study.

The Mannville Y pool, co-owned and operated by Provident Energy Ltd. and Enerplus Resources Fund, produces oil and gas from the Upper Mannville Glauconite Formation in Township 12, Range 19, west of the 4th Meridian (Figure 1.1). The gas cap of the pool was discovered in 1974 with the drilling of the 100/14-13-12-19W4 well, and the oil leg in 1992 with the drilling of the 100/1-14-12-19W4 well. The initial gas composition of the pool was 10.4% CO_2, 0.06% H_2S, 4.3% N_2, with the remainder being mostly hydrocarbon gas. At peak production the Mannville Y pool consisted of 3 gas-producing and 2 oil-producing wells (Figure 1.1). Presently, only the 100/14-13-12-19W4 well produces gas from the pool. The other wells were shut in between 1998 and 2006. In total the pool has produced 6,600 m^3 oil and 1,008 million m^3 gas.

The 100/3-25-12-19W4 well at the northern end of the pool was shut-in in January 2004 after becoming uneconomic due to low gas rates and high produced water volumes. It was converted to acid gas injection in August 2004 and is presently being used to dispose of an acid gas mixture of 1.7% H_2S, 96% CO_2, 1.8% hydrocarbon gas and 0.5% N_2. At the start of acid gas injection, the pool was producing gas from two wells, 14-13-12-19W4 and 06-24-12-19W4. Production as of December 2006 is 19 thousand m^3/d gas. The acid-gas component of presently produced gas is not available in the public database; however annual progress reports filled with ERCB indicate that at the end of 2005 the remaining producing wells 14-13-12-19W4 and 06-24-12-19W4 were producing with 40% and 70% CO_2, respectively.

Taylor Management Company Inc. manages and operates the Retlaw (Turin) Gas Plant, located in 12-19-12-18W4. At the time of the application, the Retlaw plant was grandfathered under ERCB ID 2001-03: Sulphur Recovery Guidelines, which allowed them to incinerate and emit 2.125 tonnes of sulphur/day. Taylor Management Company Inc. agreed to reduce emissions by August 2004, and applied to re-inject acid gas underground in January 2004. Approval was granted by the ERCB in July 2004, to inject 85 thousand m^3/d to (to a maximum of 310 million m^3) into the 100/03-25-12-19W4 well. Injection of acid gas was approved in July 2004 based on the severe depletion of the Mannville Y pool, and the low risk of gas leakage out of the pool. Pool pressures at the time of application were 15% of virgin reservoir pressure, with cumulative gas production having reached the expected recovery in August 2003. Additional recovery as of early 2005, includes a component of acid gas production.

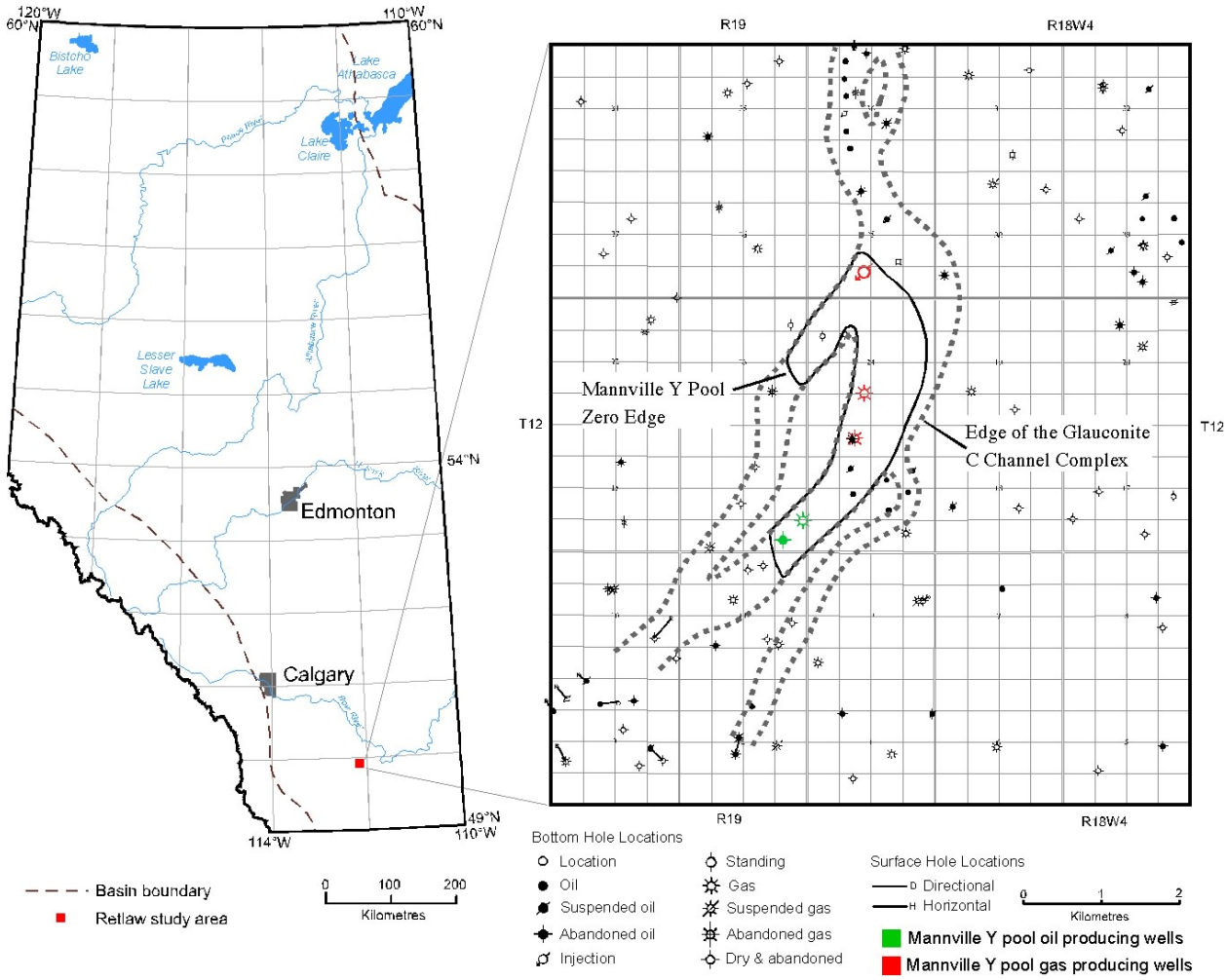

Figure 1.1: Location map of the Mannville Y pool within Alberta and of the Retlaw study area. Indicated on the study area map are the producing or past-producing oil (green) and gas (red) wells of the Mannville Y pool.

This study was initiated to model the Mannville Y pool to determine whether breakthrough at offsetting producers occurred faster than expected. In addition, this study will provide a better understanding of how acid gas migrates through depleted gas reservoirs. It is hoped through this evaluation that better modeling and reporting methods can be established to ensure that acid-gas disposal does not come at the expense of, but enhances resource development.

2. Geology

2.1 Geological Overview

The Western Canada Sedimentary Basin (WCSB) comprises the foreland Alberta Basin in the west and northwest, and the northern half of the intracratonic Williston Basin in the east. It sits on a stable Precambrian platform and is bounded by the Rocky Mountain Trench to the west and southwest, the Tathlina High to the north and the Canadian Precambrian Shield to the northeast. The Sweetgrass Arch separates the Alberta Basin from the Williston Basin to the southeast.

The Western Canada Sedimentary Basin was initiated during the late Proterozoic by the rifting of the North American Craton. It is composed of sediments deposited in two distinct tectonic environments. From the Middle Cambrian to Middle Jurassic shallow-water carbonates and evaporites (with some intervening shales) were deposited along the passive-margin on the western side of the North American Craton (Porter et al., 1982). A major change in tectonic style took place during the Middle to Late Jurassic with the start of the Columbian Orogeny and accretion of allochthonous terranes to the western margin of the proto North American continent. This tectonic style extended into the Tertiary with the Laramide Orogeny following the Columbian Orogeny and resulted in pushing sedimentary strata eastward, thrusting and folding them in the Rocky Mountain main ranges, front ranges and foothills. Folding and thrusting of strata caused lithospheric loading and isostatic flexure of the North American craton, creating conditions for foreland basin development east of the deformation front. The Precambrian basement tilted westward, with a gentle slope of < 4 m/km in the east and northeast. It steepens up to > 16 m/km near the deformation front to the west.

In the undeformed part of the basin, progressively older Jurassic to Middle Devonian strata subcrop from west to east along the sub-Cretaceous unconformity as a result of basement tilting and significant Pre-Cretaceous erosion. Deposition during the foreland stage of basin development was dominated by synorogenic clastics (predominantly silt and clay) derived from the evolving Cordillera. The basin attained maximum thickness and burial during the Laramide Orogeny in the Paleocene. Tertiary-to-Recent erosion has since removed an estimated 2000 to 3800 m of sediments, with the greatest erosion in the southwest along the deformation front. The present-day topography of the undeformed part of the basin has a general basin-scale trend of decreasing elevations, from topographic highs of 1200 m in the southwest to lows around 200 m in the north-northeast at Great Slave Lake. As a result of these depositional and erosional processes, the undeformed part of the Alberta basin comprises a wedge of sedimentary rocks that increases in thickness from zero at the Canadian Shield in the northeast to close to 6000 m in the southwest at the thrust and fold belt.

The Middle to Upper Jurassic and Lower Cretaceous sedimentary succession of the Western Canada Sedimentary Basin marks the transition in tectonic environments from a passive margin to a tectonically active foreland basin at the start of the Columbian Orogeny. Prior to the Columbian Orogeny, the WCSB was dominated by deposition of shallow-water carbonates and minor clastic deposition of quartz-dominated sandstones sourced from the craton to the east. The platform was open to the west and was bounded in the east and southeast by the uplifted Sweetgrass Arch (Poulton et al., 1994). From the Middle to Late Jurassic, loading of the craton

with thrusted strata resulted in flooding of the platform and the Sweetgrass Arch. Shallow-marine carbonates and quartz-rich sandstones gave way to deep-water marine shales as relative sea level rise shifted the sites of coarse-clastic deposition towards the east (Poulton et al., 1994). Ultimately, the Sweetgrass Arch was drowned. Following drowning of the arch, deposited strata was exposed to erosion along the Pre-Cretaceous Unconformity.

Following 40 million years of erosion along the Pre-Cretaceous Unconformity, which caps the Jurassic strata, the basin began to fill with Lower Cretaceous chert-rich synorogenic clastics. These sediments were sourced from deformed strata exposed in the south and southwest and transported northward (McLean and Wall, 1981; Zaitlin et al., 2002). The lowermost Cretaceous strata are represented by the Mannville Group, which can be subdivided into a Lower and Upper Mannville. Lower Mannville Group sediments in southern Alberta were predominantly deposited in non-marine settings (e.g., fluvial, floodplain) within a low accommodation-space basin with low sedimentation rates (Zaitlin et al., 2002). This is in contrast with the Lower Mannville Group strata in central and northwestern Alberta, which were deposited in settings characterized by moderate to high accommodation space and sedimentation rates (Zaitlin et al., 2002). Overall, preserved Lower Mannville deposits in southern Alberta are relatively thin and are commonly cross-cut by Upper Mannville channels. Towards the end of Lower Mannville deposition was a period of relative sea level rise and deposition of calcareous, restricted embayment and lacustrine sediments of the Ostracod Member. Ostracod depositional trends are similar to those of other Lower Mannville deposits, with unit thickness increasing from southern to northwestern Alberta. Overlying the Ostracod Member are brackish to non-marine sandstones, siltstones, and shales of the Glauconite Formation. The Glauconite comprises a series of stacked brackish-marine to continental sequences that prograded northward into the paleo-seaway. Associated with the top of each Glauconite sequence are incised fluvial to estuarine channels that are filled with thick sandstones. These incised channel complexes are particularly prevalent in the basal Glauconite sequence, and are interpreted to have developed during periods of forced regression and subaerial exposure during deposition of the Glauconite Fm. (Broger et al., 1997). The Retlaw Mannville Y pool is trapped within an incised channel complex developed in the basal Glauconite sequence.

2.2 Study Area Stratigraphy

The Retlaw Mannville Y pool produces from the Glauconite Formation in southern Alberta. The overall geology of the Mannville Y pool is similar to that of the Long Coulee Glauconite F pool, which also produces from the Glauconite Fm. in southern Alberta. Unlike the Glauconite F pool, however, the stratigraphy of Glauconite strata in the Retlaw Mannville Y pool area is more complex, comprising stacked sequences of sediments deposited in brackish marine settings grading upwards into continental strata. These regional sequences are crosscut by incised fluvial to estuarine channels that trended southwest-northeast (Leckie et al., 1994). The Mannville Y pool occurs within fluvial channel strata, deposited at the time of deposition of the lowermost brackish-marine to continental sequence.

In the study area (Figure 1.1), the Middle to Upper Jurassic and Lowermost Cretaceous are represented by the: Rierdon Fm. (Middle Jurassic, Bathonian); Lower Mannville Group Sunburst Member (Lower Cretaceous, Aptian); Lower Mannville Group Ostracod Member including the

Bantry Shale (Lower Cretaceous, Aptian); and, Upper Mannville Glauconite Formation (Lower Cretaceous, Albian) (Figures 2.1 and 2.2).

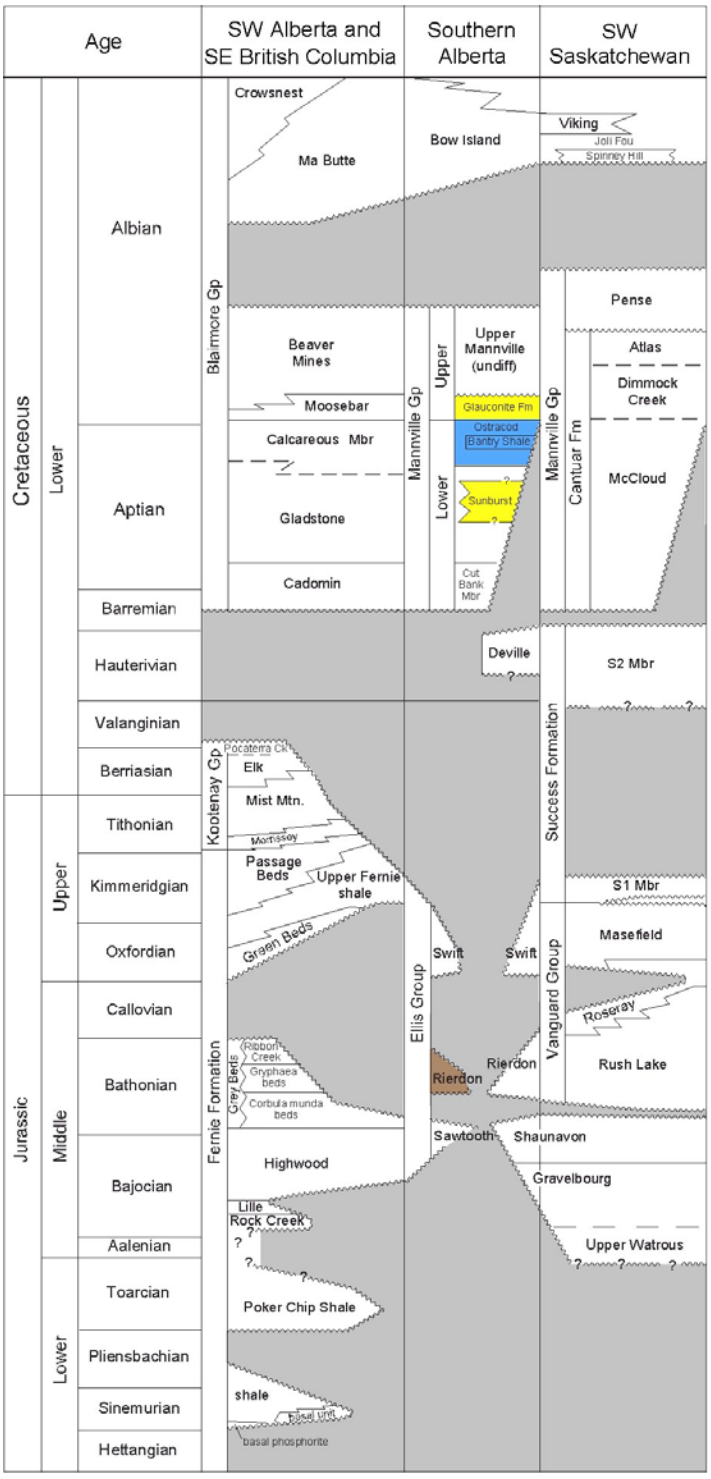

Figure 2.1: Stratigraphic chart of Jurassic and lowermost Cretaceous strata deposited in southeastern British Columbia, southern Alberta, and southwestern Saskatchewan. Highlighted in color are the formations or members identified within the Retlaw study area. The color coding on this chart match that of the units in Figure 2.2.

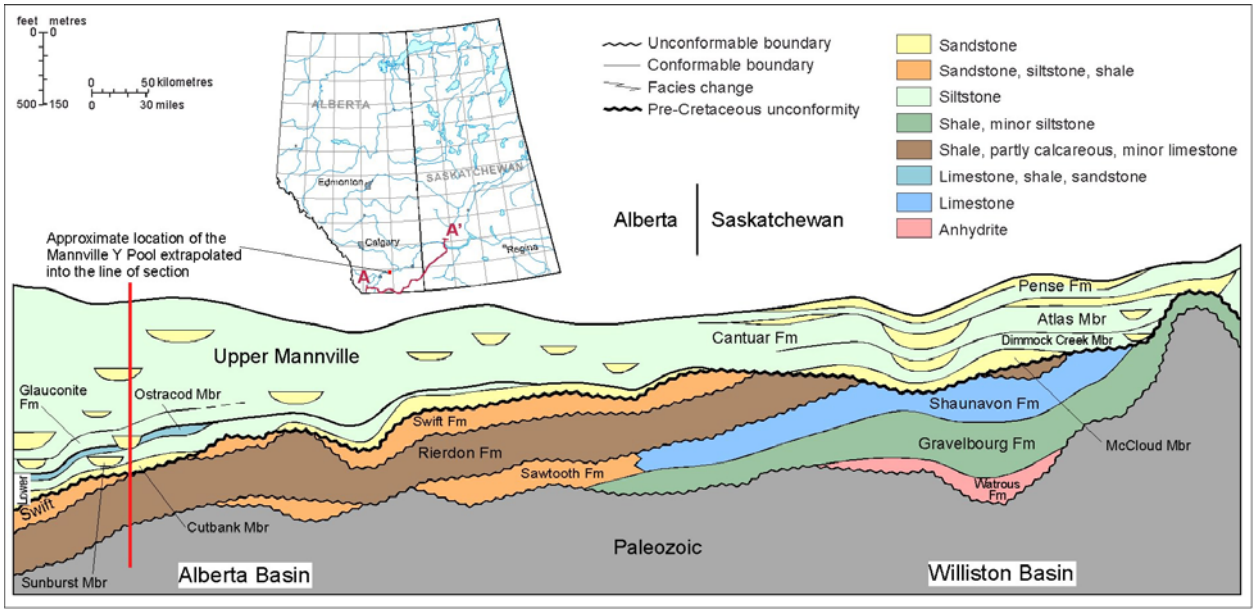

Figure 2.2: Schematic cross-section of Jurassic and Lower Cretaceous strata across southern Alberta and southwestern Saskatchewan (modified from Hayes et al., 1994, and Poulton et al., 1994). The schematic cross-section is derived using the Base of Fish Scales Zone as a datum. Indicated in red on the map is the location of the Retlaw study area. The study area location is then extrapolated into the line of section as indicated by the vertical red line.

The Sawtooth Formation does not occur within the Retlaw study area, hence the Rierdon Fm. is the first Jurassic unit observed above the Mississippian Madison Group. The Rierdon Fm. is a deep-water calcareous shale deposited as a result of tectonic loading leading to rapid transgression and extensive flooding of the continent at the start of the Columbian Orogeny (Poulton et al., 1994). The top of the Rierdon Fm. is disconformable with overlying beds of the Lower Cretaceous Sunburst Member. The Rierdon Fm. is sporadically distributed and marks the top of the Jurassic deposits (Figure 2.4) as the overlying Jurassic Swift Formation was completely eroded away during a period of uplift and erosion prior to deposition of Lower Mannville Group sediments (Figure 2.3 presents the symbols used in Figures 2.4 to 2.6). This period of erosion resulted in the development of the Pre-Cretaceous Unconformity, which represents a time gap of approximately 45 million years.

The first evidence of Lower Cretaceous deposition is the Lower Mannville Sunburst Member (Figure 2.2). These sandstones were deposited in a non-marine setting within fluvial channels that flowed from south to north and emptied into the Moosebar Sea (Farshori and Hopkins, 1989; Hayes, 1986; McLean and Wall, 1981; Zaitlin et al., 2002). Following Sunburst deposition was a period of relative sea level rise and deposition of restricted embayment and lacustrine sediments of the Ostracod Member and Bantry shale (Zaitlin et al., 2002). Overlying and incised into the Ostracod Member are marginal-marine and non-marine siltstones, sandstones and shales of the Glauconite Formation.

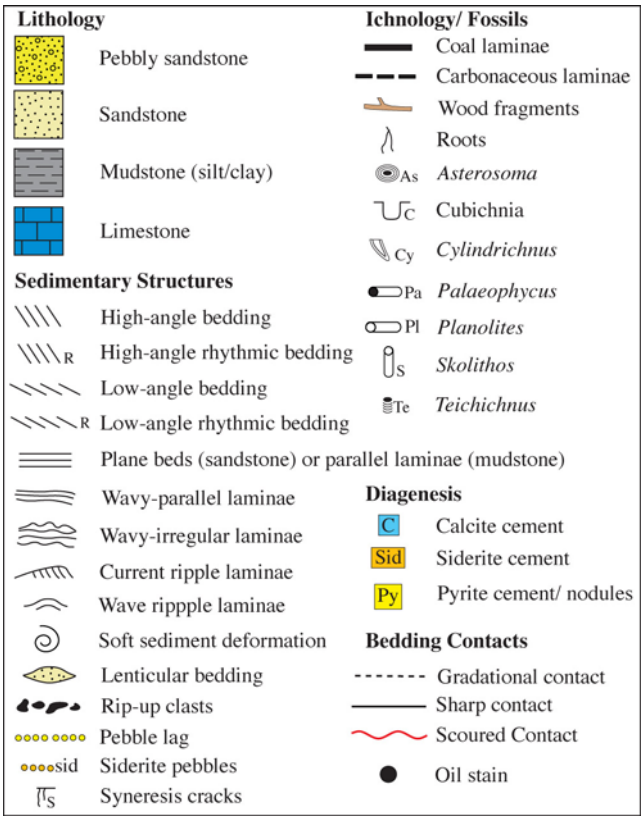

Figure 2.3: Legend for the lithology, symbols and contacts used in Figures 2.4, 2.5 and 2.6.

The Glauconite Formation at Retlaw can be subdivided into three packages (Glauconite A (youngest), B, and C (oldest)) of repeating strata that grade upwards from shales and siltstones deposited in a brackish-marine environment into sandstones deposited in a similar setting (Figures 2.4 and 2.5). The degree of marine influence decreases upward (from C to A). Each brackish-marine sequence is commonly capped by either thin, non-reservoir fluvial sandstones or silt and clay deposited in a continental setting. On logs, identifying the flooding surface that separates each sequence is not always possible, so the contact was picked at the nearest, high gamma-ray shale. This worked well as the high gamma ray shales tended to occur within 1 to 2 meters of the flooding surfaces (Figures 2.4 and 2.5). Each sequence is scoured into by incised fluvial channels that originate at horizons equivalent to the top of the brackish-marine sandstone units. The tops of the brackish-marine sandstones were not used for mapping purposes however, as the break between the marine sandstones and overlying fluvial sandstones was often difficult to pick on logs. At the top of the Glauconite Formation there is a paleosol horizon of nearly uniform thickness with high gamma ray kicks at the top and base of the paleosol. The top of the Glauconite Fm. is picked at the top of the paleosol.

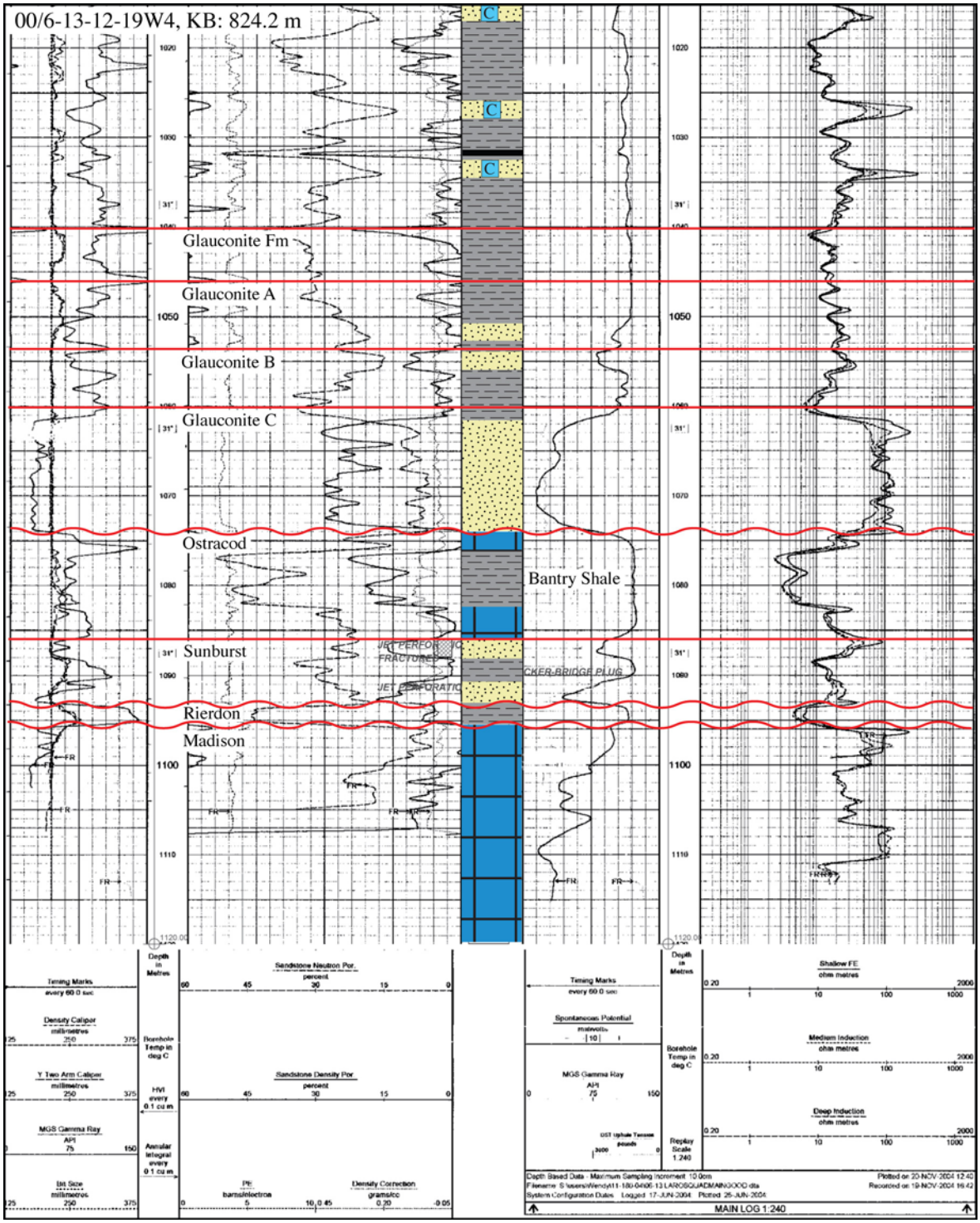

Figure 2.4: Geophysical log for the 100/06-13-12-19W4 well. Indicated on the log are the generalized lithology and tops picked in this study.

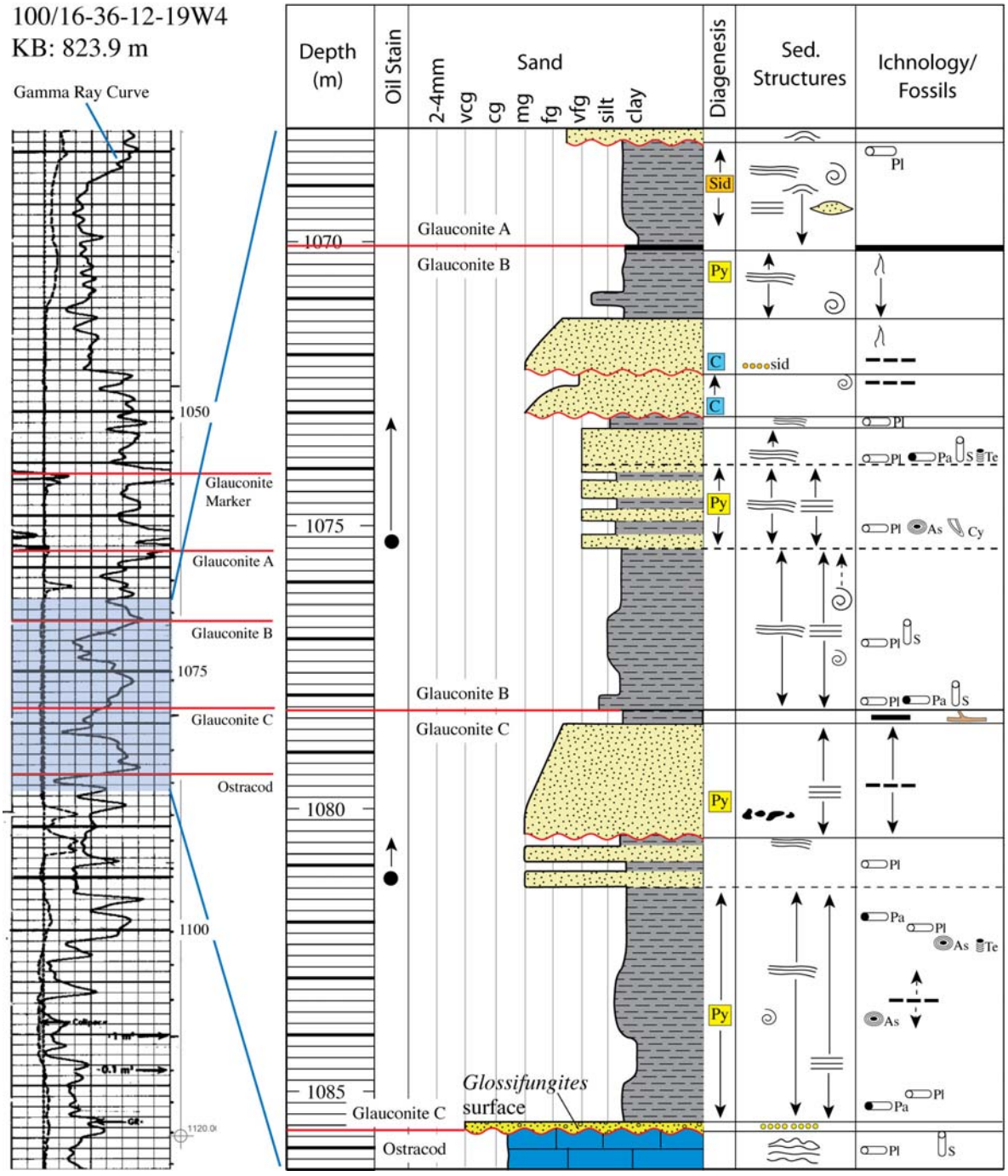

Figure 2.5: Core strip log and gamma-ray curve of the 100/16-36-12-19W4 well. This core log depicts the stacked, repeating stratal packages (Glauconite A, B, and C) that define the regional Glauconite Fm.

Large incised, fluvial to estuarine channels developed within the lower sequence of the Glauconite Formation scour into the underlying restricted lacustrine and embayment shales and calcareous sandstones of the Ostracod Member and Bantry Shale (Figures 2.4 and 2.6). The fluvial sandstones are classified as quartz arenites to sub litharenites, with 85 to 90% quartz grains. The Retlaw Mannville Y pool occurs within an incised fluvial to estuarine channel

developed in the lowermost Glauconite sequence – the Glauconite C. These incised channels exhibit high permeability and porosity, and are both narrow (400 to 800 m wide) and thick (up to 25 m). When discovered, pools within these channels tend to be prolific oil and/or gas producers (Broger et al., 1997).

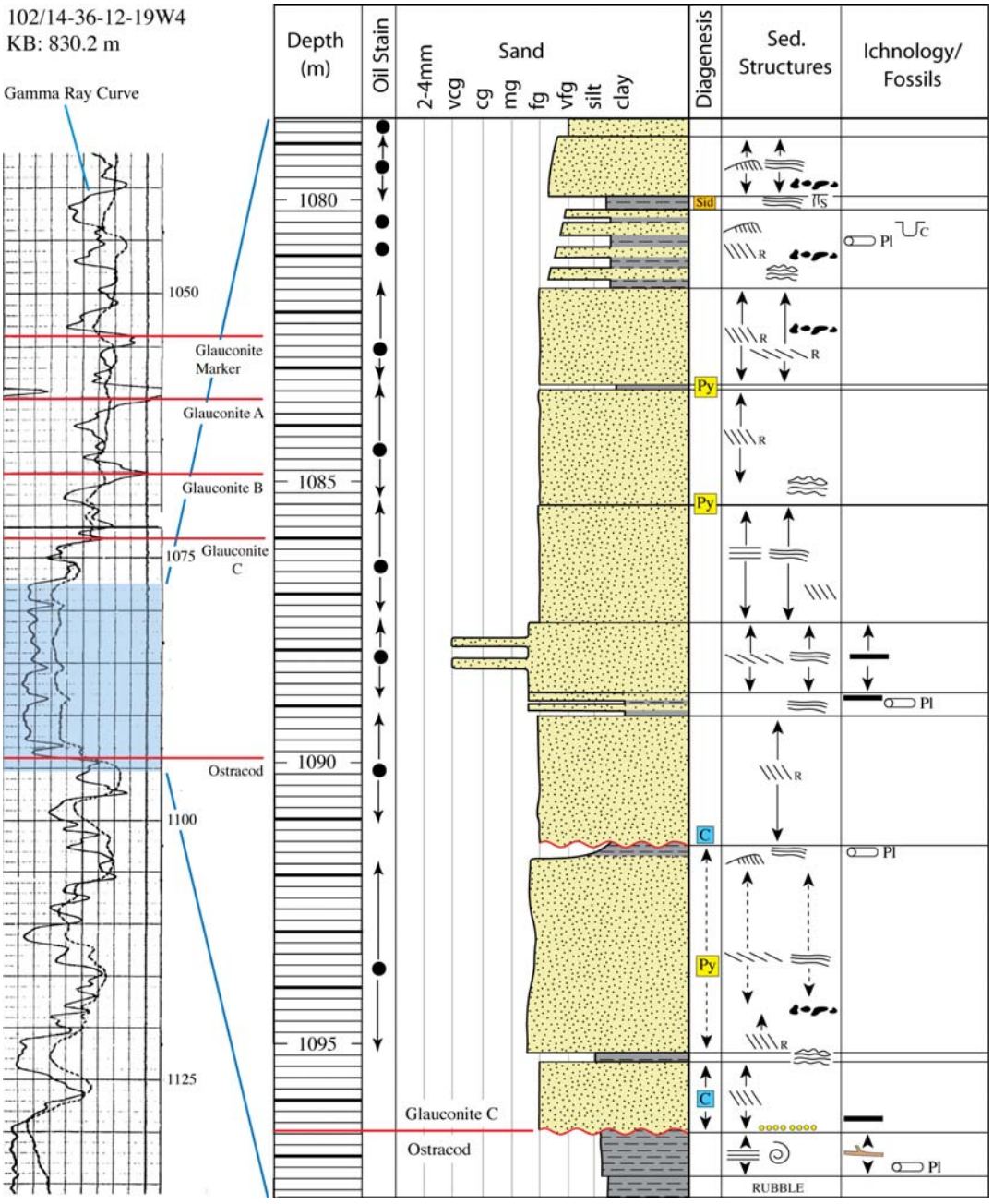

Figure 2.6: Core strip log and gamma-ray curve of the 102/14-36-12-19W4 well. This well illustrates the sedimentology and ichnology typical of incised fluvial to estuarine channels such as that which contains the Mannville Y pool. These channels are best developed in the basal Glauconite sequence – the Glauconite C. Note: depths for the core must be shifted upwards by 2.5 m to match the log depths.

In the immediate area of the Mannville Y pool, oil and gas production is reported from the basal part of the Sunburst Member, Glauconite Formation, and channels within the Upper Mannville Group. Hydraulic isolation of the Mannville Y pool from underlying Sunburst pools is discussed below, whereas overlying Upper Mannville Group pools are separated from the Glauconite Fm. by at least 80 m of impermeable Upper Mannville rocks. Maps are generated to evaluate hydraulic isolation of the Mannville Y pool, hence mapping is only done for strata between the top of the Sunburst Member and the top of the Glauconite Fm. This interval is divided into three stratal packages representing the bottom seal, reservoir and top seal. The bottom seal is considered to be the Ostracod Member, including the Bantry shale. The reservoir units are porous sandstone contained within the incised fluvial to estuarine channels in the Glauconite C zone. The top seal includes the Glauconite A and B zones as wells as the overlying paleosol. Additional mapping of permeable versus impermeable strata was not incorporated as pressure data show that the Mannville Y pool is isolated from pools contained within underlying and overlying Mannville strata (Figure 2.7).

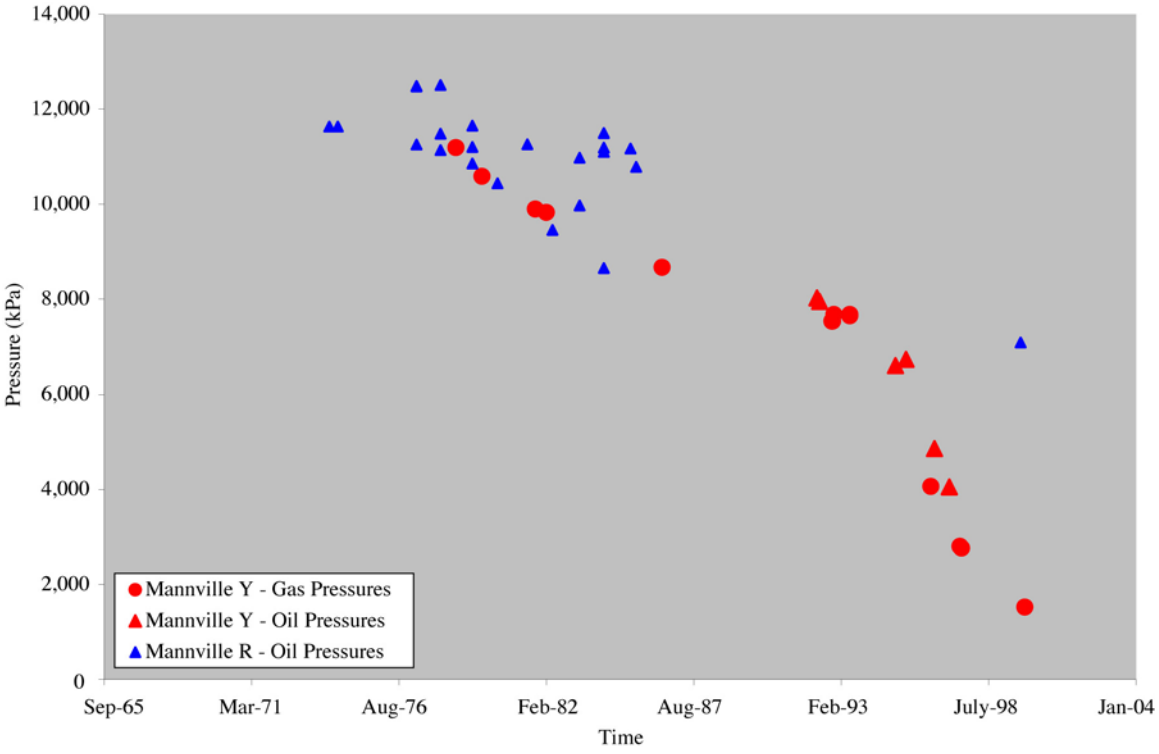

Figure 2.7: Pressure versus time plot for the Mannville Y and Mannville R pools. The Mannville R pool is contained within thin sandstone beds of the Sunburst Member and is separated from the Mannville Y pool by as little as 3 m of Ostracod shale. Pool isolation is indicated in this diagram by the significant difference in pressures of the two pools in 1999.

2.2.1 Lower Mannville Strata

In the vicinity of the Mannville Y pool, the Lower Mannville succession consists of two members – the Sunburst and the Ostracod. The Sunburst Member comprises sandstones that elsewhere host significant hydrocarbon deposits, but within the study area produce only from a

few small pools. Overlying the Sunburst Member are impermeable limestones, calcareous sandstones, and shales of the Ostracod Member. In the middle of the Ostracod Member is a 5 to 7 m thick shale succession known as the Bantry Shale. The Bantry Shale is easily recognizable on logs by low resistivity and high neutron and density porosity log responses (Figure 2.4).

Contained within the Sunburst Member and partly underlying the Mannville Y pool is the oil producing Mannville R pool. The Mannville R pool is separated from the Glauconite Fm. by 5 to 15 m of impermeable Ostracod strata (Figure 2.8), and is shown not to be in pressure communication with the Mannville Y pool (see in Figure 2.7 the pressure difference between Mannville R and Mannville Y pools in 1999).

Overlying the Sunburst are calcareous sandstones and dark grey shales of the Lower Mannville Ostracod Member. The thickness of this unit varies between 0 and 16 m (Figure 2.8). Where the Ostracod exceeds 5 m in thickness it is considered to be an effective barrier to vertical flow between the Sunburst Member and Glauconite Formation. However, thin Ostracod Member deposits occur where Glauconite C channels are incised into the underlying stratigraphy. These are potential leakage pathways for acid gas out of the Mannville Y pool. Where the Ostracod Member is eroded away or thin (less than 3 m), additional evidence is collected to prove hydraulic isolation. For example, at the northern end of the pool, immediately south of the 100/3-25-12-19W4 injection well, the Ostracod Member is completely eroded away (Figure 2.8). Evaluation of the underlying Sunburst strata reveals that, at that locale, there are no reservoir units developed near the top of the underlying Sunburst Member. In consequence, the Sunburst Member acts as the bottom seal for the pool. Pressure information was also used to determine possible leakage pathways. Between the Mannville R and Mannville Y pools the Ostracod Member is also thin. Plotting pressure versus time for these two pools indicate that they are not in pressure communication with each other (Figure 2.7).

2.2.2 Glauconite Formation

The Glauconite Formation at Retlaw comprises two distinct facies associations that occur laterally together (Figure 2.9) and repeat vertically within the formation. Facies Association one (FA1) consists of brackish-marine shales grading upward into brackish-marine sandstones and capped by fluvial sandstones, and/or siltstones and shale deposited in a continental setting (Figure 2.5). The top of each succession is marked by a minor marine flooding surface. Facies FA1 repeats three times vertically though the Glauconite Fm., with each younger sequence exhibiting reduced marine influence (Figure 2.5). The three sequences are referred to as the Glauconite A, B, and C, where the Glauconite C is the oldest zone and occurs at the bottom of the Glauconite Fm. The top of the Glauconite Fm. is marked by a regionally extensive 5 to 7 m thick paleosol comprising rooted, red (oxidized) and green (reduced) mudstone and siltstone (Figure 2.10).

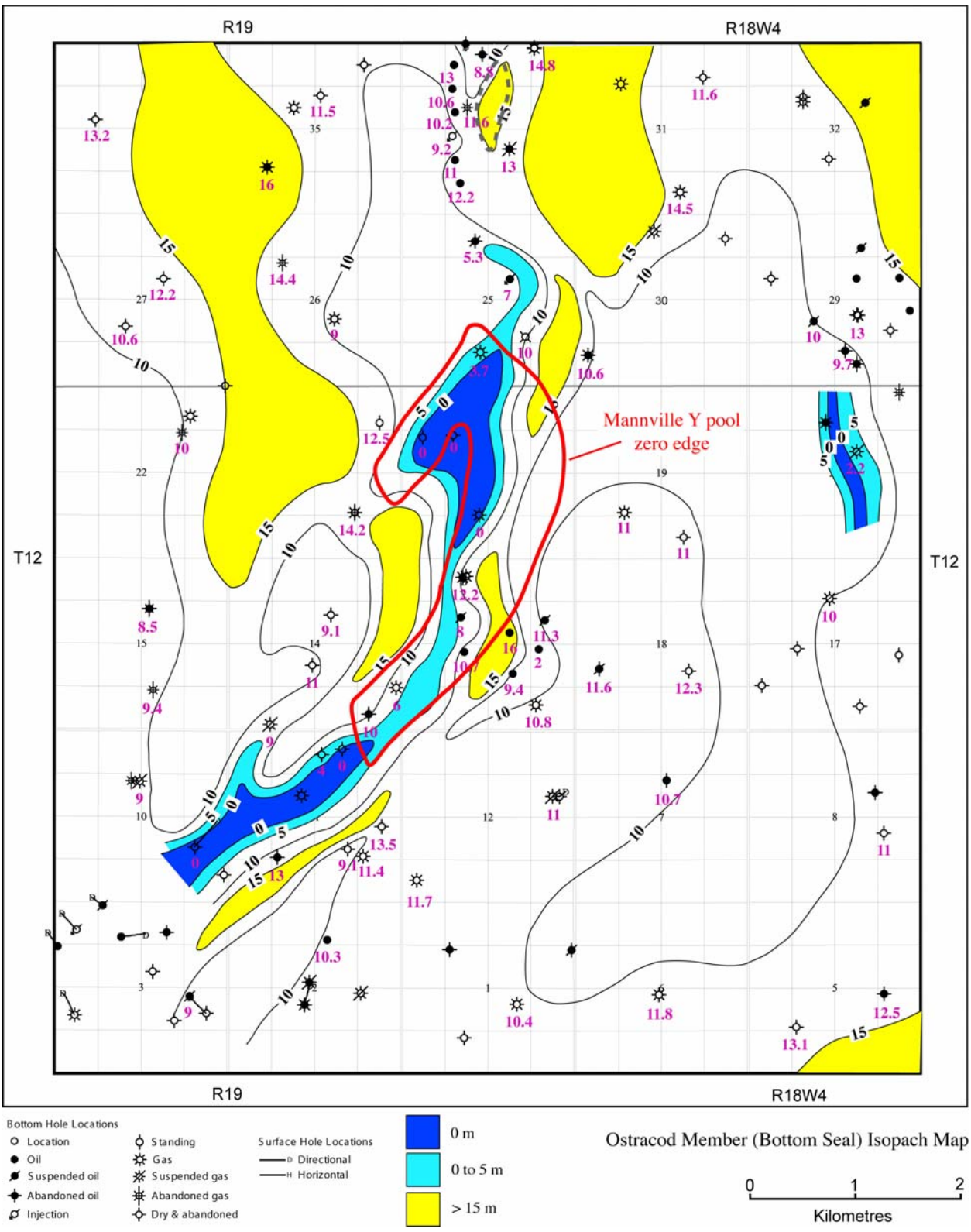

Figure 2.8: Isopach map of the Lower Mannville Ostracod Member, including the Bantry Shale. The Ostracod Member is the bottom seal for the Mannville Y pool (contour interval = 5 m).

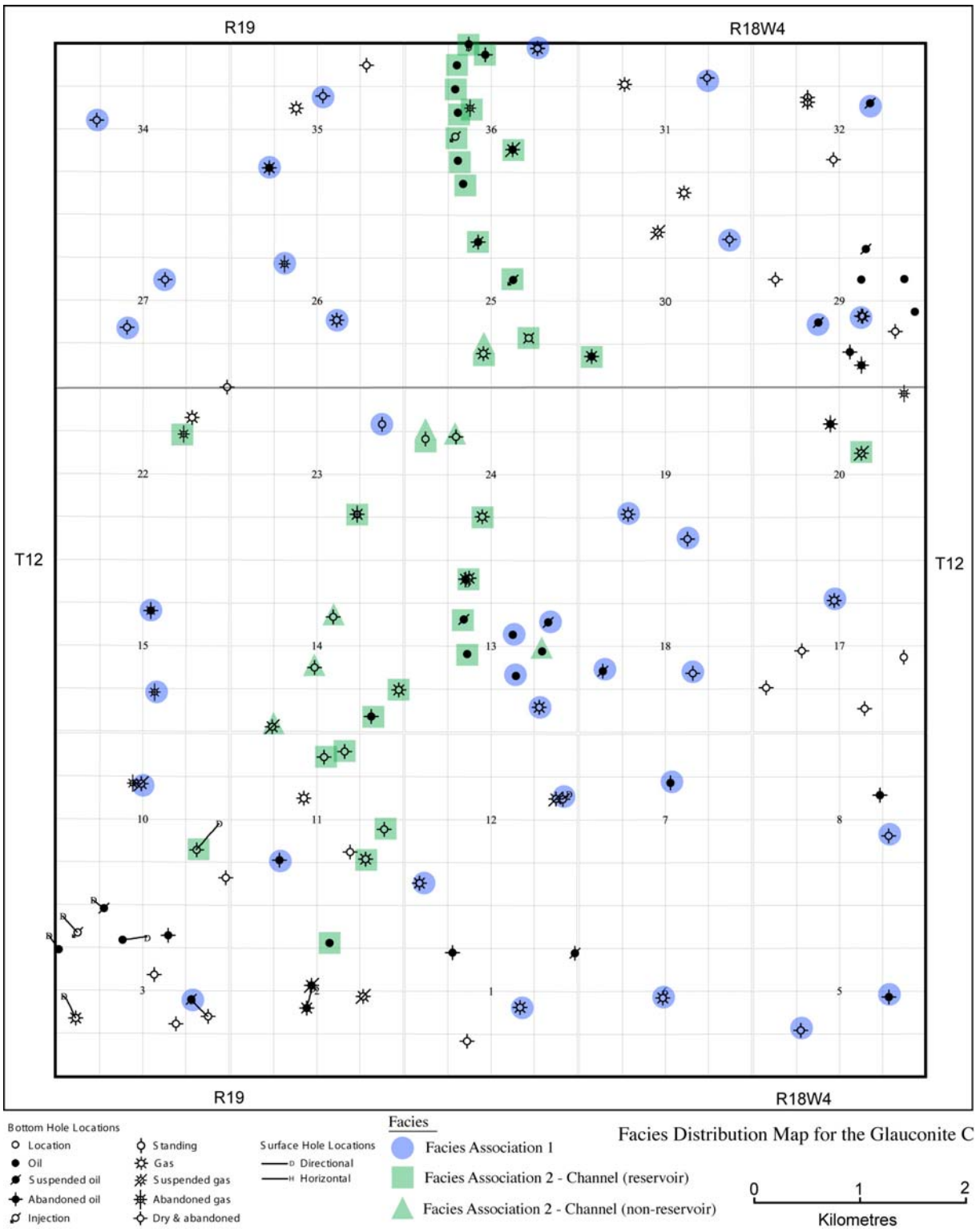

Figure 2.9: Facies distribution map of the Glauconite C zone. Facies Associations 1 and 2 are described in the text. Facies FA2 is subdivided into reservoir and non-reservoir units. A green triangle on top of a green square is used to indicate non-reservoir channel deposits capping reservoir channel deposits.

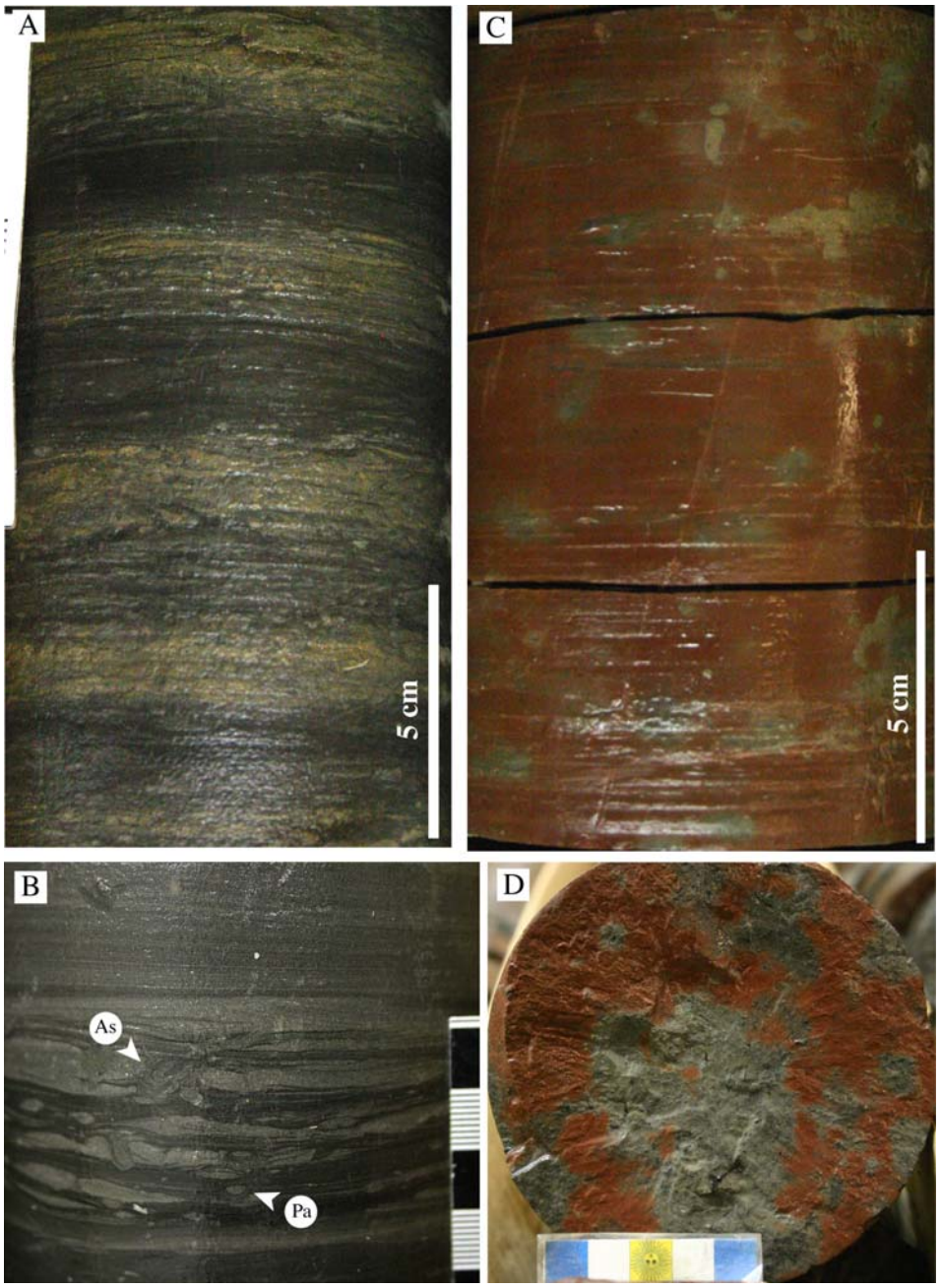

Figure 2.10: Images of the sedimentology and ichnology of the top seal, Facies Association 1 and the regional paleosol, for the Mannville Y pool. A. Rhythmic sand and mud beds deposited in the transition zone from brackish-marine mudstones to brackish-marine sandstones of the Glauconite B zone (1074 to 1074.3 m, 100/16-36-12-19W4). B. Close-up of the bioturbated brackish-marine mudstones and sandstones of the Glauconite C zone. Note the diminutive size and low density of the traces within this unit, which reflects the relatively brackish nature of the depositional environment at the time of deposition. Diminutive *Asterosoma* (As) and *Palaeophycus* (Pa) are indicated on the photo (1081.7 m, 100/16-36-12-19W4). C. Red and green beds of the regionally extensive paleosol. The red coloration indicates oxidized sediments and the green coloration reduced sediments (1054.6 m, 100/10-25-12-19W4). D. Plan view of the regionally extensive paleosol indicating the patchy distribution of red (oxidized) and green (reduced) sediments (1055.4 m, 100/10-25-12-19W4).

Developed from horizons within all three repeating sequences of FA1 are channels of Facies Association 2. These channels generally originate at the top of the brackish-marine sandstones and cut into the underlying strata. Channels associated with the A, B and C sequences all produce oil and/or gas, but it is the incised channels within the Glauconite C (Figure 2.11) that are the main play for the Glauconite in southern Alberta (Broger et al., 1997). Acid-gas injection is into the Mannville Y pool, which occurs within incised fluvial to estuarine channel sandstones of the Glauconite C zone. The channel sandstones are quartz arenites to sublitharenites, are very porous and permeable, and are excellent reservoir rocks. The channel complex containing the Mannville Y pool is oriented north-south across the study area (Figure 2.11). The channel is variable in width from 400 to 800 m, and attains a maximum sand thickness of 25 m (Figures 2.12 and 2.13). Reservoir sandstones mainly comprise shallow to steeply dipping beds, some of which appear to be rhythmic. Plane beds, wavy lamination, thin shale interbeds, and shale rip-up clasts are also observed (Figures 2.6 and 2.13). Bioturbation is minimal, comprising rare *Planolites* in interbedded shales (Figure 2.6). A single resting trace (cubichnia) was also observed at the top of one channel succession (Figure 2.13).

The Mannville Y pool is defined by the edges of the incised channel complex as well as the structural dip of the porous sandstone. Within the study area, the stratigraphy exhibits an overall dip towards the southwest with topographic highs and lows occurring locally (Figure 2.14). Top of porosity structure for the Mannville Y pool partly mimics the regional structure with an overall dip towards the northeast. The up dip pitchout of the pool is defined by the edge of the incised channel sandstones, whereas the lateral pool edges (to the north and south) are defined by structural lows. The lateral seals for the pool are brackish-marine shales and calcite-cemented sandstones. The top seal is composed of the Glauconite A and B sequences and regional paleosol (Figures 2.5 and 2.10), and varies in thickness from 17 to 35 m with an average thickness of 25 m (Figure 2.15). The top seal includes porous and permeable channels within the Glauconite A and B sequences; however, there are no porous and permeable channels at those horizons that occur directly above the Mannville Y pool.

2.3 Mannville Y Pool Reservoir Characteristics

2.3.1 Reservoir Isolation

The Mannville Y pool resides within incised channel sandstones of the Upper Mannville Glauconite Formation. The pool consists of an oil leg and gas cap, with net-pay thicknesses up to 25 m (Figure 2.16). The pool is highest in the northern half of section 24-12-19W4 and dips away from that high in all directions (Figure 2.17). The original oil-water contact for the Mannville Y pool was identified in the 100/1-14-12-19W4 well at -261.3 m. A gas-water contact, considered equivalent to the gas-oil contact for the pool, was identified at the northern end of the pool in the 100/3-25-12-19W4 well at -256.3 m.

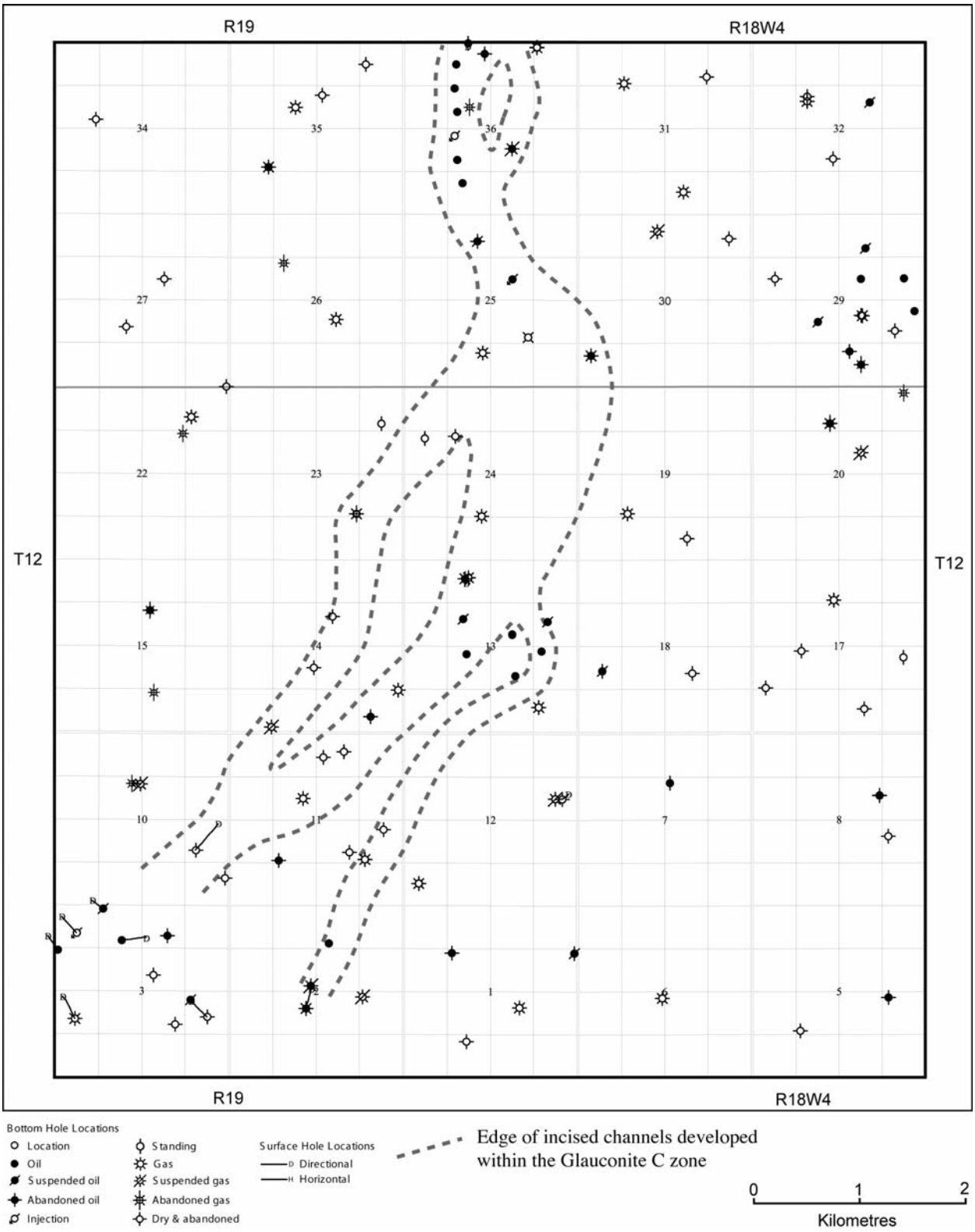

Figure 2.11: Edges of the incised fluvial to estuarine channels developed within the Glauconite C zone. The channels are relatively narrow, varying in width from 400 to 800 m.

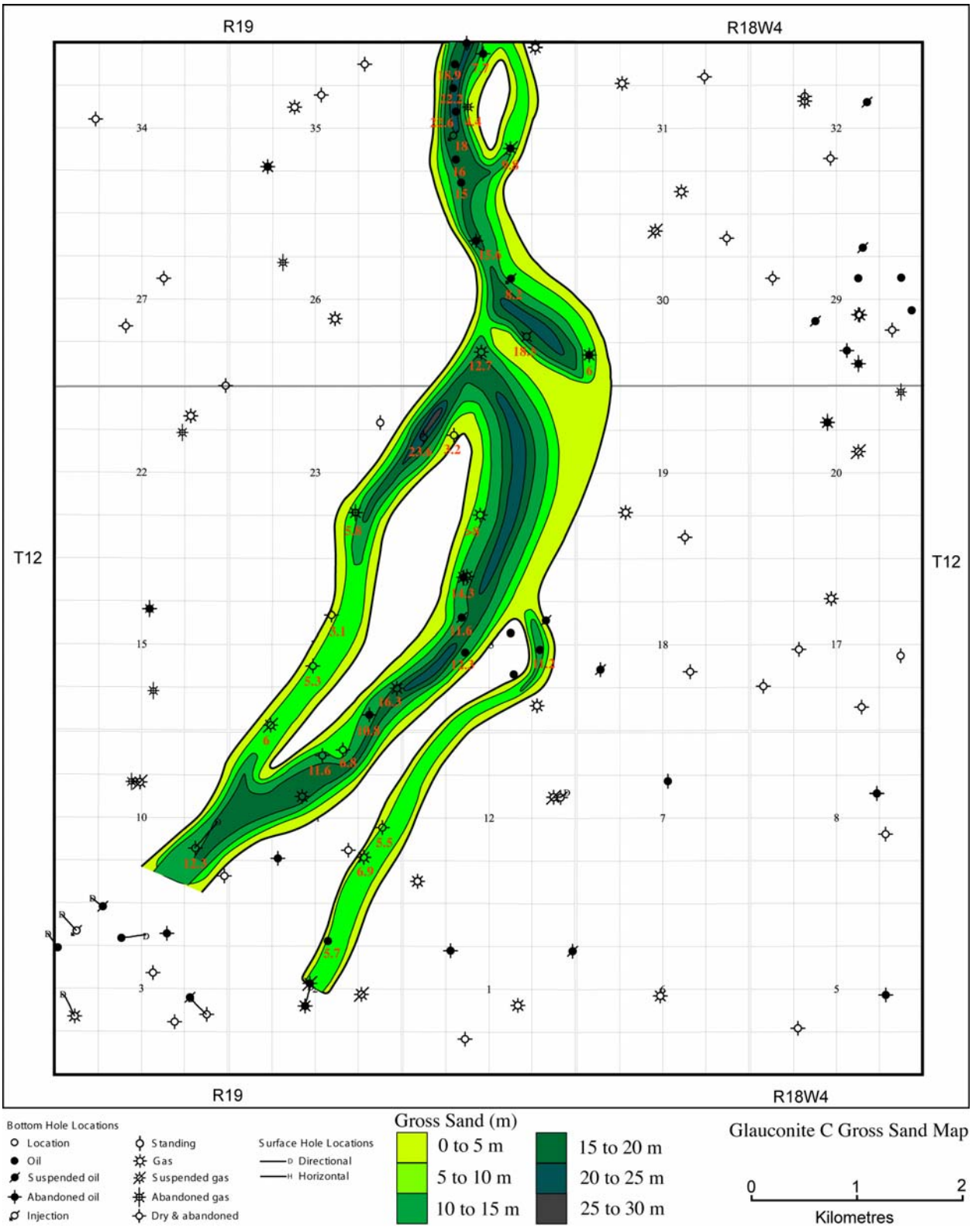

Figure 2.12: Hand-contoured gross sand map of the porous sandstones within the Glauconite C incised channel complex (contour interval = 5 m). Gross sand was determined using a 75 API gamma-ray cutoff.

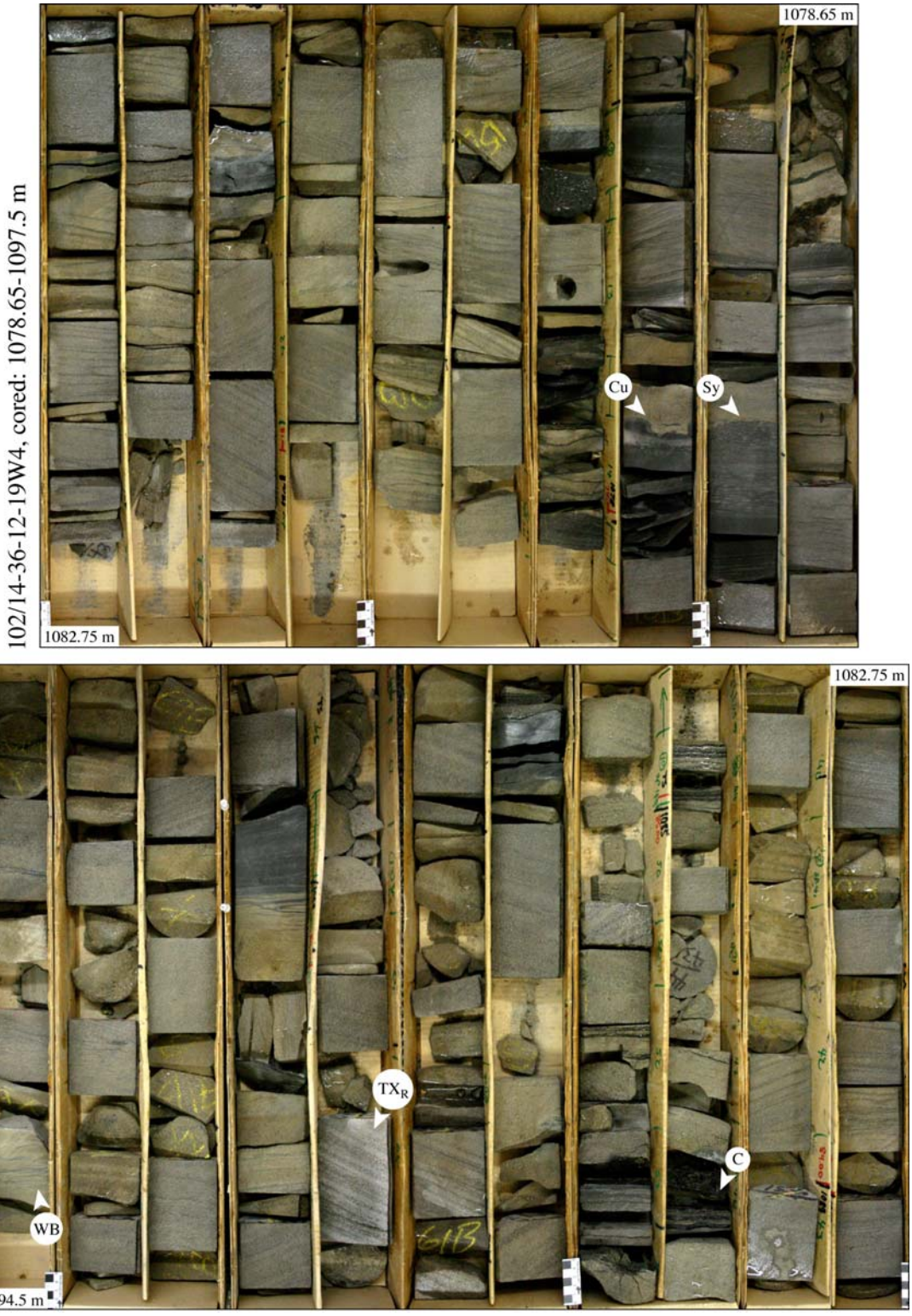

Figure 2.13: Core box pictures of the 102/14-36-12-19W4 well. This is the same well depicted graphically in Figure 2.6. Note the wavy bedding (WB), rhythmic trough cross-bedding (TX_R), coal (C), resting trace fossil – cubichnia (Cu), and syneresis cracks (Sy). The bottom of the core is in the bottom left hand corner of the page (1094.5 m). The top of each core box is the bottom of the core box to its right.

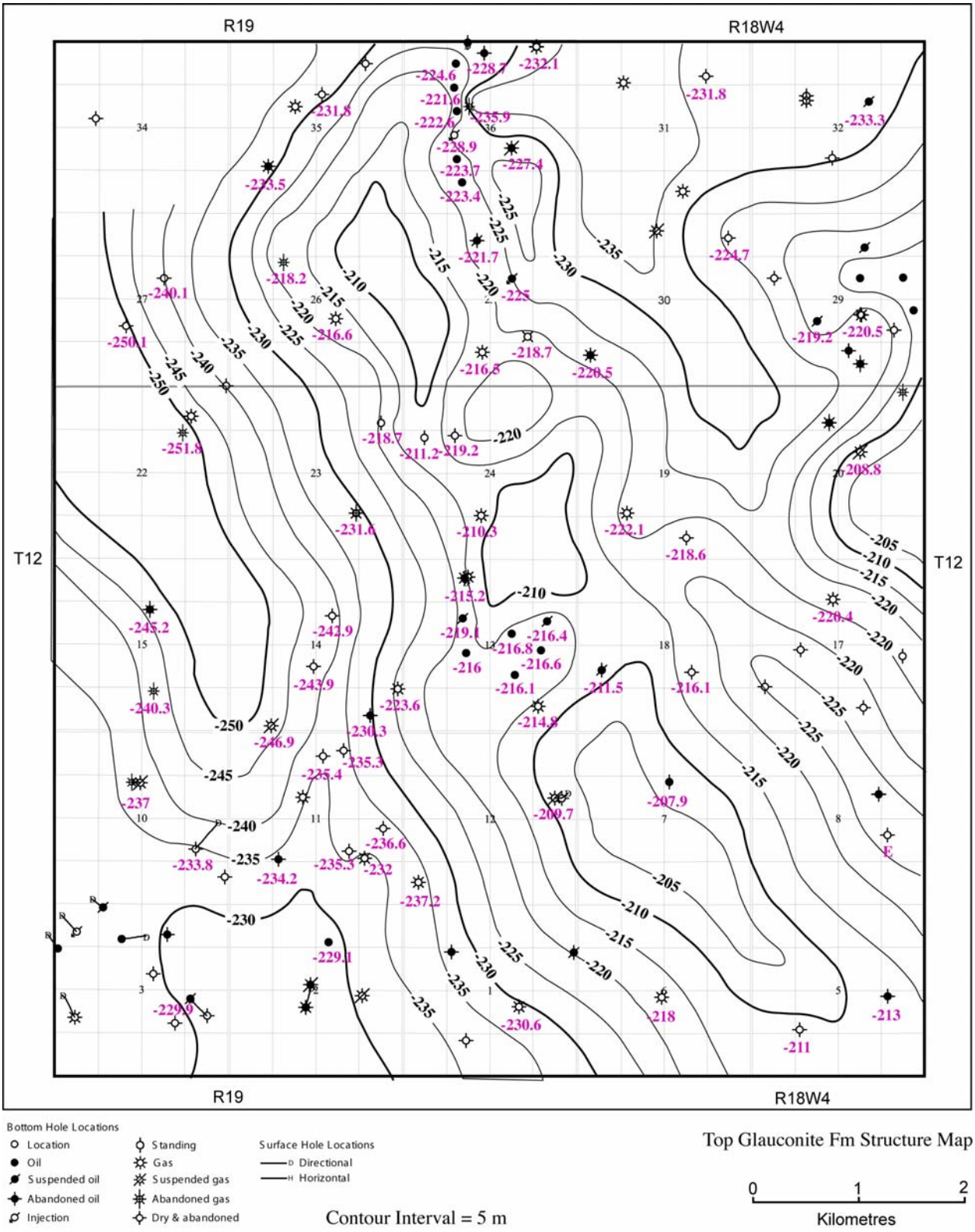

Figure 2.14: Hand-contoured top of the Glauconite Fm. structure map (contour interval = 5 m).

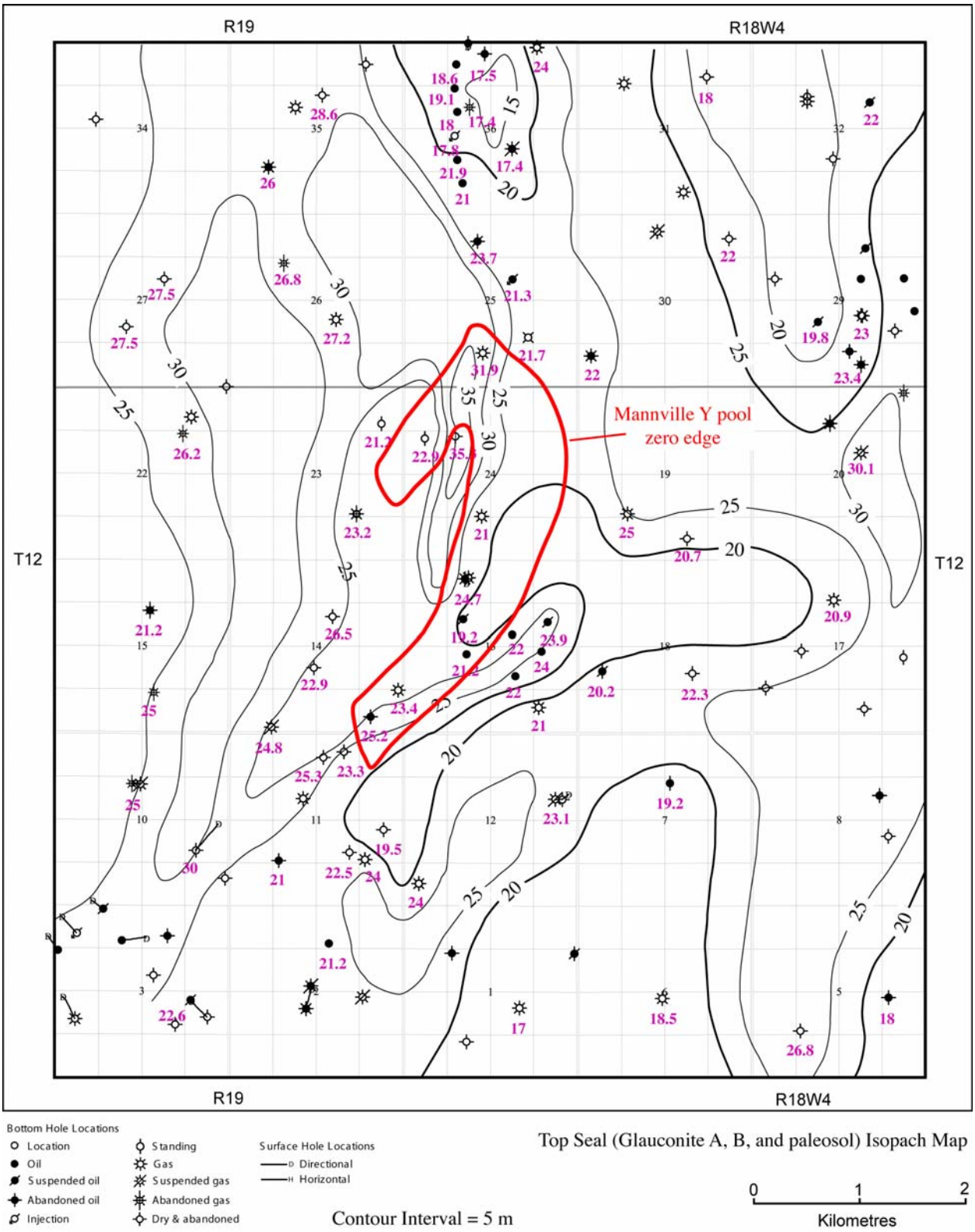

Figure 2.15: Hand-contoured isopach thickness map of the top seal for the Mannville Y pool. The top seal includes the Glauconite A and B zones, as well as the regionally extensive paleosol (contour interval = 5 m).

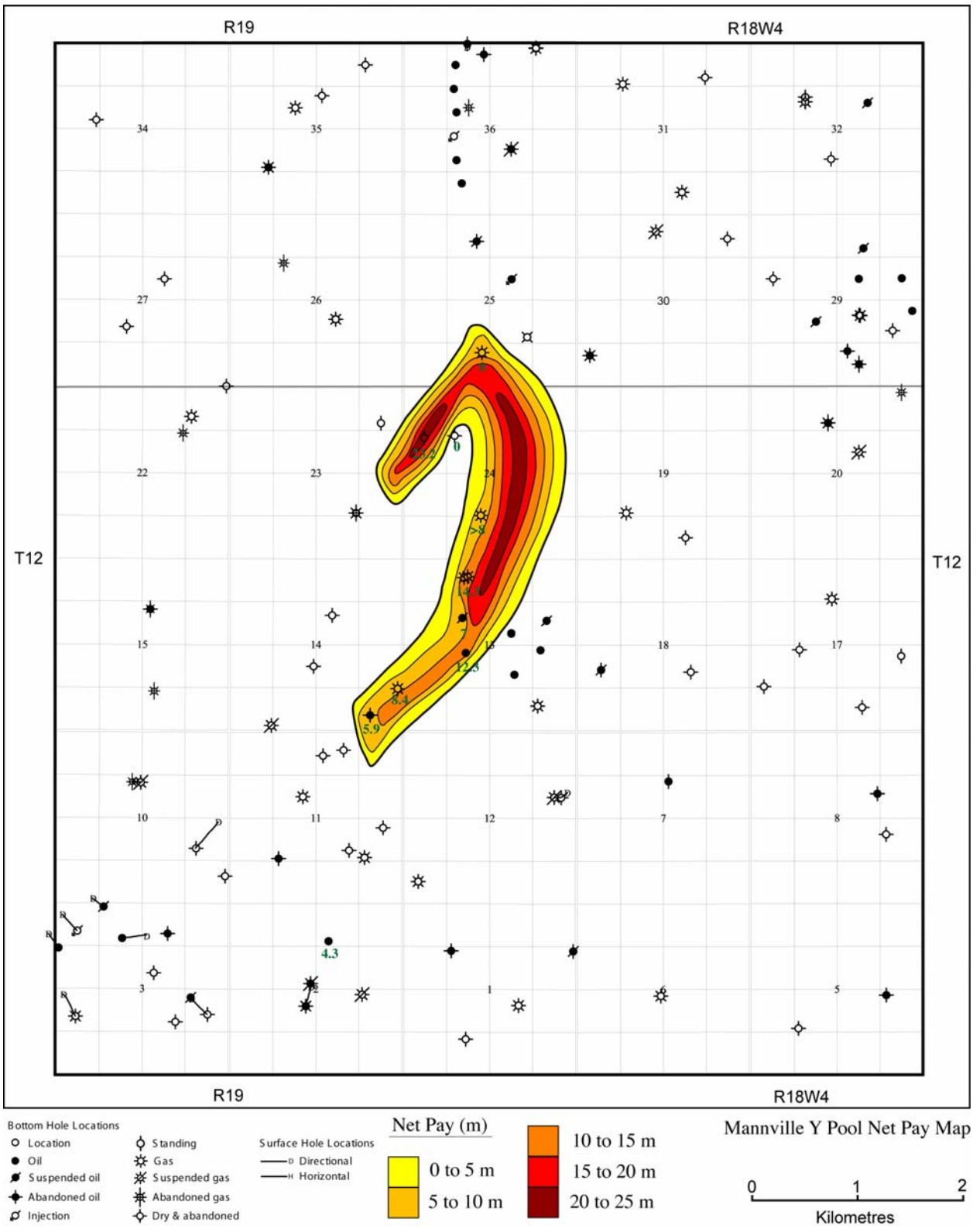

Figure 2.16: Hand-contoured net-pay map of the Mannville Y pool (contour interval = 5 m).

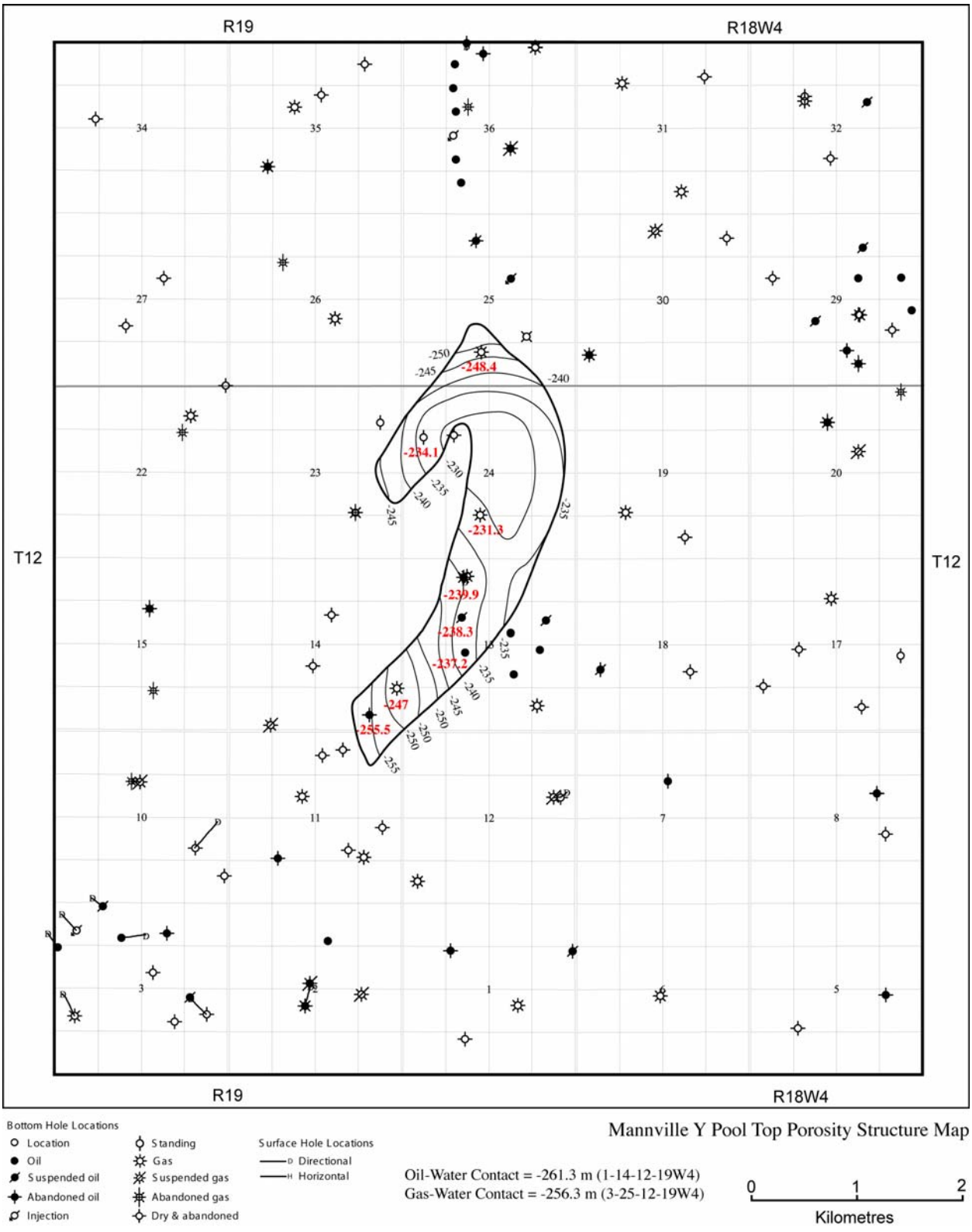

Figure 2.17: Hand-contoured top of porosity structure map in meters below mean sea level (contour interval = 5 m).

The trapping mechanism for the Mannville Y pool is both stratigraphic and structural. The up dip (east) and down dip (west) pool edges are defined by the edges of the incised channel. Within the channel complex the lateral pool edges, to the north and south occur at structural lows. At the northern end of the pool, the pool edge is further defined by a change in depositional environment from sandstone deposition to shale deposition. Potential leakage pathways exist between pools within the Glauconite C incised channel complex and between Glauconite pools and underlying Sunburst pools where the Ostracod Member is either thin or is completely eroded away. Acid-gas leakage from the Glauconite into the underlying Sunburst is unlikely based on pressure data from the Mannville Y pool and underlying Mannville R pool (pressure difference between Mannville R and Mannville Y pools in 1999, Figure 2.7). Assessment of potential leakage between Glauconite pools contained within the same channel complex, however, requires further investigation.

There are two pools within the Glauconite C incised channel complex – the Mannville EEE, and LL pools (Figure 2.18) - that may be in communication with the Mannville Y pool. Separation of the Mannville Y pool from the Mannville LL and Mannville EEE pools is determined from pressure data. The Mannville Y and EEE pools exhibit distinct pressures trends over time, where the Mannville EEE pool has a lower pressure than the Mannville Y pool (Figure 2.19). The Mannville Y and LL pools are considered to be separate hydrocarbon accumulations based on the distinct hydrocarbon phases they contain and their separate pressure decline histories. The Mannville Y pool produces mainly gas, whereas the Mannville LL pool produces mainly oil. In terms of pressure, the two pools started out with the same reservoir pressure and declined at the same rate for the first four years of production. After four years, the two pools exhibit significantly different decline histories likely because the Mannville LL pool was placed on secondary recovery using water (Figure 2.20).

The Mannville Y pool is overlain by an additional 17 to 35 m (Figure 2.15) of impermeable Glauconite Formation strata. These strata include brackish-marine shales and sandstones (Figure 5) and calcite-cemented fluvial sandstones of the Glauconite A and B sequences, and a regionally extensive 5 to 7 m thick paleosol horizon (Figure 2.10). The Glauconite A and B sequences have porous and permeable fluvial channels associated with them that occasionally contain economic accumulations of oil and gas. These channels present a possible leakage pathway for injected acid gas; however, the only channel with the A or B sequences that occurs directly above the Mannville Y pool is a shale channel (observed in the injection well 100/3-25-12-19W4) that has eroded into the underlying porous Glauconite C incised channel. Brackish-marine sandstones of both the A and B sequences can also contain hydrocarbons and are laterally extensive. It is unlikely though that the brackish-marine sandstones within each sequence are in hydraulic communication with sandstones in other sequences as they are encased in regionally extensive brackish-marine to continental siltstones and shales. The top of the Glauconite Formation is marked by a regional marker identified on logs by a low resistivity spike associated with a high gamma-ray count and porosity spikes in both the neutron and density curves. This marker is approximately 25 m above the top of the Mannville Y pool.

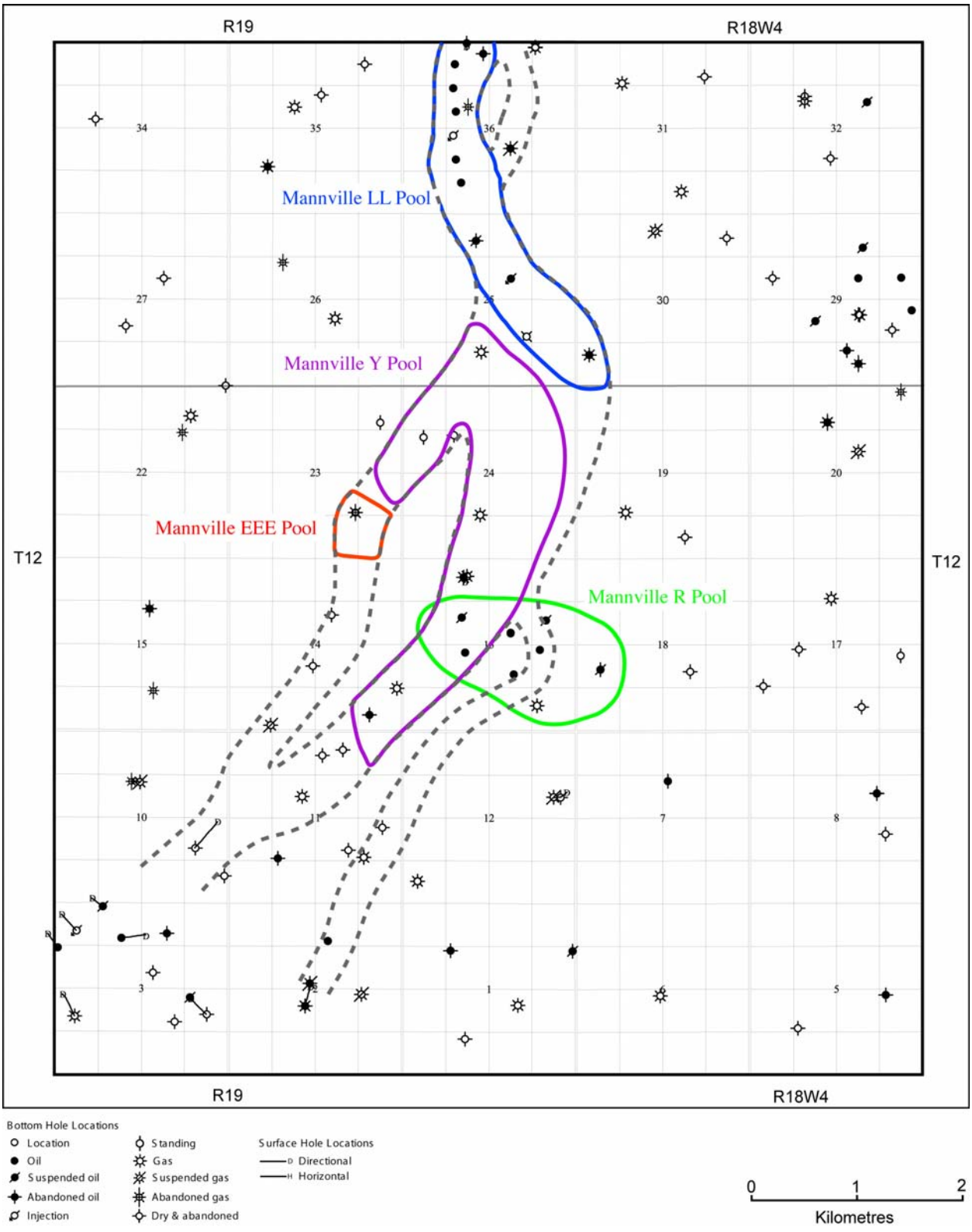

Figure 2.18: Map of the distribution of pools that may be in hydraulic communication with the Mannville Y pool. These include pools contained within the underlying Sunburst Member (Mannville R pool), and those within the same incised fluvial to estuarine channel complex (Mannville EEE and LL pools).

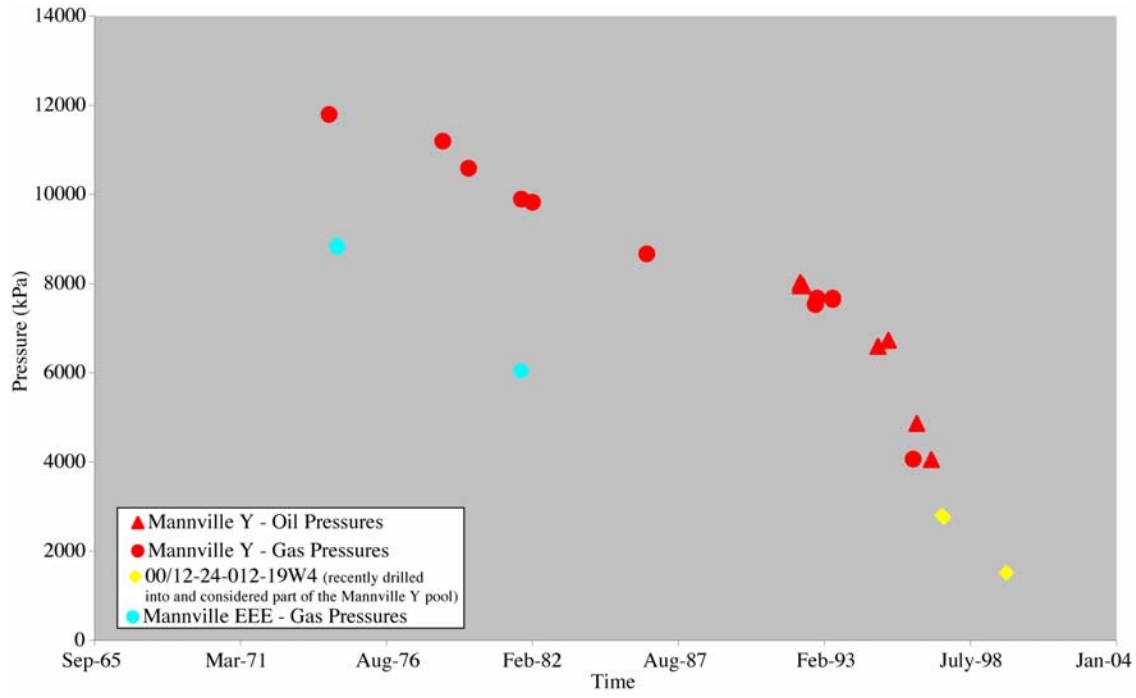

Figure 2.19: Pressure versus time graph for the Mannville Y pool (red circles and triangles) and the Mannville EEE pool (blue circles). Also included are pressure data from the recently drilled 100/12-24-12-19W4 well (yellow diamonds), which indicate that this well is part of the Mannville Y pool.

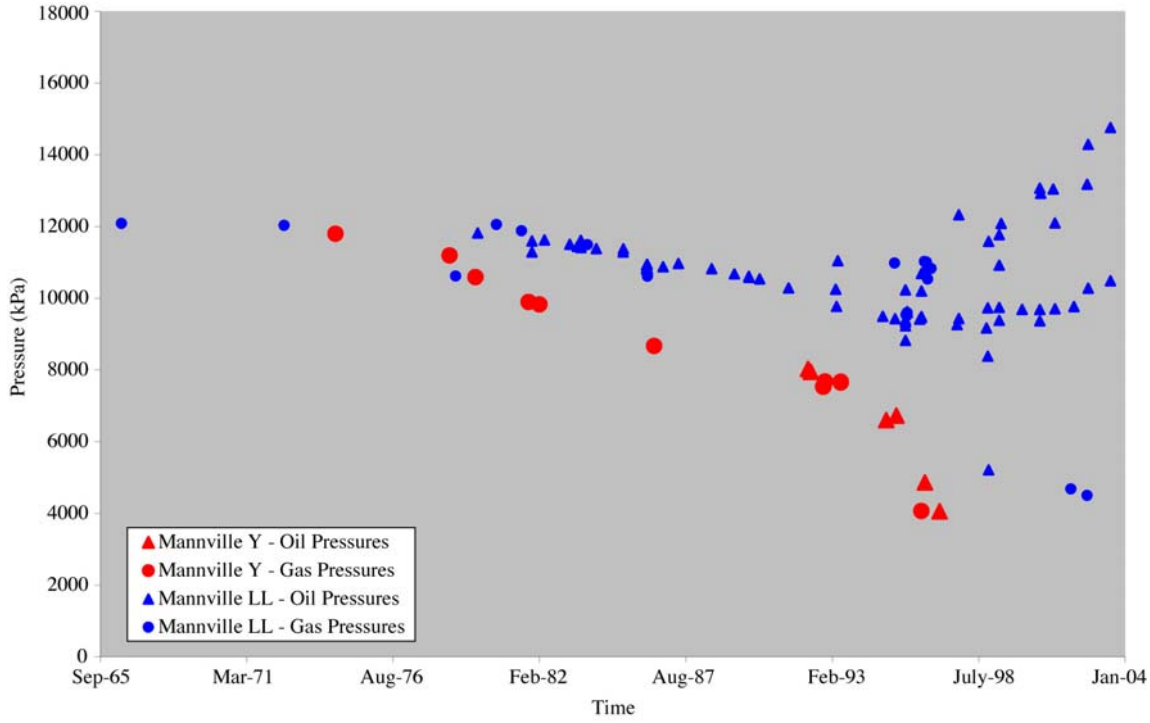

Figure 2.20: Pressure versus time graph for the Mannville Y pool (red circles and triangles) and the Mannville LL pool (blue circles and triangles). In 1978, the pressure curves for the two pools diverge significantly (likely due to waterflooding of the Mannville LL pool) indicating that they are not in hydraulic communication.

2.3.2 Rock Properties

Weighted average (by thickness) net-pay porosity values for the Glauconite C incised channel sandstones obtained from porosity logs (using a 9% porosity cut off) do not vary significantly across the pool. The low average porosity is 17.7% with a maximum measured average porosity of 23.9% (Figure 2.21).

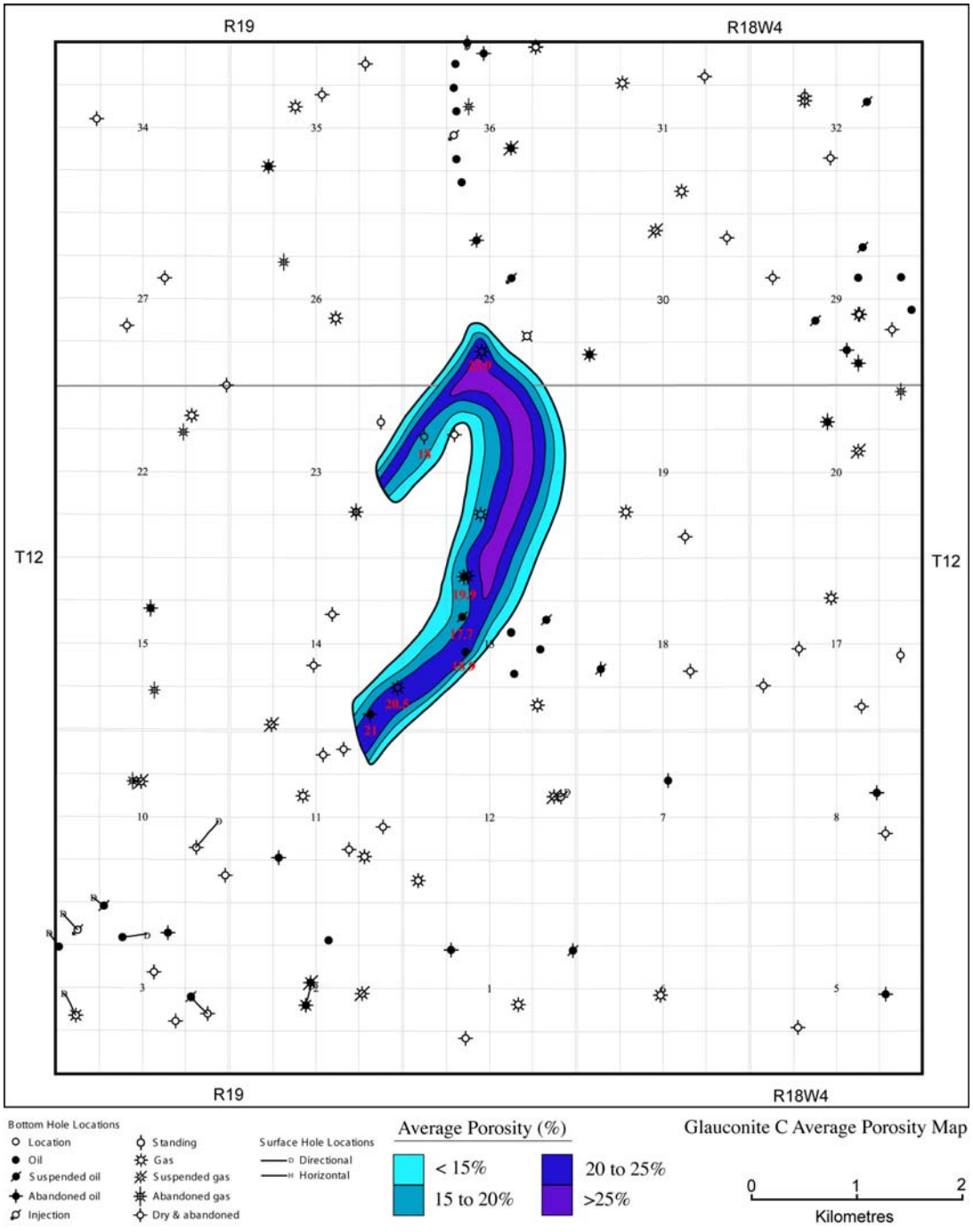

Figure 2.21: Hand-contoured net-pay average porosity map of the Mannville Y pool (contour interval = 5% porosity).

Log-derived porosity closely matches core-derived porosity, likely reflecting the quartz-rich nature of the channel sandstones, lack of shale interbeds, and limited variability in the porosity of the sandstones. Core-derived porosity is more reliable than log-derived porosity; however, no wells that produce from or penetrate the Mannville Y pool are cored in the Glauconite Fm. Log-derived porosity is, therefore, the only mechanism available to predict the porosity and permeability of the Glauconite C sandstones that contain the Mannville Y pool. To accurately determine porosity and permeability of the Mannville Y pool it is first necessary to derive the relationship between log porosity and core porosity for wells cored in the Glauconite Fm. (Figure 2.22). Core porosity can then be used to predict the permeability, in three directions, of the Glauconite C sandstones. This is accomplished by comparing core porosity to the maximum horizontal permeability (k_{max}), and then k_{max} to vertical permeability (k_v) and horizontal permeability (k_{90}) at 90 degrees to k_{max} to determine permeability anisotropy.

The mathematical relationship between core- and log-derived porosity was determined for nine wells (10 distinct sandstone bodies) cored in the Glauconite Fm. within a 3-mile radius of the Mannville Y pool (well location is given in Figure 2.22). This relationship is given by:

$$\Phi = 0.8146\Phi_{LOG} + 0.0453$$

where the core porosity (Φ) and log porosity (Φ_{LOG}) are expressed as fractions. The relationship between these two values is depicted graphically in Figure 2.23.

Maximum horizontal permeability as measured in core is proportional to the core-derived porosity and can be estimated using the following equation:

$$k_{\max} = 10^{(15.944\Phi - 0.7979)}$$

where the core porosity (Φ) is expressed as a fraction and maximum horizontal permeability (k_{max}) is expressed in millidarcies (md). This relationship is illustrated graphically in Figure 2.24. As presented in Figure 2.24, the permeability of the Glauconite C zone is variable and ranges from an average of 4.34 md at 9% porosity to 1068 md at 24% porosity.

The Glauconite Fm. also exhibits a significant degree of vertical permeability anisotropy. The maximum horizontal permeability of the Glauconite Fm. is significantly greater than the vertical permeability (k_v) as seen in Figure 2.25, and can be expressed mathematically by:

$$k_v = 0.107 k_{\max}^{1.0194}$$

Based on this relationship, it can be stated that the vertical permeability is approximately one tenth that of the maximum horizontal permeability.

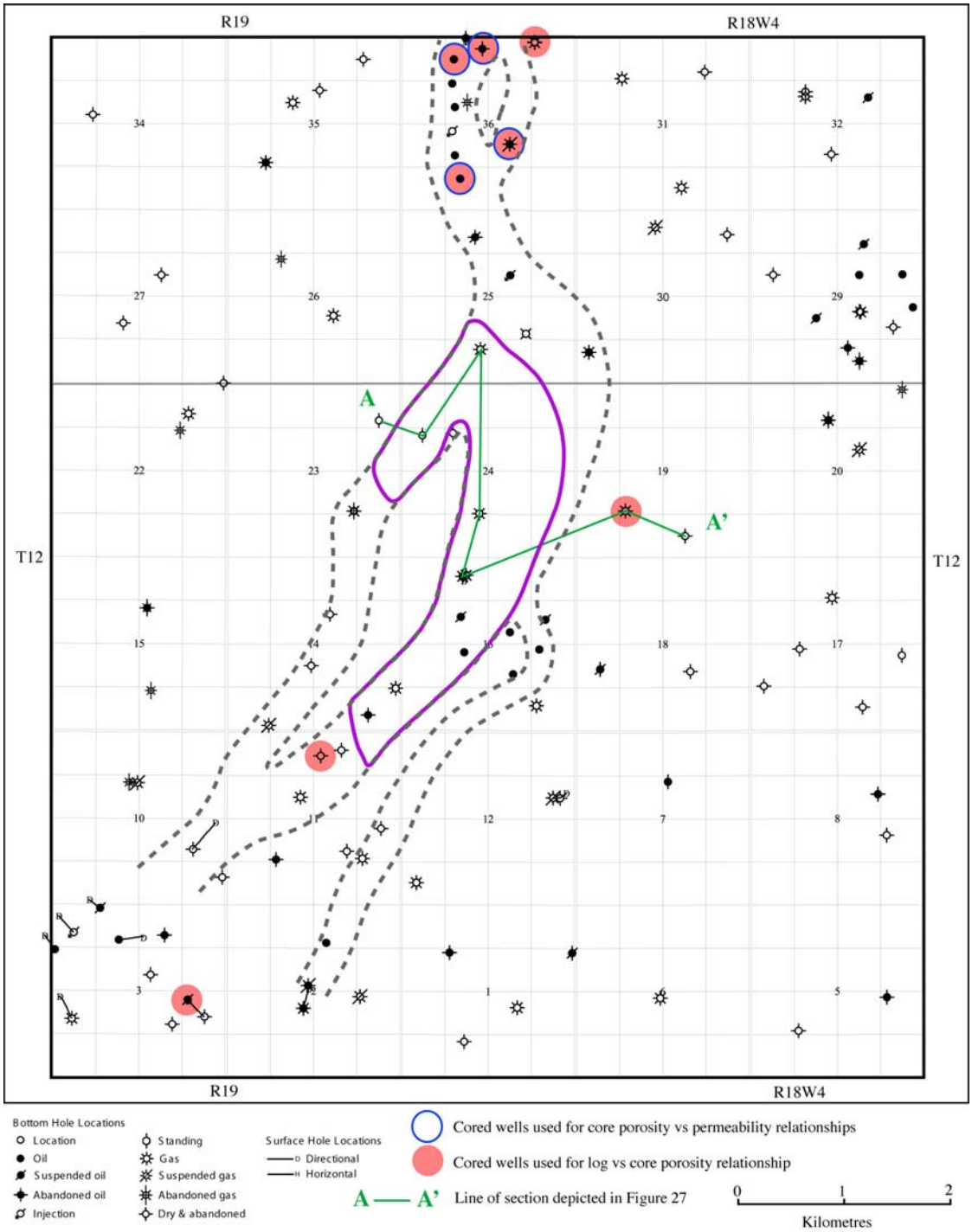

Figure 2.22: Map of the study area with wells cored in the Glauconite Fm. and used in determining porosity and permeability relationships. Filled red circles indicate wells used in determining the relationship between log-derived and core-derived porosity. Hollow blue circles indicate wells cored through the Glauconite C incised channel deposits that were used to determine the relationship between core-derived porosity and core-derived permeability. Outlined with a dashed grey line is the edge of the Glauconite C incised channel complex. The solid purple line indicates the zero edge of the Mannville Y pool. The green line marked A-A' is the line of section schematically illustrated in Figure 2.27.

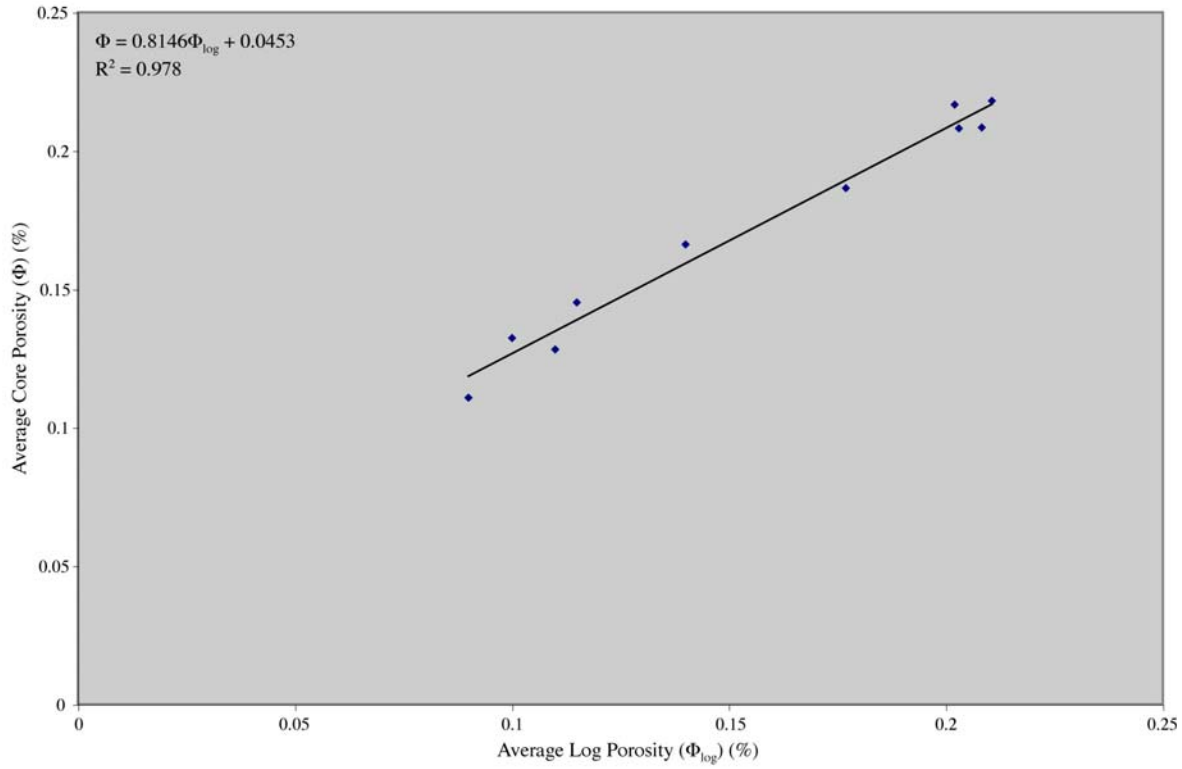

Figure 2.23: Graphic relationship between average Glauconite porosity determined from density or neutron-density logs and average porosity derived from core analyses of Glauconite Fm. sandstones.

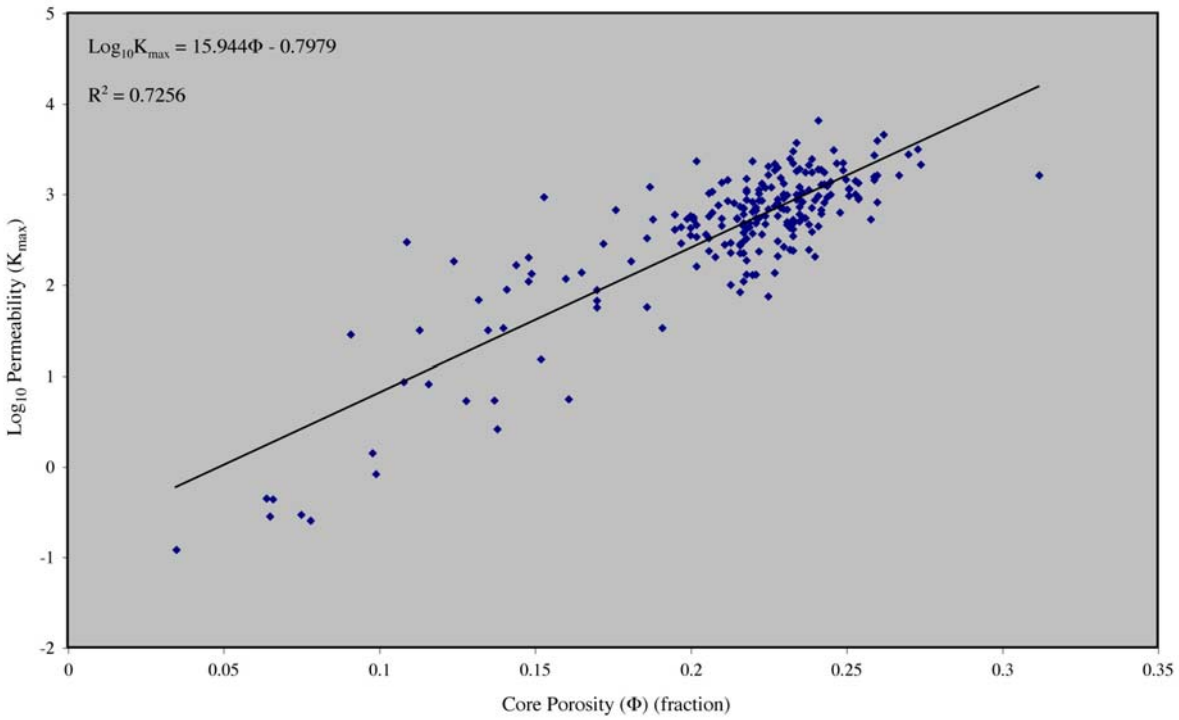

Figure 2.24: Graphic relationship between core-derived porosity (Φ) and core-derived maximum horizontal permeability (k_{max}).

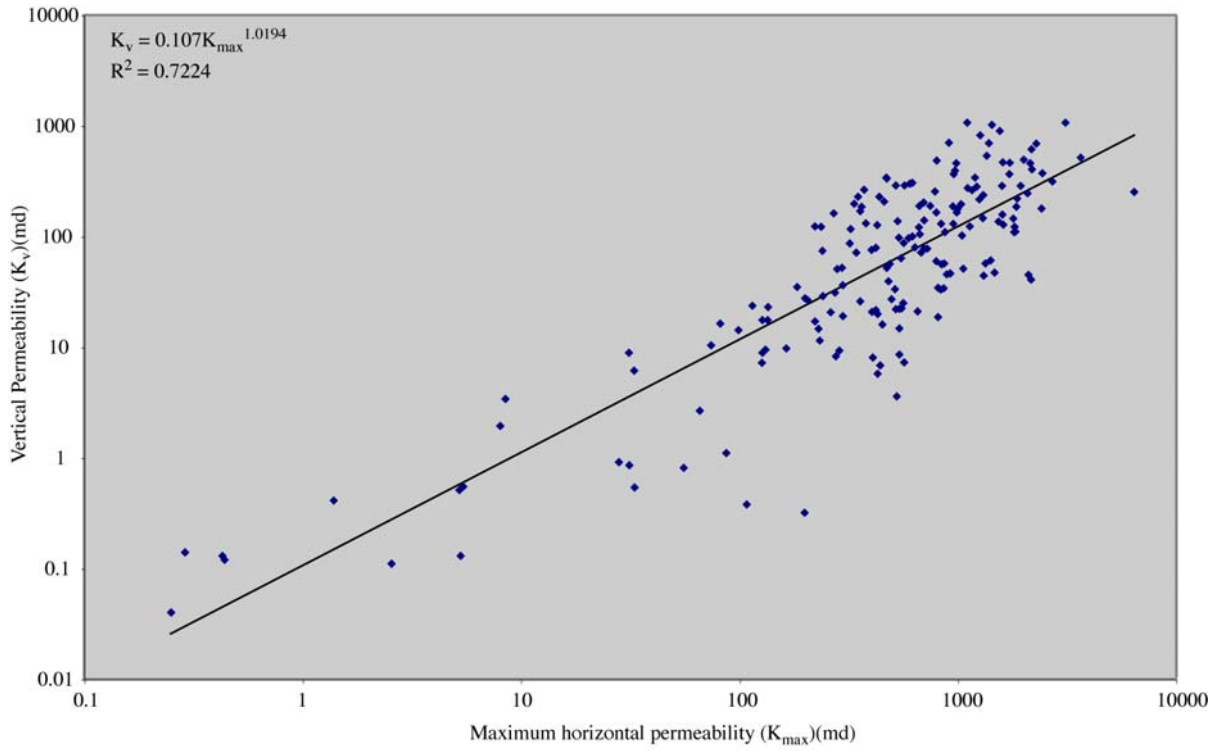

Figure 2.25: Graphic relationship between vertical permeability (k_v) and maximum horizontal permeability (k_{max}). This relationship defines vertical permeability anisotropy within Glauconite C incised channel sandstones.

Horizontal permeability anisotropy is shown graphically in Figure 2.26 and can be expressed by the relation:

$$k_{90} = 0.7634 k_{\max}^{1.016}$$

where k_{90} is the horizontal permeability oriented at 90° to the maximum horizontal permeability k_{max}. The k_{90} permeability is approximately 75% that of k_{max} suggesting that there is significant horizontal permeability anisotropy within Glauconite C incised channels.

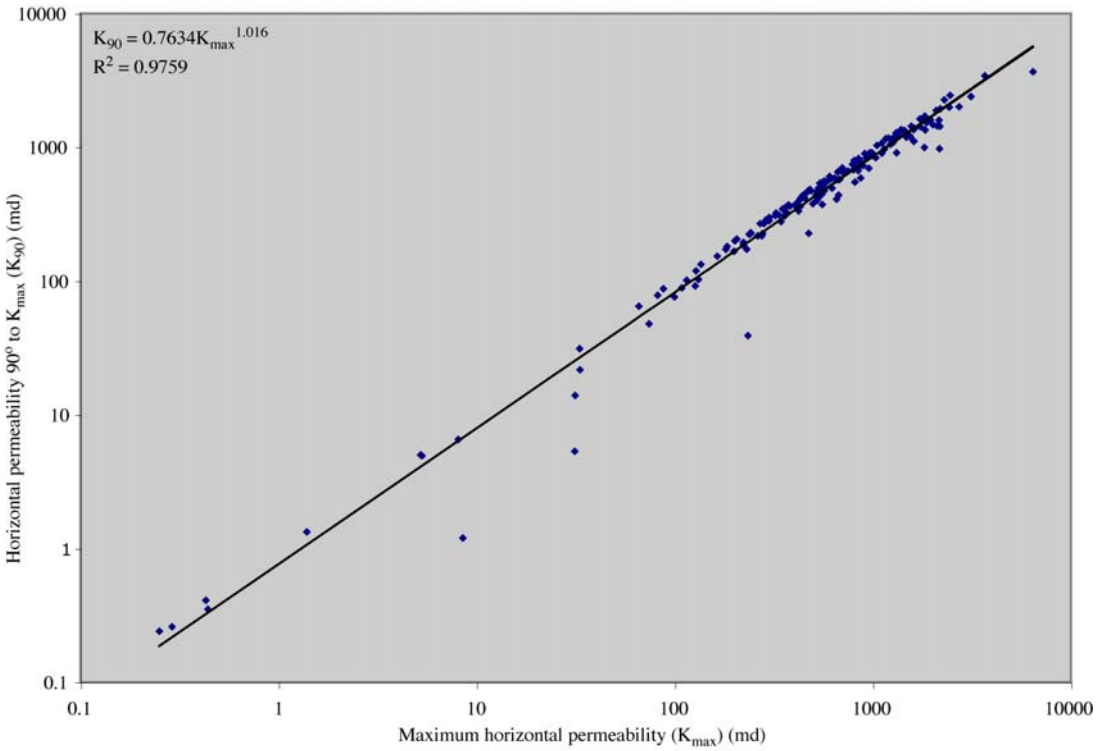

Figure 2.26: Graphic relationship between maximum horizontal permeability (K_{max}) and horizontal permeability measured at 90 degrees to k_{max} (k_{90}). This relationship defines horizontal permeability anisotropy within Glauconite C incised channel sandstones.

2.4 Summary

1) The Mannville Y pool is contained within quartz arenite to sublitharentie sandstones deposited in an incised fluvial to estuarine channel complex in the basal sequence of the Glauconite Fm. – the Glauconite C. Within the study area, this channel changes direction from southwest-northeast to north-south.
2) The Mannville Y pool is hydraulically isolated from the underlying oil-producing Mannville R pool.
3) The Mannville Y pool is hydraulically isolated from the stratigraphically equivalent Mannville LL and EEE pools.
4) There is a good relationship between horizontal permeability and porosity in Glauconite Fm. incised channels in the Retlaw area.
5) The rocks of the Glauconite Fm. incised channels exhibit pronounced and well-defined permeability anisotropy in both the vertical and horizontal planes. Vertical permeability is approximately one tenth that of maximum horizontal permeability. The horizontal permeability at 90 degrees to k_{max} is only 75% of k_{max}.

A not-to-scale cross-section through the Mannville Y pool is illustrated in Figure 2.27.

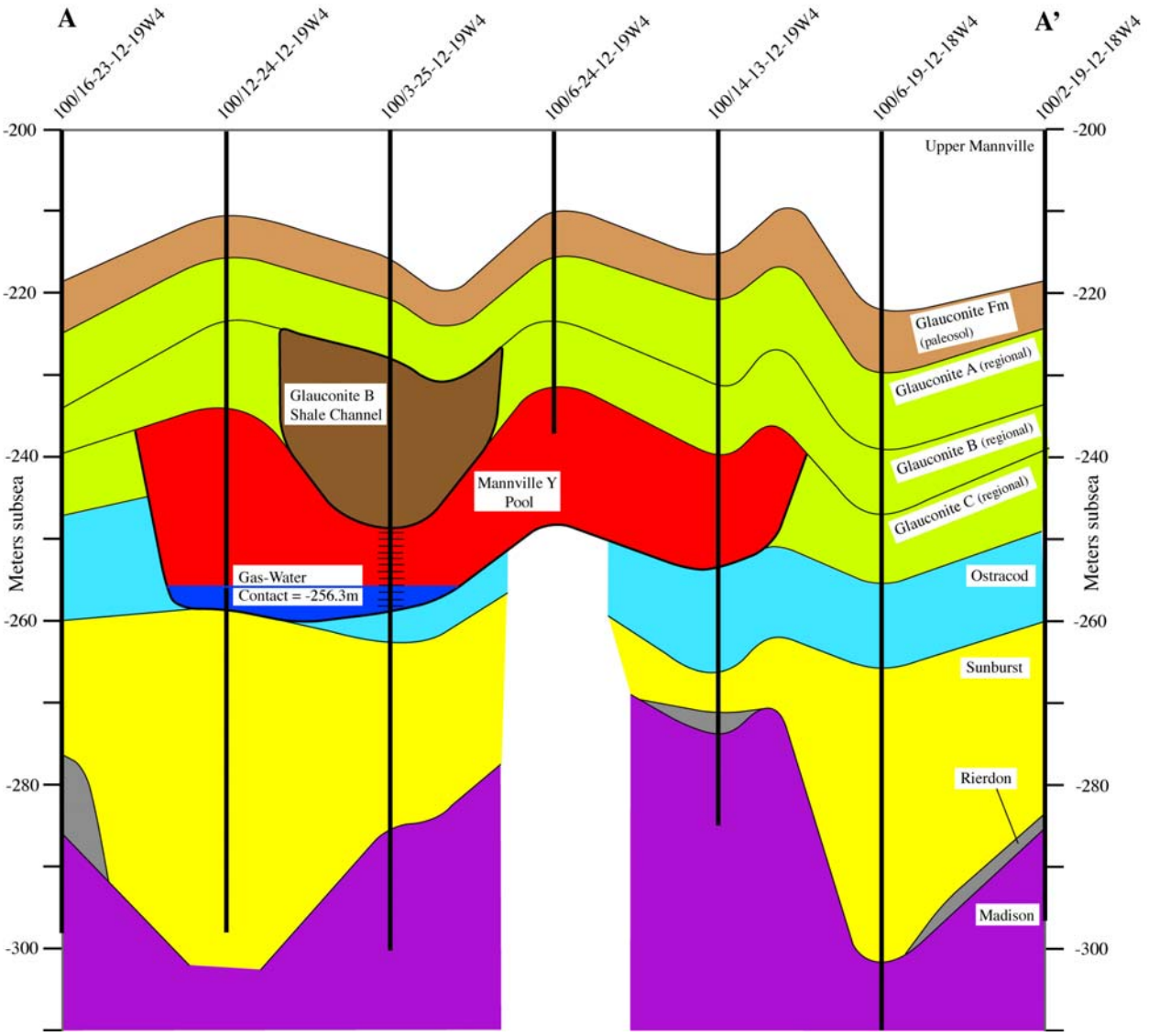

Figure 2.27: Not-to-scale schematic cross section depicting the location of the Mannville Y pool and its relationship to other stratigraphic units from the top of the Mississippian Madison Group to the top of the Glauconite Fm. The acid-gas disposal zone is identified in the 100/3-25-12-19W4 well by horizontal bars. The line of section (A-A') is shown on Figure 2.22.

3. Production Data Analysis

3.1 Data Analysis

The Retlaw Mannville Y pool has produced from four gas wells and from one oil well in Range 19 of Township 12 (Figure 3.1). Production commenced from one gas well in August 1976. Oil production started later, from one well only, in April 1992. One gas well was subsequently converted to an acid gas injector, in December 2003. As of November 2006, the cumulative gas and oil production are 1.009×10^9 Sm^3 and 6,610 Sm^3, respectively.

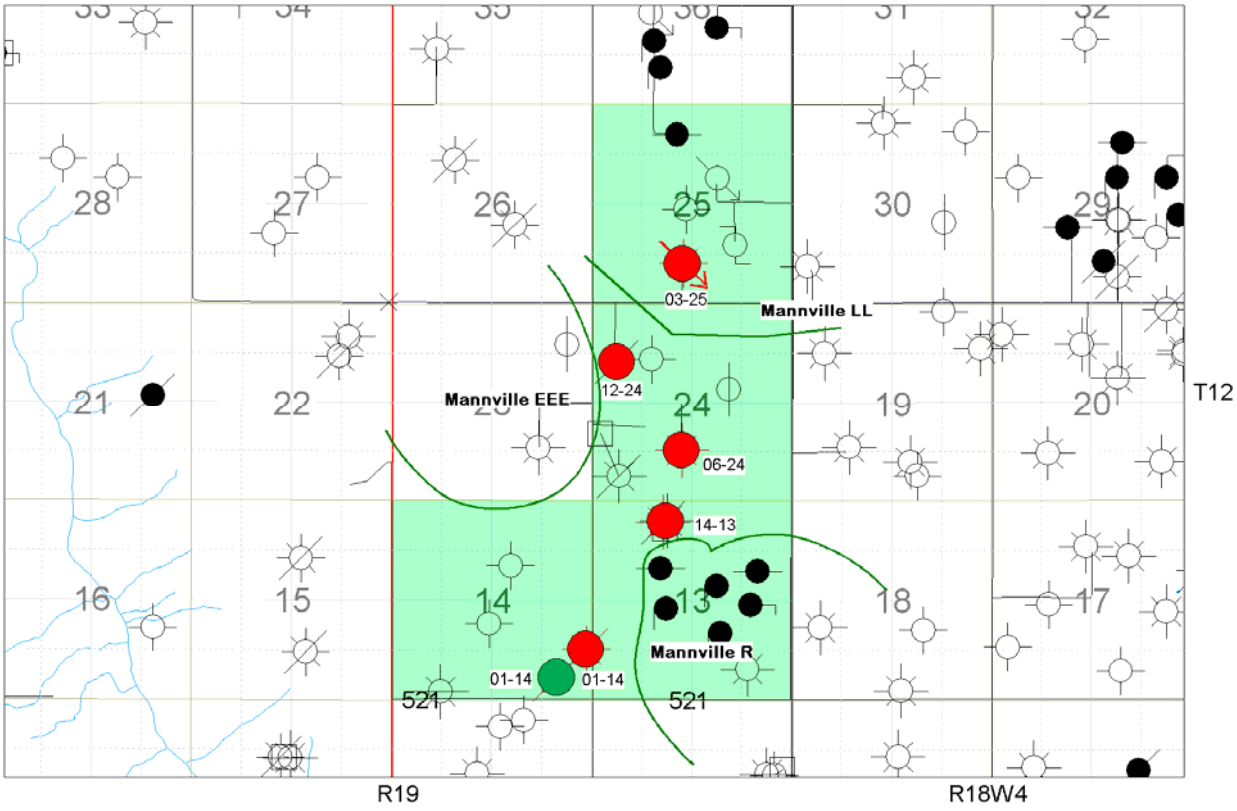

Figure 3.1: Location of the oil and gas producing wells, and of the acid gas injection well in the Retlaw Mannville Y pool.

Data from ERCB's public databases were used for estimating in-place hydrocarbons. Using this information, the original oil and gas in place (OOIP, and OGIP) are estimated at 222,000 Sm^3 at 1.208×10^9 Sm^3, respectively. Using material balance techniques, the pool OGIP is re-evaluated in this report after a review of the pressure and production information. The OGIP estimated using the material balance technique (see below), is significantly greater than the OGIP that one would estimate when using the average reservoir properties given by the ERCB[1].

[1] The different values of possible OGIP are further discussed under "Discussions".

Well Completions. All the wells in the Retlaw Mannville Y pool are vertically drilled, and perforated through the Glauconite C channel. Well 14-13 was initially completed to produce from the Sunburst but no commingling occurred.

Pressure History. The pressure data for the Mannville Y pool sourced from publicly available databases, including static gradient and build-up tests, are shown in Figure 3.2, indicating an initial pressure of about 11,790 kPa. The reservoir, situated at an average depth of 1,100 m, was thus originally at normal hydrostatic conditions.

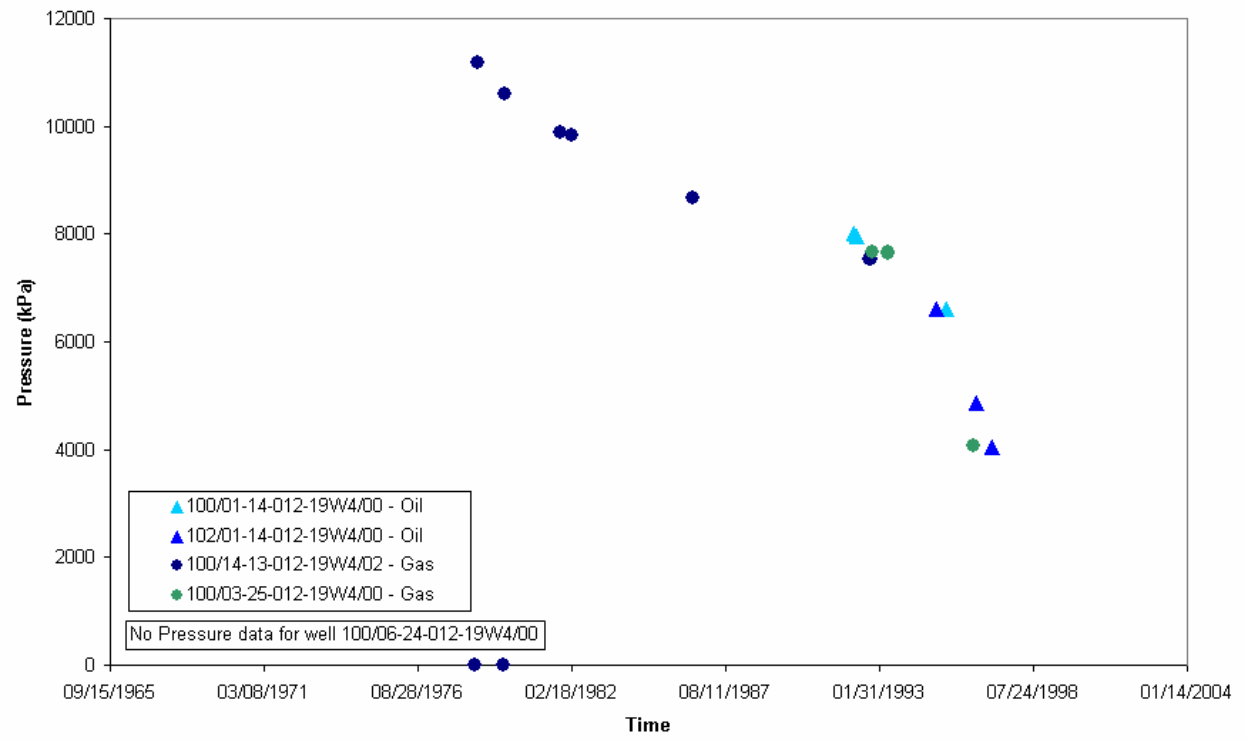

Figure 3.2: Historical reservoir pressures in the Retlaw Mannville Y pool.

Upon production of the 14-13/02 well starting in August 1976, reservoir pressure declines gradually, followed by a sharper decline in early 1993, after the start of well 03-25 as a gas producer and well 01-14 as an oil producer. The pressure declines further in 1995 when wells 102/01-14 and 06-24 are both put on gas production. No pressure data are available after February 1997, but the Taylor Management Company Inc. progress reports to ERCB, dated after 2004 when gas injection is initiated at well 03-25, indicate an average reservoir pressure maintained constant or slightly increasing at around 2,500 kPa.

Production. Production analysis was performed separately on the oil and gas legs of the reservoir. The list of the 5 wells producing from the Retlaw Mannville Y pool is shown in Table 3.1 below. Plots of the total oil and gas production versus time are shown in Figures 3.3 and 3.4, respectively.

Table 3.1 Operational characteristics of the 5 oil and gas wells in the Retlaw Mannville Y pool.

UWI	Well Name	Completion Date	Cumulative Oil (m3)	Cumulative Gas (m3)	Cumulative Water (m3)	Last Production
100/14-13-012-19W4/02	PROVIDENT RETLAW 14-13-12-19	4-Jul-74	-	611,699,000	1,192	Current
100/01-14-012-19W4/00	JEFFCO RETLAW 1-14-12-19	9-Mar-92	2,919	1,990,000	5,532	Jan-98
102/01-14-012-19W4/00	PROVIDENT RETLAW 1-14-12-19	24-Sep-94	82	901,000	272	Nov-98
100/06-24-012-19W4/00	PROVIDENT RETLAW 6-24-12-19	24-Jan-95	-	221,104,000	205	Current
100/12-24-012-19W4/00	PROVIDENT RETLAW 12-24-12-19	1-Jul-97	-	-	-	-
100/03-25-012-19W4/00	TMI RETLAW 3-25-12-19	24-Oct-92	944	173,113,000	47,752	Dec-03

UWI	Status	Cumulative Acid Gas Injected (m3)	On Injection	Last Injection
100/14-13-012-19W4/02	Flowing GAS	-	-	-
100/01-14-012-19W4/00	ABD OIL	-	-	-
102/01-14-012-19W4/00	ABD Reentered GAS	-	-	-
100/06-24-012-19W4/00	Flowing GAS	-	-	-
100/12-24-012-19W4/00	Drilled & Cased	-	-	-
100/03-25-012-19W4/00	Acid GAS Disposal	57,013,000	Aug-04	Current

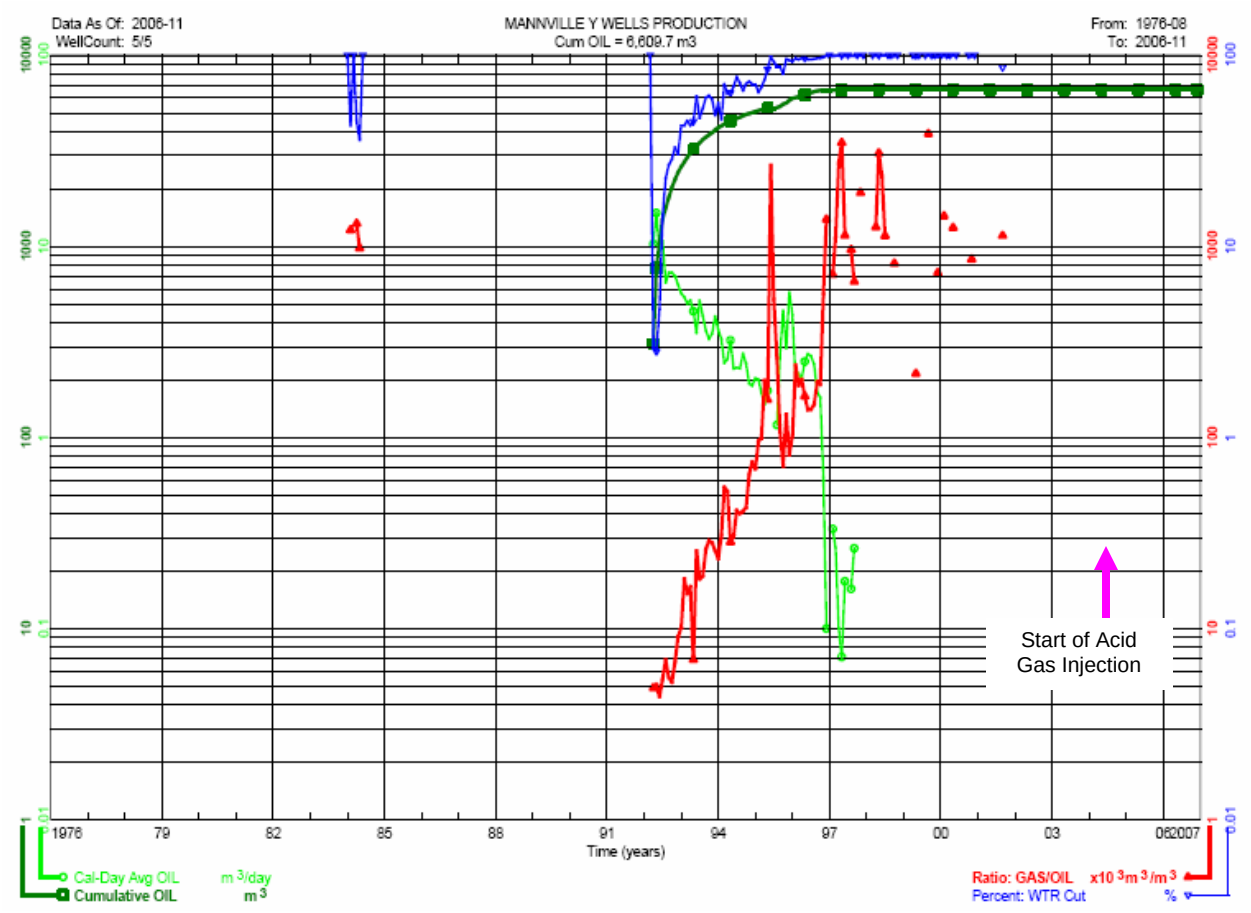

Figure 3.3: Oil production from the Retlaw Mannville Y pool.

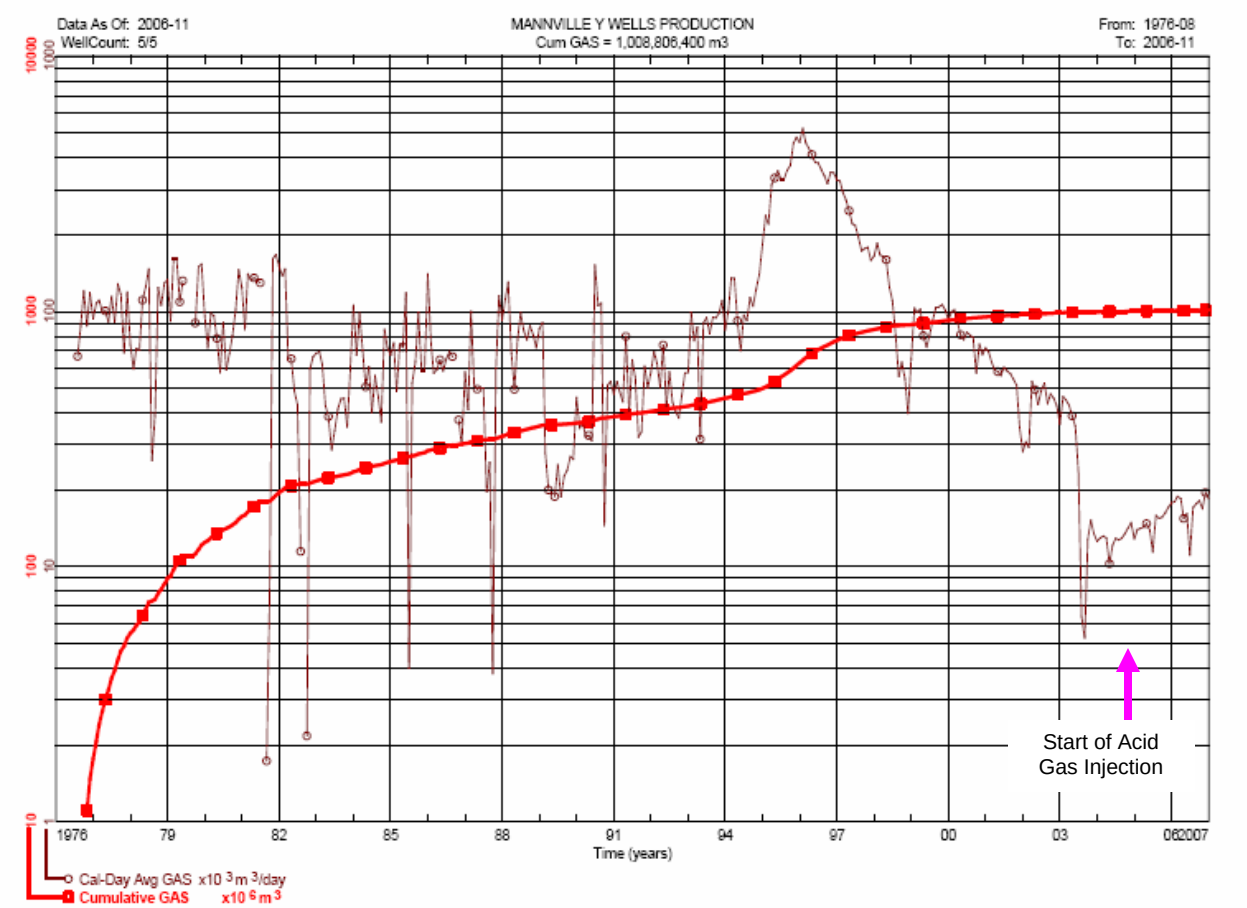

Figure 3.4: Gas production from the Retlaw Mannville Y pool.

The following trends are evident in Figures 3.3 and 3.4:

Gas Production:

- Gas production in the Mannville Y pool starts in August 1976 from the 14-13 well, at a rate of 100,000 Sm^3/d.
- New gas wells (01-14, 06-24 and 03-25) are put on production in 1992, 1994 and 1995. As a result, the production rate is increased and peaks in 1996 at 500,000 Sm^3/d. As all wells start to decline, the rate drops to 40,000 Sm^3/d in early 2003. In late 2004, well 03-25 is converted to an acid gas injector and production from14-13 and 06-24 starts again at a rate of 13,000 Sm^3/d. The rate as of December 2006 is 19,000 Sm^3/d.
- Total gas production (including from the oil well) is 1.009×10^9 Sm^3. This value also includes the acid gas that was produced from the two wells that showed breakthrough. To estimate the cumulative volume of *hydrocarbon* gas recovered from this pool, the cumulative gas production from these two wells up to the time that CO_2 concentration reached 50% was added to that of the three other wells in the field. These latter wells were shut-in prior to start of acid gas injection. As such the cumulative hydrocarbon gas produced from this reservoir is estimated at 1.004×10^9 Sm^3 (see text below and Figure 3.5 for more details).

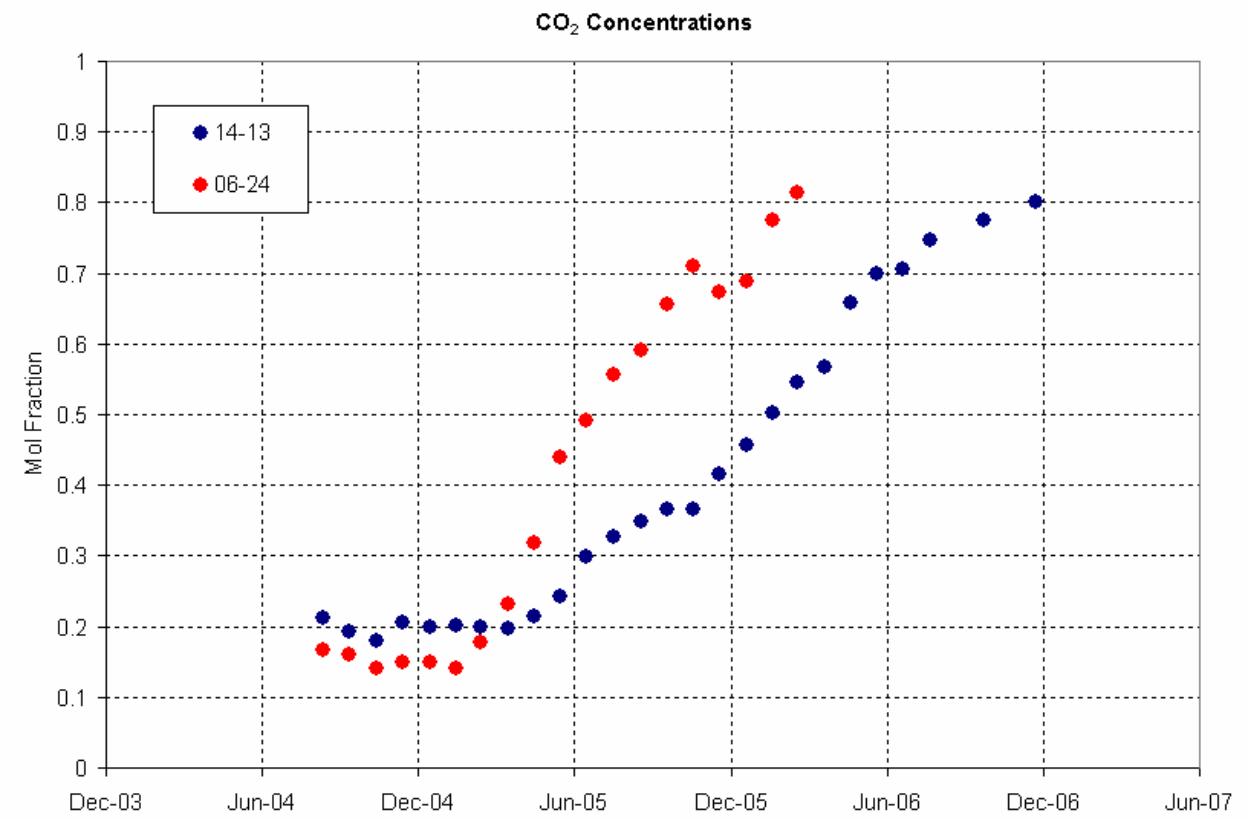

Figure 3.5: CO_2 concentration in gas wells that continued production after the start of acid gas injection in the Retlaw Mannville Y pool.

Oil Production:

- Oil production in the Mannville Y pool starts in March 1992 from well 01-14 at a rate of 21 Sm^3/d, initially drilled assuming a separate pool. Well 01-14 continues producing until mid to late 90's, when GOR (Gas-Oil Ratio) increases to above 100,000 Sm^3/Sm^3.
- No further oil production is reported since 1998.

Acid Gas Injection:

- Well 03-25 is converted into an acid gas injector in December 2003. It is located in the northern part of the pool. The composition of the injected gas is roughly 96% CO_2, 1.7% H_2S, 0.5% N_2, and 1.8% light hydrocarbon gases.
- Total acid gas injection as of November 2006 amounts to 57 million Sm^3. Average rate of injection is in the order of 66,000 Sm^3/d.
- The progress reports filed by Taylor Management Company Inc. with ERCB show an increase of CO_2 concentration in producing wells. The measured results are plotted in Figure 3.5 and indicate that in March 2005, the 06-24 well showed an increase in CO_2 concentration. This increase continued until March 2006, when the well was shut-in because of high CO_2 concentrations (more than 80%). Breakthrough of CO_2 into the 14-13 well was observed in May 2005. Acid gas concentration in this well was at 80% as of December 2006. By this time the rate of recycling was reported at 11% of the injected rate. Measurements shown in Figure 3.5 were used to account for the cumulative volume of the acid gas produced as explained previously.

Total pool:

- The cumulative hydrocarbon gas production, including from the oil well, is estimated at 1.004×10^9 Sm^3.
- The cumulative oil production is 6,610 Sm^3 as of November 2006.
- The cumulative water produced until November 2006 is 54,950 m^3.
- The gas production rate does show an increase after acid gas injection started (see Figure 3.4). Less than a year and half later, acid gas breaks through (as evidenced in Figure 3.5) contributing to the production rates shown in Figure 3.4.

Decline Analysis. Decline analysis has been performed on the gas-producing wells only. Figure 3.6 shows an extrapolation for the gas in the pool. Traditional exponential decline analysis based on data prior to start of the acid gas injection leads to an estimated ultimate recovery (EUR) of 1.027×10^9 Sm^3. While this value is greater than the estimated cumulative volume of hydrocarbon gas that has been produced from the pool (by 23×10^6 Sm^3), this difference is within the range of uncertainty of the estimated EUR.

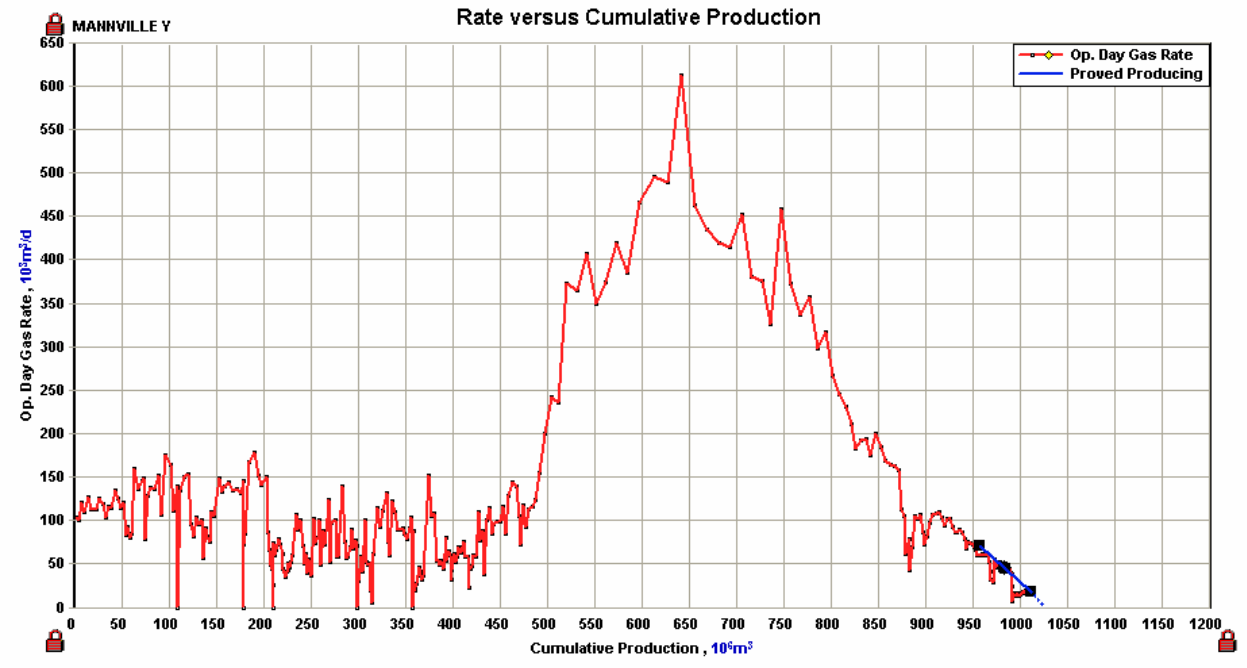

Figure 3.6: Exponential decline analysis of gas production rate versus cumulative gas production from the Retlaw Mannville Y pool.

Material Balance Calculations. Figure 3.7 shows material balance p/Z plots for gas production from the Retlaw Mannville Y pool. Pressures are reported up to 1997 and do not include readings performed during acid gas injection. Cumulative gas production to 2004 (prior to acid gas injection) is shown by the yellow triangle, and corresponds to a value of 995.8×10^6 Sm^3. Figure 3.6 indicates that the OGIP as determined by the material balance technique is 1.067×10^9 Sm^3, which is 63×10^6 Sm^3 greater than the pool production.

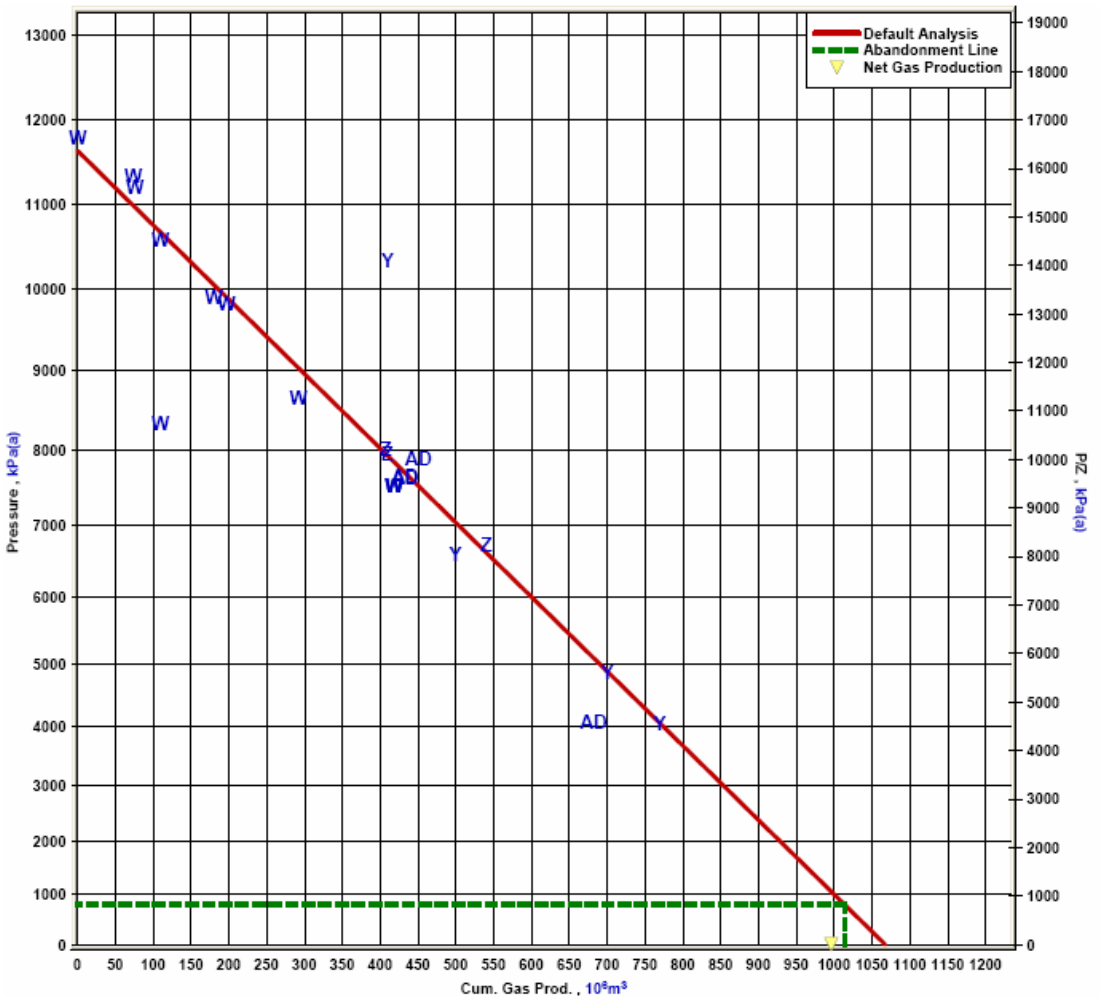

Figure 3.7: Plot of p/Z material balance for gas produced from the Retlaw Mannville Y pool.

3.2 Discussion

The cumulative gas production up to December 2003 is 995.8×10^6 Sm^3. The rate decline and material balance calculations just performed give an estimated ultimate gas recovery of 1.027×10^9 Sm^3 and an OGIP of 1.067×10^9 Sm^3, respectively. In the following a discussion of various estimates of reservoir pore volume (PV) is given.

Calculations using ERCB data. Using the average reservoir characteristics (see Table 3.2) recorded by the ERCB for the Mannville Y pool, the total pore volume is $PV_{ERCB} = 4.9\times10^6$ m^3. This pore volume corresponds to an OGIP of 0.59×10^9 Sm^3, which is roughly half the OGIP given by the ERCB (of 1.2×10^9 Sm^3).

Table 3.2: ERCB's Average reservoir characteristics for the Retlaw Mannville Y gas pool (extracted from GeoScout).

ERCB values	
Area A (ha)	372
Thickness h (m)	5.44
Porosity	0.242
Gas Saturation	0.85
Z-factor Z	0.796
Initial pressure (kPa)	11,790
Temperature (K)	313

Calculations using Geology data. In "Chapter 2: Geology" of this report, maps of the net pay thickness and porosity of Retlaw Mannville Y pool were generated (Figures 2.16 and 2.21, respectively). These provide a total pore volume of roughly $PV_{Geol} = 7\times10^6$ m^3, which corresponds to an OGIP[2] of 0.84×10^9 Sm^3. While this total pore volume and OGIP are larger than the corresponding values as determined from ERCB average properties given in Table 3.2, these are still not large enough to accommodate the observed production. In the following a sensitivity study is performed to investigate whether the uncertainties in different reservoir parameters can account for the observed discrepancy between calculated reservoir pore volume and production to date and/or OGIP calculated using various methods.

Sensitivity on reservoir parameters. Using production data and material balance calculations, one can estimate OGIP, and then calculate the reservoir pore volume. Such an estimate is affected by uncertainties in a number of parameters including initial pressure, gas composition, and reservoir pressure (at a certain cumulative production). The data were reviewed and a representative range of values is given in Table 3.3 below.

Table 3.3: Range of values affecting material balance calculations for the Retlaw Mannville Y pool (extracted from GeoScout).

Range of properties	
CO_2%	10 - 15%
H_2S%	0.1 - 0.2%
Gas Gravity	0.73 - 0.8
Initial Pressure, P_i (kPa)	11600 – 11800
Temperature T (°C)	39 – 40
Cumulative Production (10^6 m^3)	450
Pressure P (kPa)	7500 – 7800
Gas saturation (S_g)	0.85

Based on the data above, the range of OGIP and total pore volume are estimated using Monte-Carlo simulations, using the material balance equations of $OGIP = \frac{G_p B_g}{B_g - B_{gi}}$, and $HCPV = OGIP \times B_{gi}$, where G_p (Sm^3) is the cumulative gas production, B_{gi} and B_g (m^3/Sm^3) are

[2] For the OGIP calculations, the PVT properties given in Table 3.2 are used.

the gas formation volume factors at the initial and current pressure, and *HCPV* is the hydrocarbon pore volume (m^3) (Craft and Hawkins, 1959). An initial water saturation of 15% as suggested by the ERCB is assumed valid.

Figure 3.8 below shows the estimated range of pore volume and indicates a mean value of $PV = 11.1 \times 10^6$ m^3 with a range of $PV = 10.8 - 11.4 \times 10^6$ m^3. The OGIP corresponding to the estimated pore volume is 1.12 to 1.17 $\times 10^9$ m^3. The range of *PV* estimated using this exercise is significantly larger than the *PV* that the geological interpretation presented in Chapter 2 suggests, rendering any numerical simulation meaningless. Nevertheless, to demonstrate the large discrepancy between the reported cumulative gas production and the volumetric estimates, a short simulation study was performed.

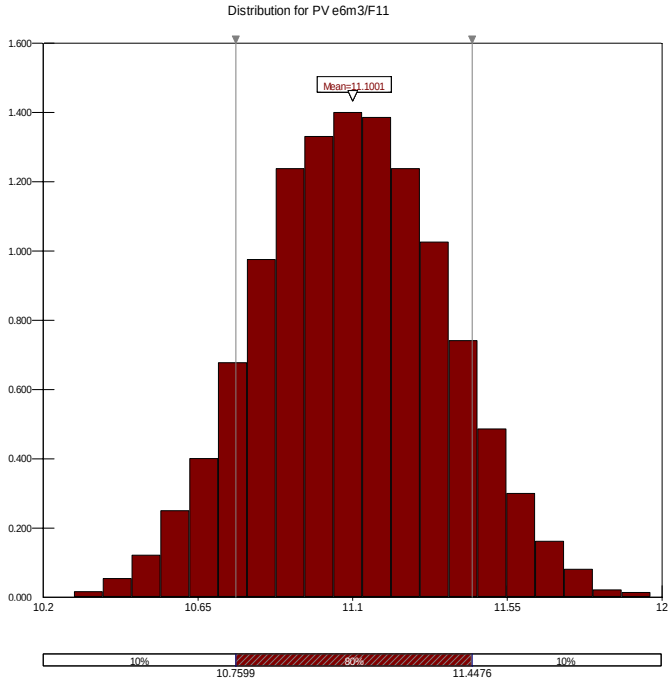

Figure 3.8: Monte Carlo simulation of the pore volume for the Retlaw Mannville Y pool.

3.3 Revision of Pool Size

The large discrepancy between the calculated volumetric gas reserves based on the maps in Chapter 2 (0.84×10^9 Sm^3) versus the gas reserve estimates calculated by the engineering material balance method (1.067×10^9 Sm^3) is significant. The authors believed consultation with the Energy Resources Conservation Board (formerly Alberta Energy Utilities Board - AERCB) would be appropriate and contacted the Geology and Reserves Group (GRG) which is responsible for estimating oil, conventional gas, coalbed methane gas, coal and bitumen reserves for the entire province of Alberta on an annual basis. These estimates are utilized by numerous Alberta and Federal government agencies, industry and any other individual or organizations that require this information.

Estimation of reserves by GRG is an iterative process. Initially, when the first well is drilled, reserves estimates are based on the net pay encountered in the well, porosity, water saturation, compressibility engineering parameters and the area of the drilling spacing unit.

Subsequent to the initial discovery, additional wells are mapped into the pool if they exhibit appropriate characteristics which indicate that they are in a common accumulation. Such characteristics include: same stratigraphic interval, similar gas-water or oil-water contacts if present, close proximity to other wells (usually within one or two sections) and pressures. At this stage of pool development volumetric reserve methodology are used to estimate gas reserves in place. Recovery factors used are based on historical data obtained from established pools. In the case of gas pools, recovery factors typically range from 75 to 80 percent.

After a few years of production (typically more than 5 years) sufficient engineering data (pressures, production) for the pool become available. These data permit an additional method for determination of reserves. If the engineering methodology of reserve estimation significantly differs from the volumetric method, the pool is identified and an iterative process between geology and engineering staff is initiated. The goal of this exercise is to identify potential explanations and find resolution for the reserve discrepancy.

In the case of the Retlaw Mannville Y pool, the engineering methodology and results were reviewed by GRG staff. It was determined that these data were sufficient to provide a representative gas in place (determined by material balance) and producible gas (determined by production decline). It was noted that the volumetric gas in place determined by geological mapping was significantly lower. Based on these observations, GRG undertook a review of the volumetric gas in place, which consisted of the following:

- reviewing the net pay at each well, the average porosity and water saturation
- reviewing the zero edge of the pool. (does the existing well control prevent extension of the zero edge beyond the existing limits)
- evaluating all zones of the pool in the wells proximal to the pool (in this case, GRG had not initiated the evaluation of the Mannville Y pool in the well 00/12-24-012-19W4/0)

After reviewing the data based on the above criteria, the Retlaw Mannville Y pool isopach was revised. The primary revision consisted of extending the zero edge of the pool (since there was no control preventing this revision), and evaluating the Mannville Y pool accumulation in the well 00/12-24-012-19W4/0. The resulting isopach revision resulted in a rock volume of 4827 ha metres (determined by a pool area of 576 ha with an average net pay of 8.38 metres); average pool water saturation of 20 percent and porosity of 21.8 percent. Utilization of these parameters resulted in a revision of the volumetric original gas in place to 1.143×10^9 Sm^3, which broadly matches the values obtained by the other two engineering methods. The following figures present the AERCB current isopach maps of the gas and oil accumulations of the Retlaw Mannville Y pool. These maps were subsequently used for simulation studies in Section 4 of this report.

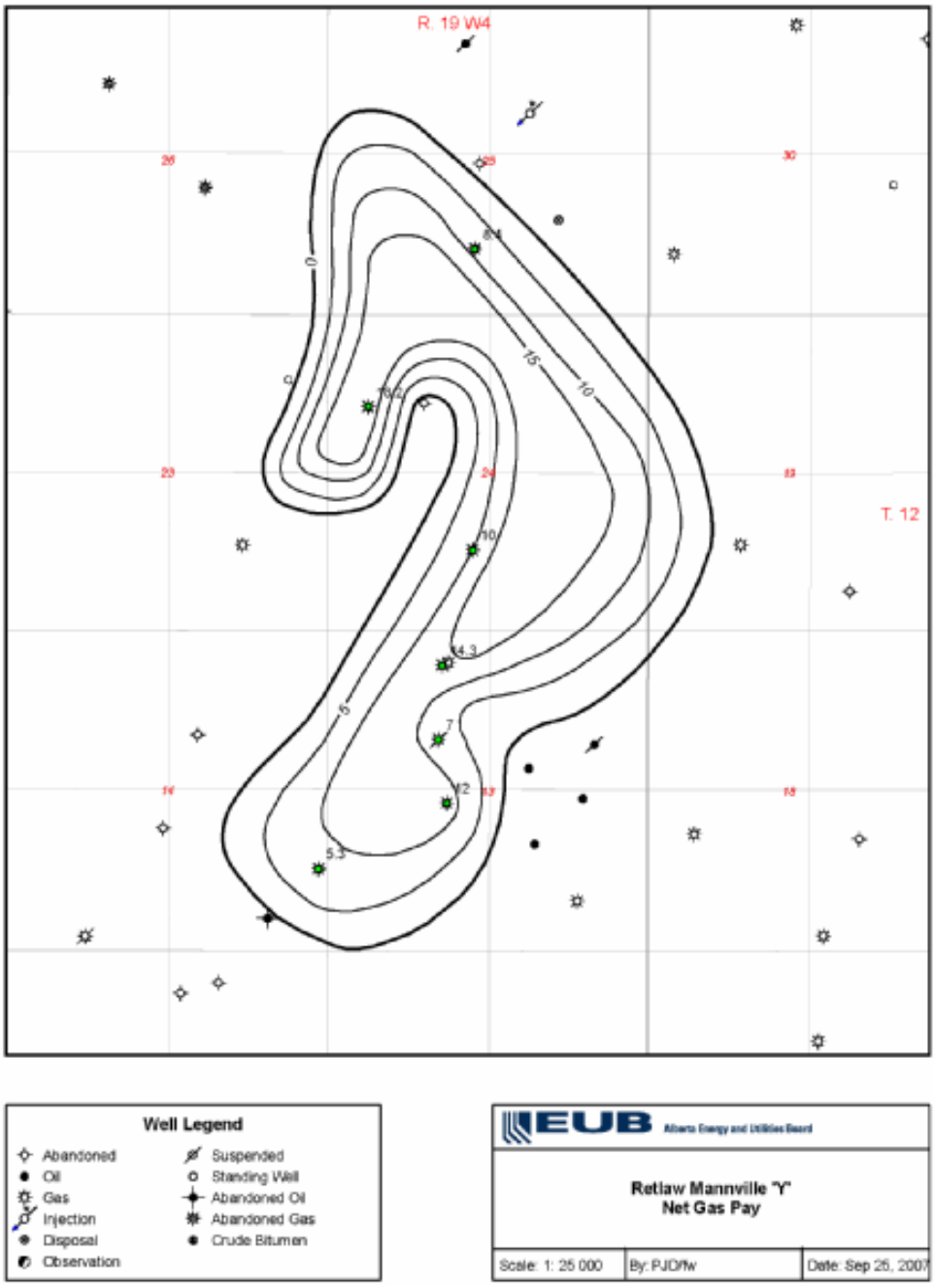

Figure 3.9: Revised outline and isopach map of the gas accumulation in the Retlaw Mannville Y pool.

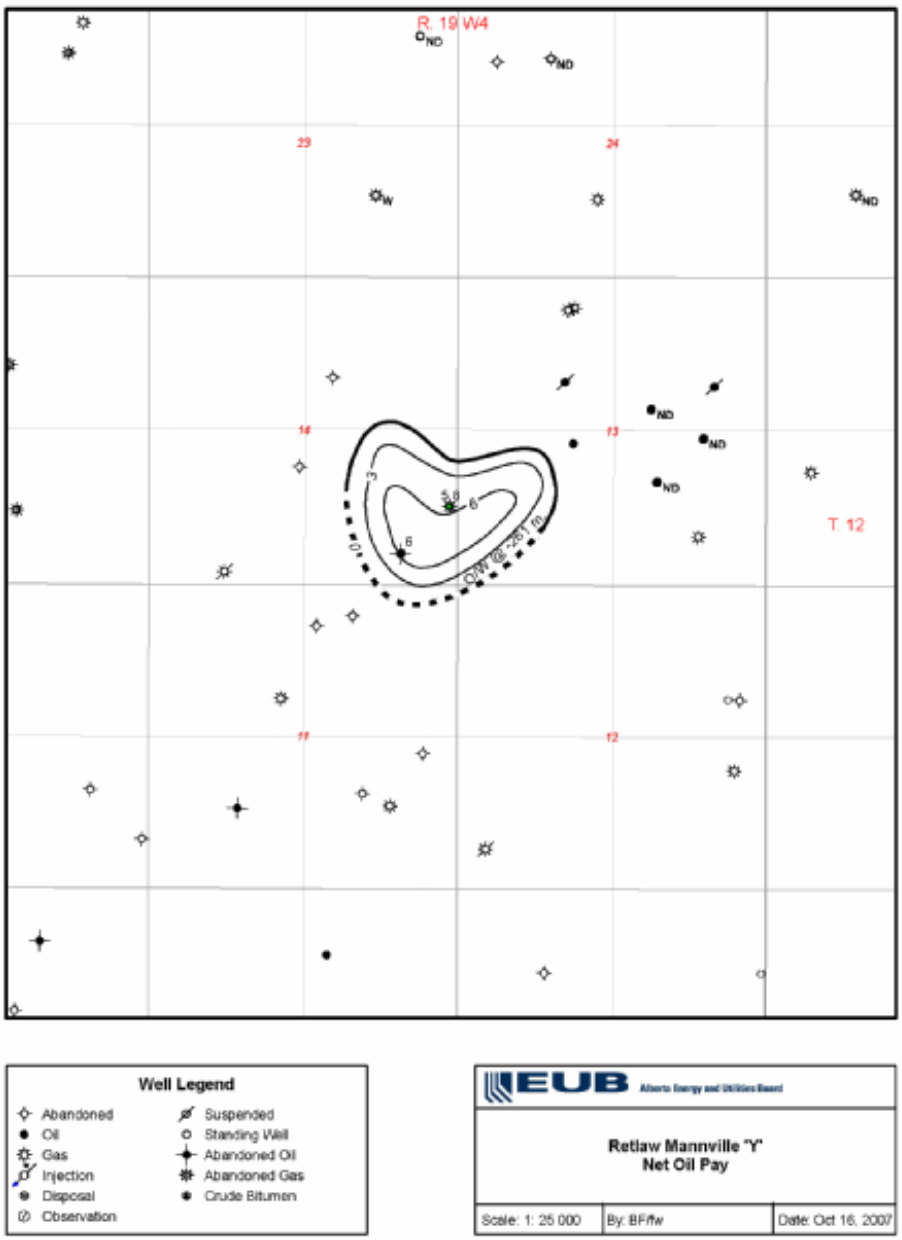

Figure 3.10: Revised outline and isopach map of the oil accumulation in the Retlaw Mannville Y pool.

4. Numerical Simulation

In this section, reservoir simulations are presented to model reservoir performance prior to, and during acid gas injection, as well as to forecast its behavior. The numerical simulation work has been conducted in 3 phases:

1) Production history-matching based on a black oil model simulation using the maps of the Retlaw Mannville Y reservoir generated in Chapter 2;
2) Production history matching based on a black oil model simulation using the revised ERCB mapping of the Retlaw Mannville Y reservoir;
3) Production history matching and forecast based on a compositional model simulation using the revised ERCB mapping of the Retlaw Mannville Y reservoir.

This chapter will describe each of the phases separately. The initial geological mapping, PVT and other data used in the simulations are presented first, followed by history matching that led to some modifications of the initial input, and closing with predictive simulations of reservoir behavior.

4.1 Black-oil Model Simulation using the Original Geology

Chapter 3 on Production Data Analysis concludes that both the geological interpretation of Chapter 2 on Geology and the ERCB original estimate of OGIP can not accommodate the much larger cumulative gas production to date from the Mannville Y pool. To illustrate this discrepancy, a short simulation study was performed and is presented next. The reservoir was simulated as a black oil model using CMG-IMEX^{TM} (CMG, 2006a). Simulated production and pressure are compared with the historical data.

4.1.1 Input Data

The maps of structure top, porosity, permeability and thickness (based on the maps given in Chapter 2), were incorporated in the numerical simulator (see Figures 4.1 to 4.4). The relationship between permeability and porosity presented in Figure 2.24 was used. Well locations are also shown in Figure 4.1.

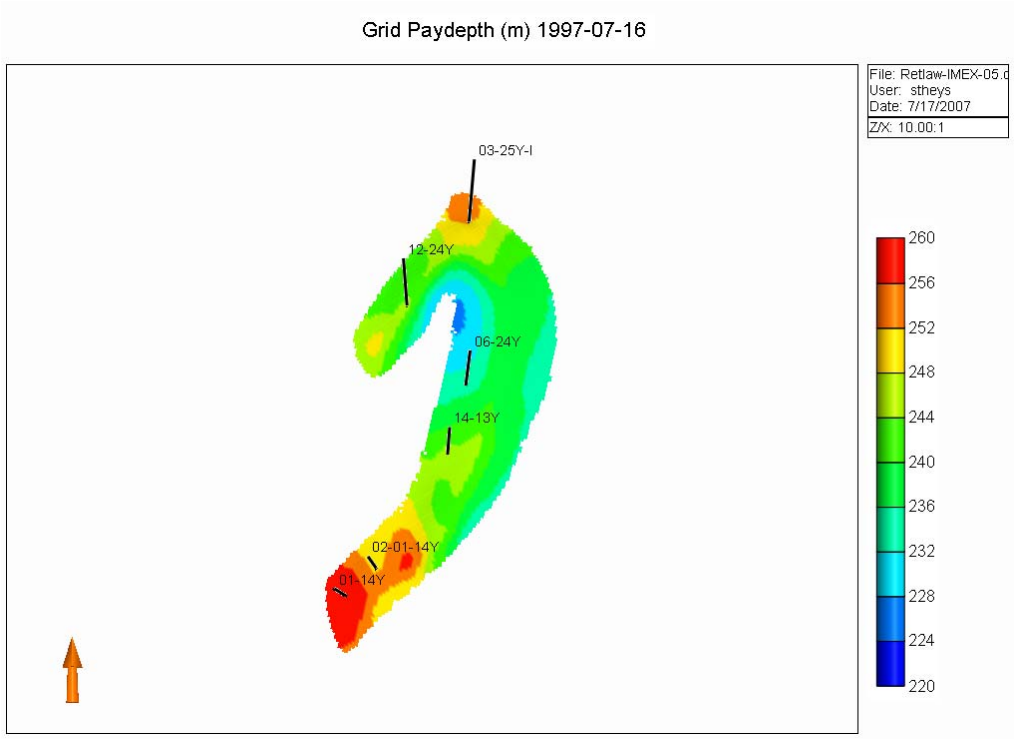

Figure 4.1: Discretized structure top of the Retlaw Mannville Y pool used in numerical simulations.

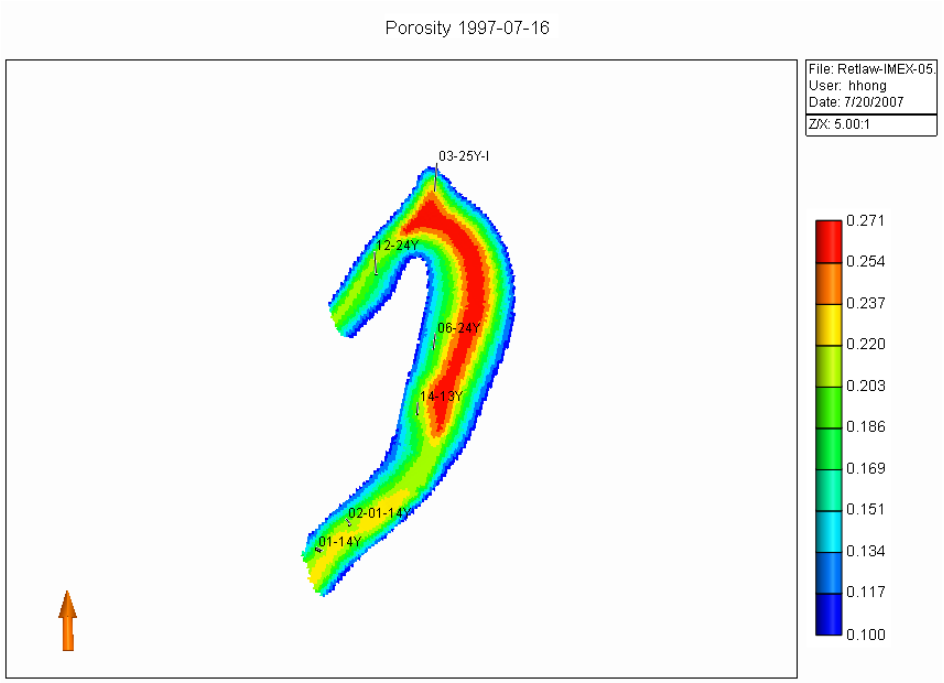

Figure 4.2: Discretized porosity distribution of the Retlaw Mannville Y pool used in numerical simulations.

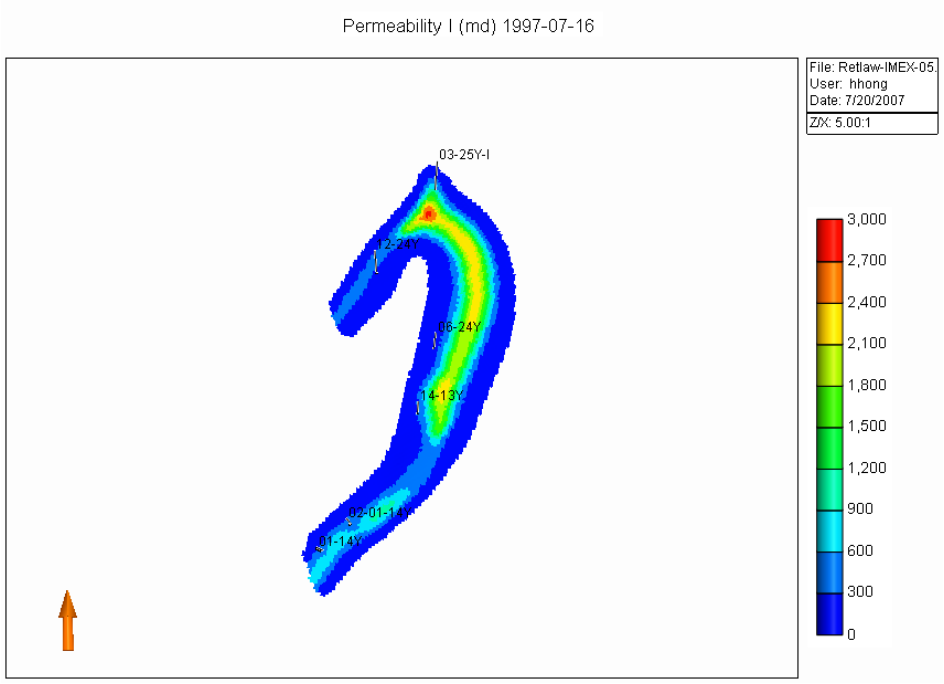

Figure 4.3: Discretized permeability distribution of the Retlaw Mannville Y pool used in numerical simulations.

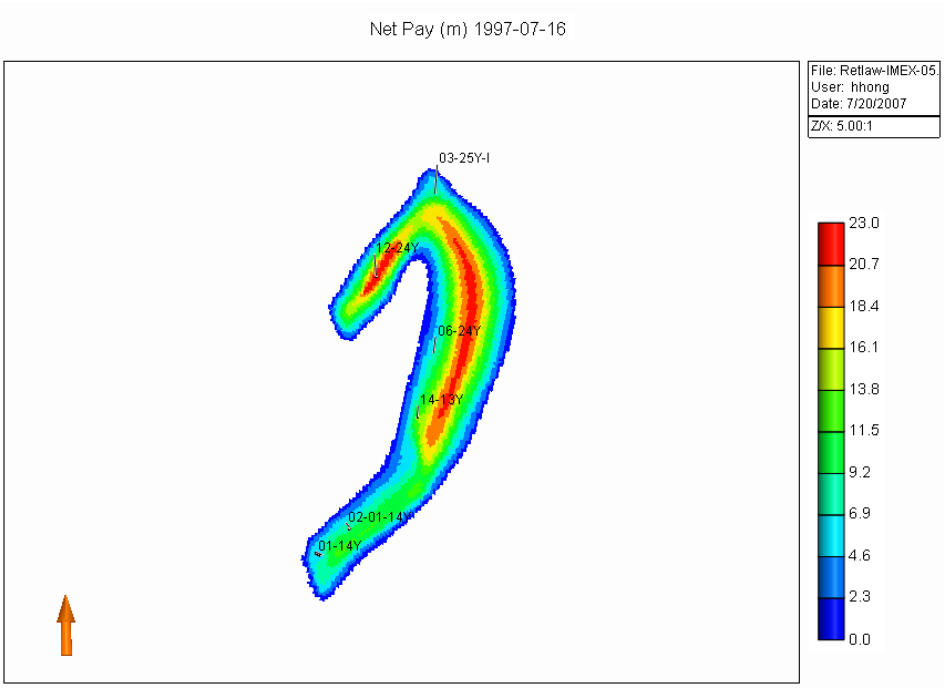

Figure 4.4: Discretized thickness distribution of the Retlaw Mannville Y pool used in numerical simulations.

No experimental relative permeability data were available. Instead, conventional Corey-type relative permeability functions (Craft and Hawkins, 1959) were used with parameters presented in Table 4.1.

Table 4.1: Relative permeability characteristics used in numerical simulations of production from, and injection into Retlaw Mannville Y pool.

Parameter	Value
Irreducible water saturation: S_{wirr}	0.15
Residual Oil Saturation to water: S_{orw}	0.28
Residual Oil Saturation to gas: S_{org}	0.20
Critical Gas Saturation: S_{gc}	0.05
End-point value of relative permeability of oil: k_{ro}^0	0.80
End-point value of relative permeability of water : k_{rw}^0	0.50

The historical pressure data indicate an initial pressure of approximately 11,790 kPa[3] (estimated at the datum depth of 256.3 m subsea, at the gas-oil contact). Therefore the reservoir oil is assumed saturated at the time of the discovery, with a bubble point pressure of 11,790 kPa at the gas-oil contact. In the absence of experimental information, the Standing correlation (Craft and Hawkins, 1959) was used to generate the necessary PVT properties for reservoir oil. Table 4.2 below gives the hydrocarbon PVT properties that were used in the simulation.

Table 4.2 – PVT properties at bubble point pressure of the oil and gas in the Retlaw Mannville Y pool.

Parameter	Unit (metric)	Value
API Gravity	-	23.8
Gas Gravity	-	0.76
Reservoir Temperature	°C	40
Bubble Point (P_b) Pressure	kPa	11,790
Solution Gas Oil Ratio (R_s) @ P_b	Sm^3/Sm^3	58
Formation Volume Factor (B_o) @ P_b	m^3/Sm^3	1.15
Viscosity μ_o @ P_b	mPa·s	3.7

The model was then initialized. Table 4.3 summarizes the fluid in-place volumes.

The historical gas and oil production rates were used as constraints for the gas and oil producing wells respectively. The wells were set to produce at the specified rates, unless bottomhole flowing pressure dropped below a minimum value of 200 kPa, at which time the wells would produce at a constant bottomhole flowing pressure. Regarding the completion information, a skin factor of –3 was incorporated for all the producing wells.

[3] The initial pressure of 11,790 kPa reported by the ERCB for the Retlaw Mannville Y pool is taken at a datum elevation of 245 m SS in 1974.

Table 4.3: Calculated original oil and gas in place in the Retlaw Mannville Y pool (Black Oil Model & original geological interpretation).

Parameter	Units	Entire Field
Total pore volume	m^3	6.99×10^6
HC pore volume	m^3	4.69×10^6
OOIP	Sm^3	0.11×10^6
OGIP (free)	Sm^3	0.861×10^9
OGIP (solution)	Sm^3	0.01×10^9
OGIP (Total)	Sm^3	0.871×10^9

4.1.2 History Matching

A history match was deemed acceptable when the following conditions were simultaneously met: (i) the wells produced the designated primary production values, (ii) the reservoir pressure was matched, and (iii) the gas production of the oil producing wells was reasonably matched. This simulation did not include the period since 2004, when acid gas injection is occurring.

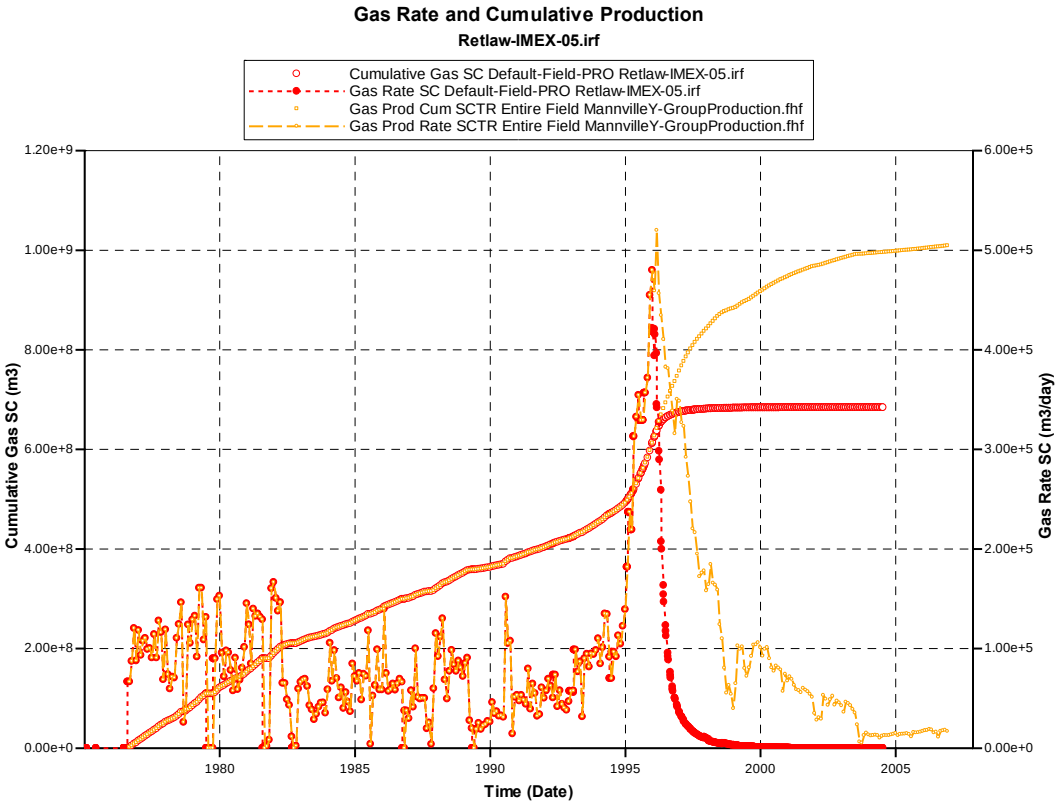

Figure 4.5: Comparison between the historical production data and simulation of the Retlaw Mannville Y pool using the initial mapping of the reservoir.

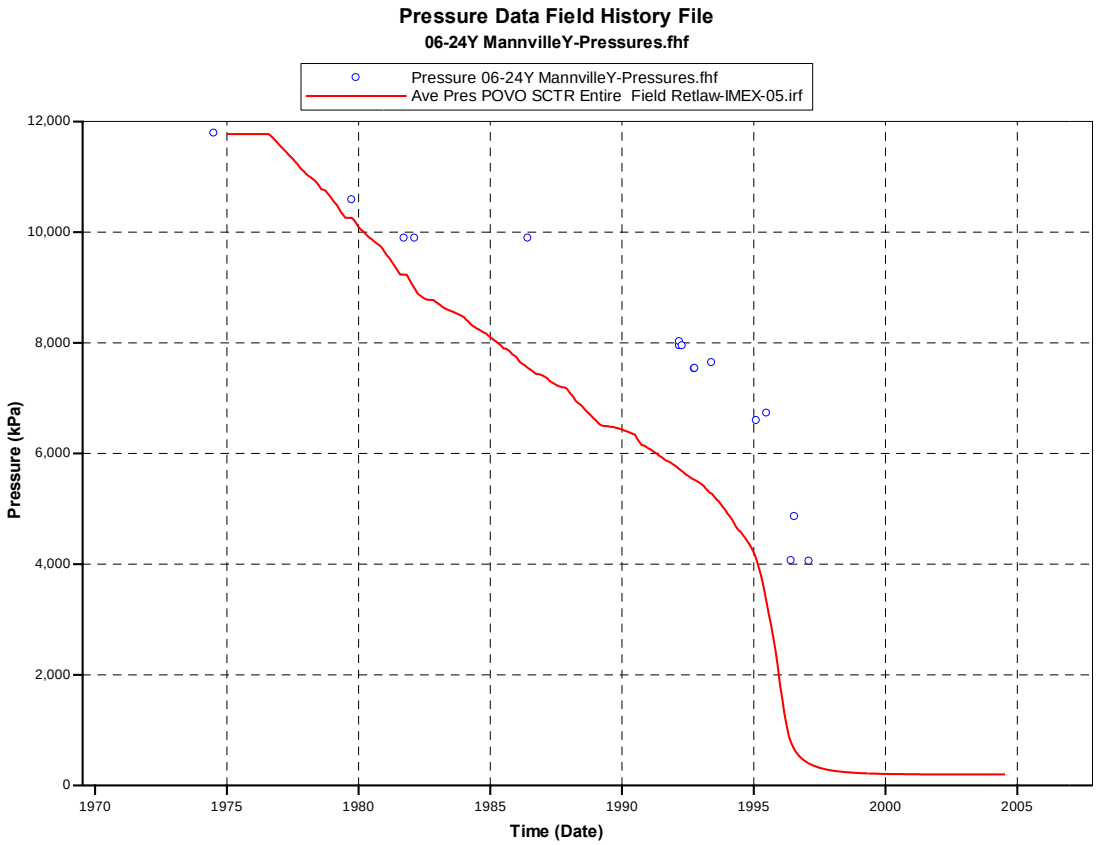

Figure 4.6: Comparison between the historical pressure data and simulation of the Retlaw Mannville Y pool using the initial mapping of the reservoir.

As expected, the results shown in Figures 4.5 and 4.6 indicate that the model cannot honor the historical production rates and pressures. After 1996, the simulated production fails to match the historical data. Cumulative gas production in the model sums to only 0.684×10^9 Sm^3, which is 68% of the historical cumulative gas produced prior to acid gas injection. In the meantime, the model, while producing significantly less gas, shows pressures that are 2,000 kPa less than the historical readings (see Figure 4.6). These combined results confirm that the mapped size of the Retlaw Mannville Y reservoir is too small to contain the entire amount of hydrocarbons already produced until 2004.

4.2 Black-oil Model Simulation using the Revised Geology

As the maps from the geological interpretation in Chapter 2 cannot contain the cumulative gas produced up to 2004, the new net pay maps provided by the ERCB for the oil and gas legs of the reservoir (Figures 3.9 and 3.10) were merged into one isopach map, digitized and incorporated in the black oil model CMG-IMEX^{TM}, (CMG, 2006a) (see Figures 4.9 to 4.13). The combining of the two oil and gas legs required additional geological interpretation as to how the two reservoir legs tied together. In particular, Figure 4.7 shows a saddle shape of the structure in the southwest of the pool, where the oil leg lays (note that the vertical direction is exaggerated by a factor of 40).

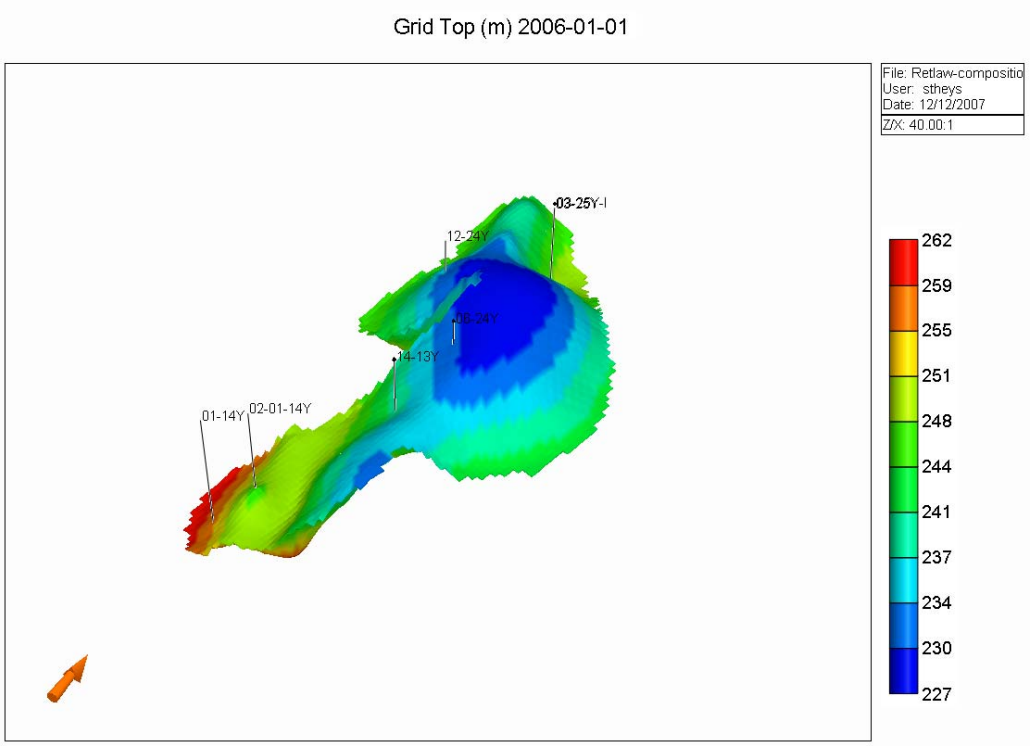

Figure 4.7: Discretized structure top of the updated Retlaw Mannville Y pool.

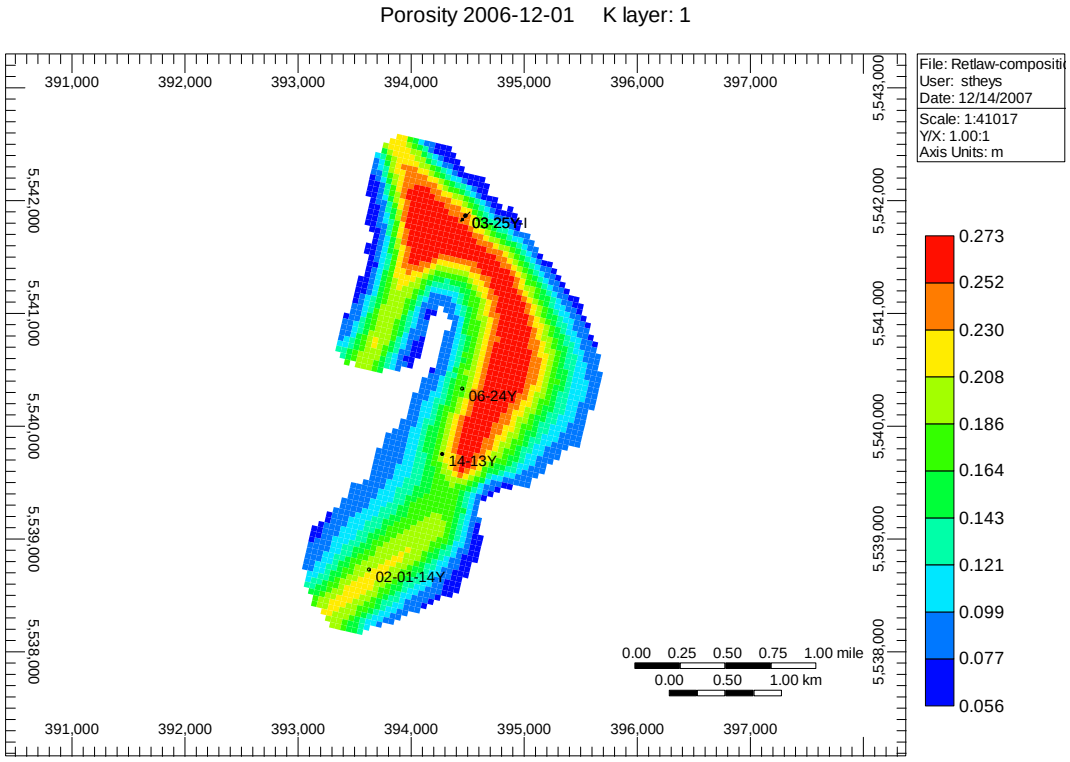

Figure 4.8: Discretized porosity distribution of the updated Retlaw Mannville Y pool.

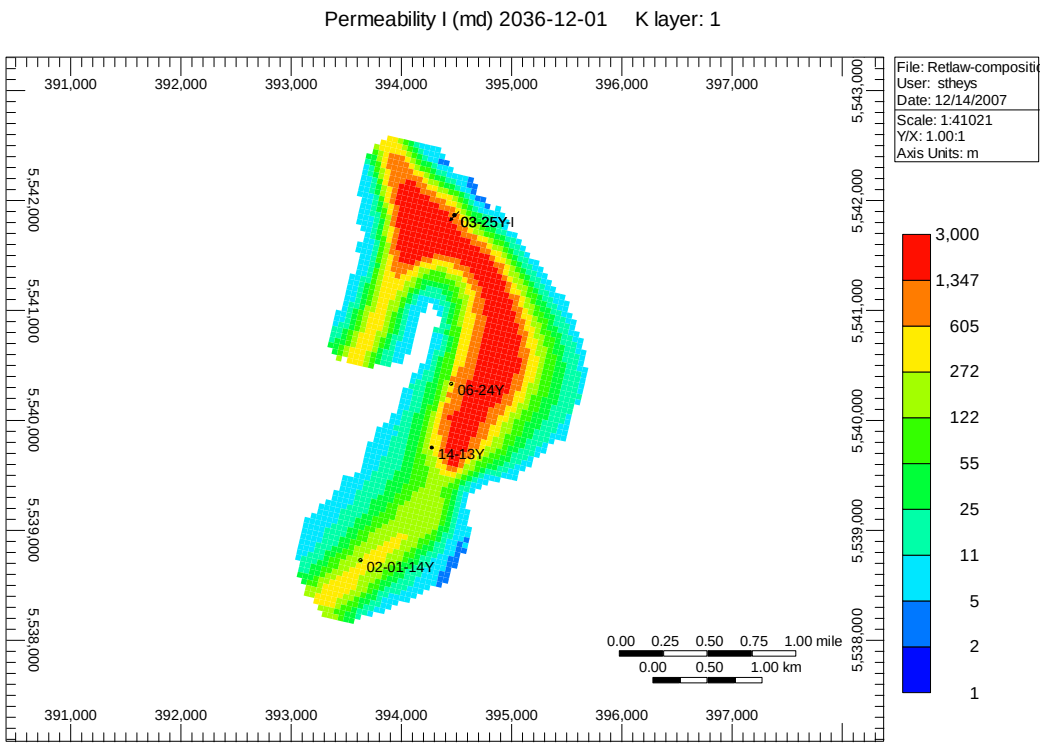

Figure 4.9: Discretized permeability distribution of the updated Retlaw Mannville Y pool.

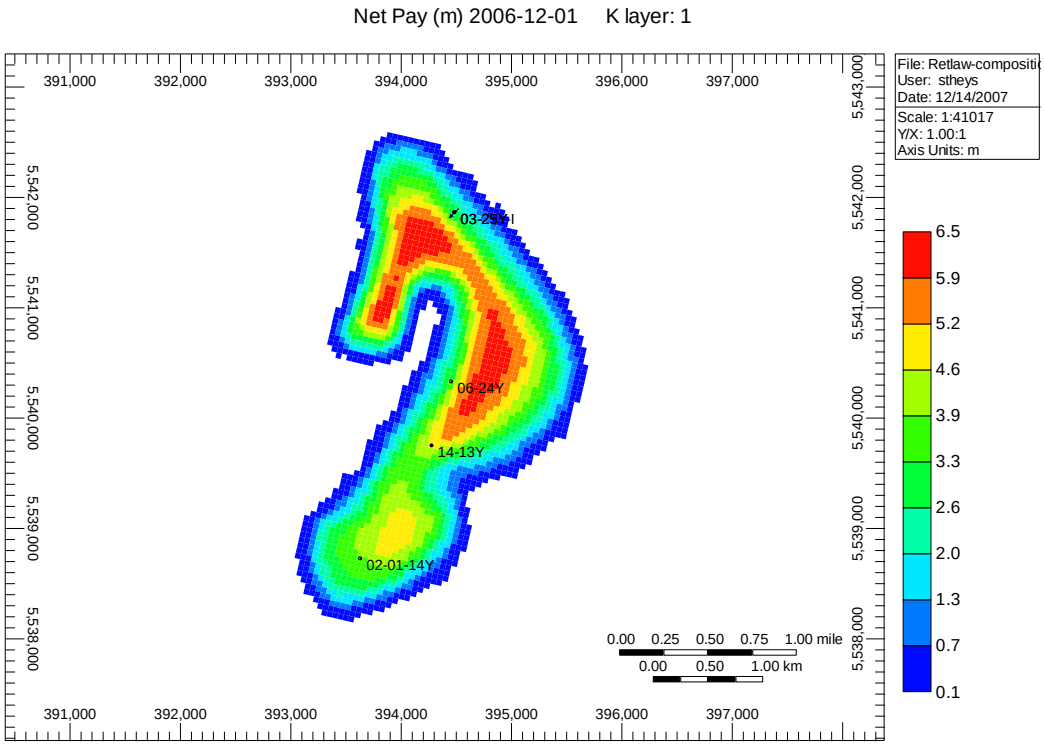

Figure 4.10: Discretized thickness distribution of the updated Retlaw Mannville Y pool.

Since no saturation maps were generated for this project, the OOIP, OGIP and OWIP are calculated at initial equilibrium of the model, after setting a gas-oil-contact (GOC) and water-oil-contact (WOC). Depending on the settings of WOC and GOC and considering that the saddle shape creates a structural low, the OOIP and OWIP may be much larger than originally estimated. Relationship between permeability and porosity follow the same relationship as that presented in Figure 2.24. Relative permeability parameters remain unchanged from the first simulation runs (See Table 4.1). The reservoir is considered saturated at time of discovery and PVT properties are listed in Table 4.2. The pool history prior to acid gas injection was considered like in the first simulations, and well production settings were left with a 200 kPa minimum bottomhole flowing pressure and skin factor of -3 on the producing wells.

4.2.1 Fluid Regions

Well 03-25 has produced 1/6th of the total oil produced from the Retlaw Mannville Y pool. It is also the biggest producer of water. At the same time, although it is located in a structural low on the northeastern side of the pool, it is still higher than the 01-14 oil well located in the oil leg in the southern part of the pool. In other words, well 3-25 in the north produces a significant amount of water, while well 01-14 in the south, while lower in the structure, produces mostly oil. To accommodate this behavior, two regions with different fluid contacts were introduced (both regions have the same fluid properties and initial pressure conditions), illustrated in Figure 4.11: region 1 (in blue) and region 2 (in red).

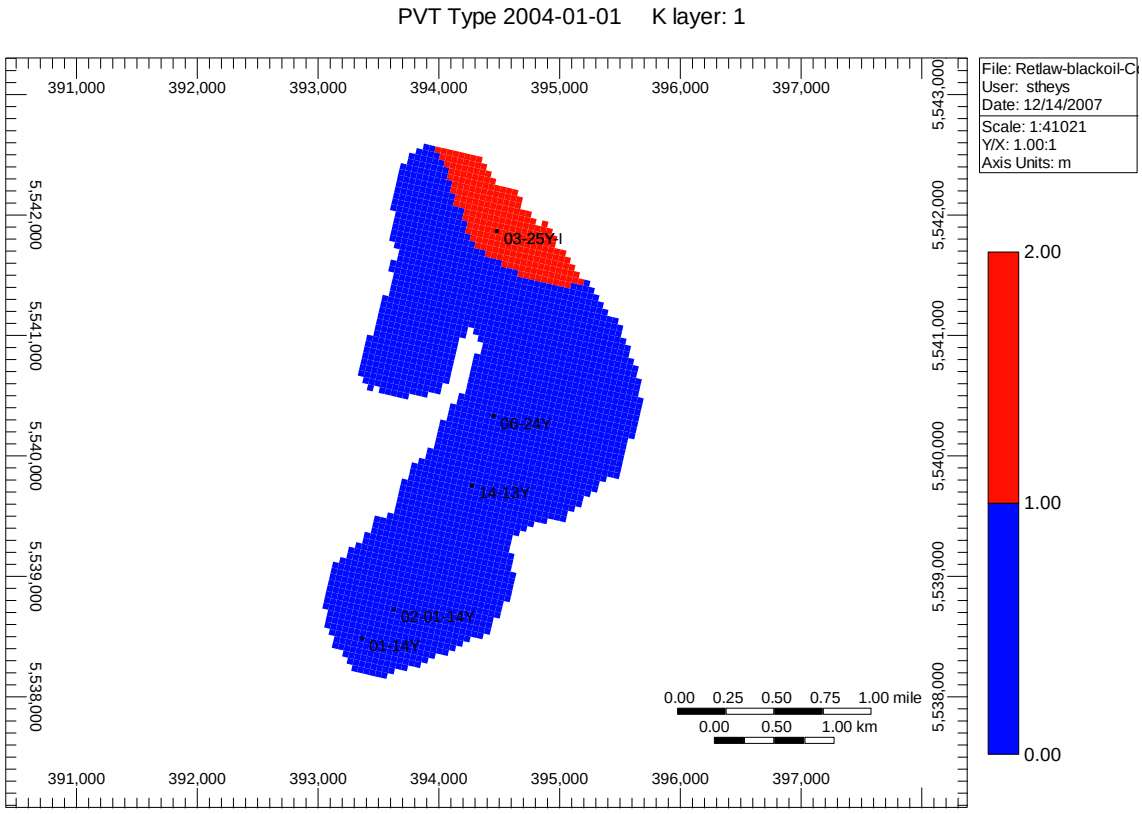

Figure 4.11: PVT regions set in the black oil model to allow control of Water-Oil and Gas-Oil contacts.

Gas-oil and water-oil capillary pressure curves given in Figure 4.12 are used to allow transition from water at the bottom to oil and then to gas on top.

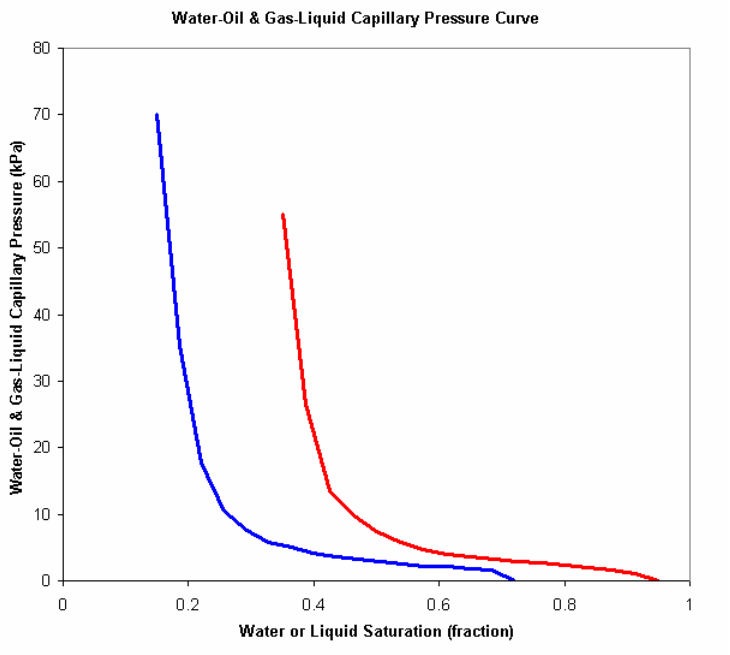

Figure 4.12: Water-Oil (Red) and Gas-Liquid (Blue) capillary pressure curves.

The simulation model was then initialized and the in-place volumes reported (see Table 4.4). The OGIP given in Table 4.4 is in-line with the cumulative volume of gas produced.

Table 4.4: Calculated original oil and gas in place in the Retlaw Mannville Y pool (Black Oil Model & new ERCB maps).

Parameter	Units	Entire Field
Total pore volume	m^3	10.74×10^6
HC pore volume	m^3	8.40×10^6
OOIP	Sm^3	1.68×10^6
OGIP	Sm^3	1.03×10^9
OWIP	Sm^3	2.34×10^6
OGIP (Total)	Sm^3	1.03×10^9

4.2.2 History Matching

A simulation run was conducted for August 2004, before the acid gas injection started. Results shown in Figures 4.13 and 4.14 indicate that the model now exhibits pressures that are in agreement with historical values, indicating a pressure of 470 kPa at the end of the history match period, while at the same time honors the historical production volume. These results confirm that the updated maps of the Retlaw Mannville Y reservoir are now adequate to accommodate the entire amount of hydrocarbons produced until 2004. The estimated recovery factor if 97%.

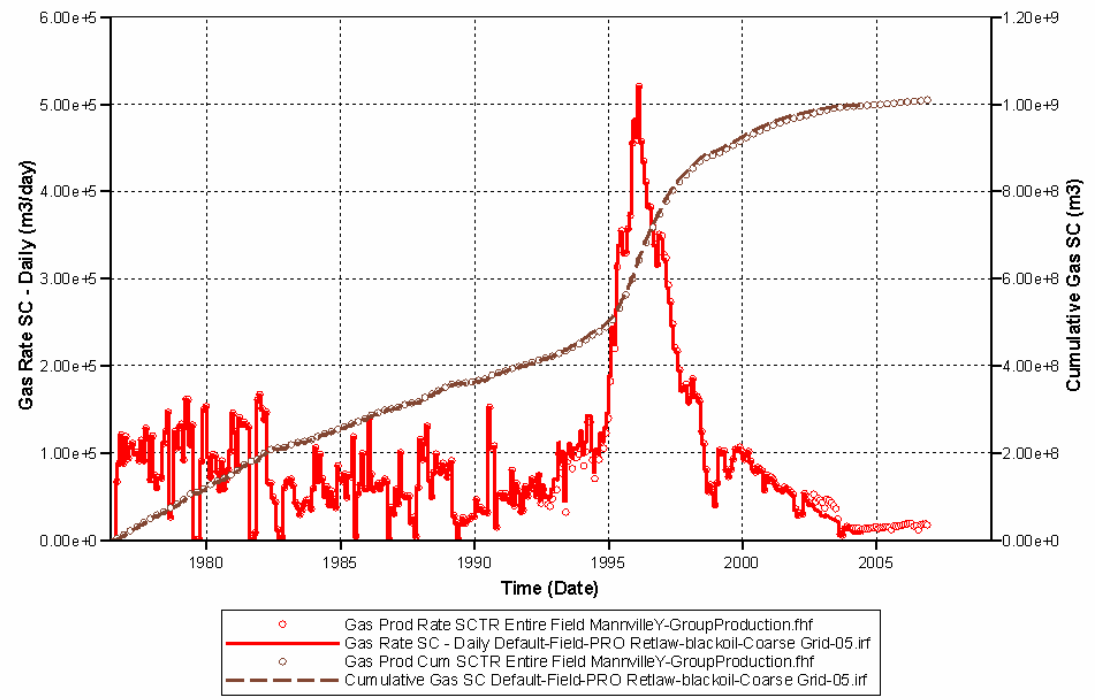

Figure 4.13: Comparison between the historical production data and simulation of the Retlaw Mannville Y pool using the updated mapping.

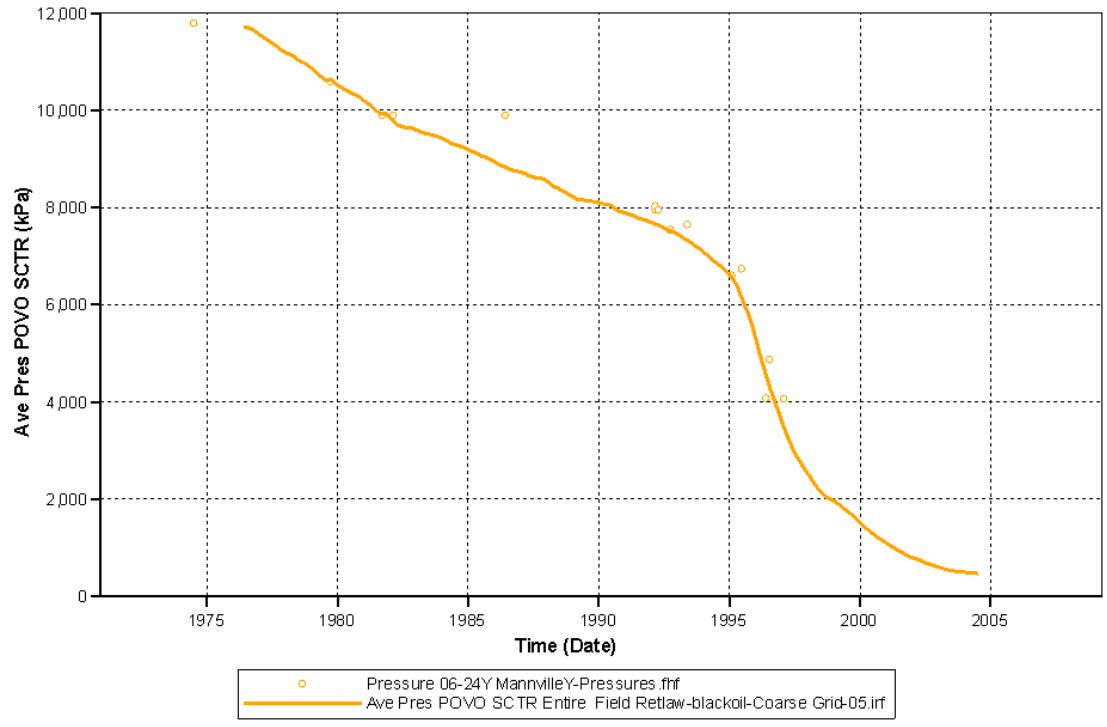

Figure 4.14: Comparison between the historical pressure data and simulation of the Retlaw Mannville Y pool using the updated mapping.

4.3 Compositional Model Simulation using Revised Geology

In the third phase, the simulation study is revised by accounting for the composition of the fluids in place and of the injected gas using CMG-GEM^{TM} compositional reservoir simulator (CMG, 2006b). The objective of this phase is to study the effect of acid gas injection within the Retlaw Mannville Y pool. The same reservoir geometry and characteristics were used as in the black-oil simulations (Section 4.2). The characterization of the components and fluids composition are discussed first and original fluids in place are reported. The results of the simulation study are presented subsequently.

4.3.1 Fluid characterization

Five components, H_2S, CO_2, CH_4, C_{2-6} and C_{7+}, are considered in this compositional model. Default properties of H_2S, CO_2 and CH_4 in GEM are used. Pseudo-component of C_{2-6} is grouped from C_2 to C_6 components based on the composition in the gas analysis and the assumption of ideal gas mixing rules. Pseudo-component of C_{7+} is a heavy component in the oil phase. Gas gravity of 0.76 was used for estimating the other physical properties. Critical temperature, pressure and volume were estimated by Twu's correlation (Twu, 1984), and the acentric factor was estimated by using Lee-Kesler's correlation (Lee & Kesler, 1975), as listed in Table 4.5.

Table 4.5: Parameters of Pseudo-Components used in compositional model simulations.

Parameter	C_{2-6}	C_{7+}
MW	35.5	235
AC	0.0846	0.7712
PC, atm	42.58	19.97
TC, K	266.06	798.76
VC, l/mol	0.1802	0.98

The fluid compositions listed in Table 4.6 are assumed in the gas cap and oil zone. The composition of gas is taken from one of the gas analysis reports (publicly available). The oil composition is not available. Instead, the oil phase composition has been estimated using Henry's law and adjusted to match the reported OOIP, R_s and B_o. Despite the uncertainty in the oil properties, this difference does not affect the result significantly because the oil only occupies only a small region of the whole reservoir. The pseudo-components listed in Table 4.5 and compositions listed in Table 4.6 resulted in reasonable fluid properties at initial conditions and initial oil in place as listed in Table 4.7, which are in general agreement with the properties in the black-oil model.

An average acid gas composition of 96% of CO_2 and 1.7% of H_2S is considered as the injection gas. There are no recorded pressures at the start of acid gas injection in December 2003 and the pressure of the reservoir is currently estimated at 2550 kPa. In all cases, and considering the reservoir temperature of 40 ^oC, both CO_2 and H_2S are in a gaseous state at all times.

Table 4.6: Composition of gaseous and oil phases at initial condition.

Component	Gas Zone	Oil Zone
H_2S	0.0006	0.001
CO_2	0.104	0.09
CH_4	0.7462	0.2302
C_{2-6}	0.1491	0.0966
C_{7+}	0.0001	0.5822

Table 4.7: Fluid Properties at initial conditions of 11790 kPa and 40ºC (bubble point pressure).

Parameter	Compositional Model	Black-Oil Model
B_o, rm^3/sm^3	1.13	1.15
B_g, rm^3/sm^3	$7.37e^{-3}$	$6.87e^{-3}$
R_s, sm^3/sm^3	62	58
Viscosity of oil @ P_b, cP	3.9	3.7

4.3.2 History Matching

Figures 4.15 and 4.16 show, respectively, the history-matched and forecasted gas production and pressures in the Retlaw Mannville Y pool. Since the acid gas content in the 14-13 and 06-24 producing wells has been monitored in the field, matching of the gas composition in these wells is of particular interest. Compositional data at the producing wells show that breakthrough times of CO_2 in the producers are earlier than that of H_2S. Breakthrough of CO_2 for wells 06-24 and 14-13 are February and April 2005, respectively. While the breakthrough of H_2S occurs in April 2005 for well 06-24, it is not clearly defined until July 2005 for well 14-13. The Long-Coulee compositional study (Pooladi-Darvish et al., 2008) showed that the preferential solubility of the H_2S is the formation brine together with its low concentration in the injected gas lead to the H_2S component being stripped off at the leading edge of the displacing gas. In the absence of mechanisms leading to significant mixing in the gaseous phase, this leads to delayed breakthrough of H_2S.

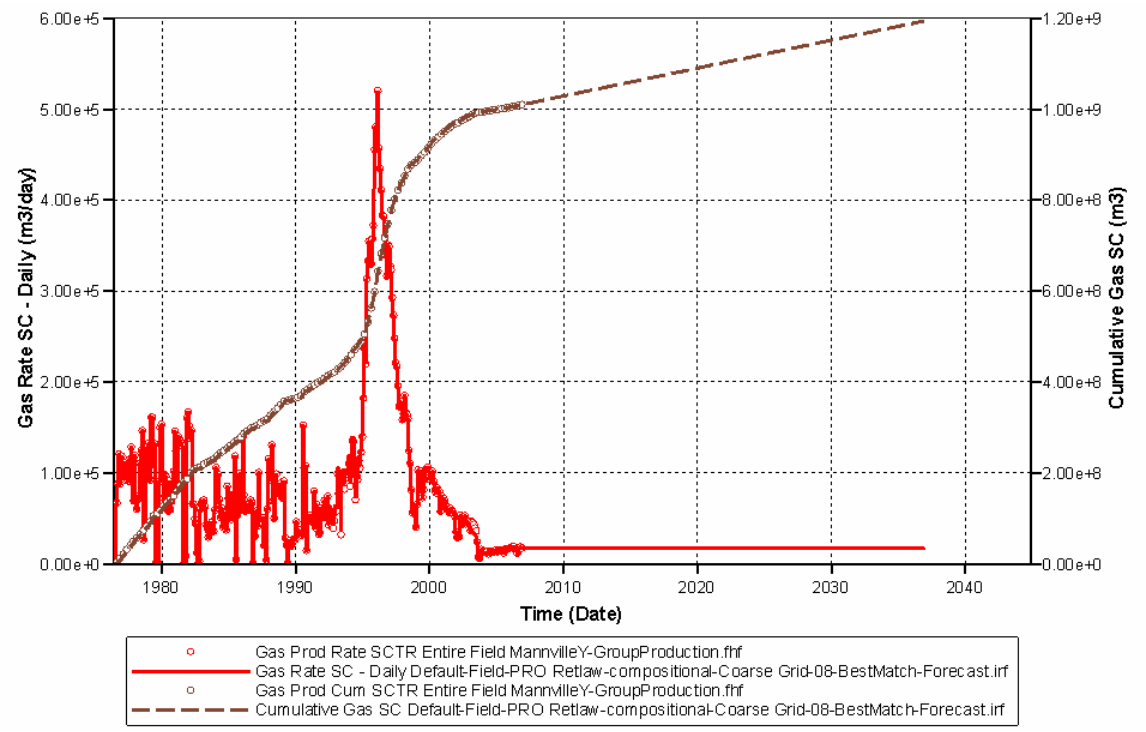

Figure 4.15: History matching and forecast of the Retlaw Mannville Y pool gas production assuming current operations (December 2006) are maintained.

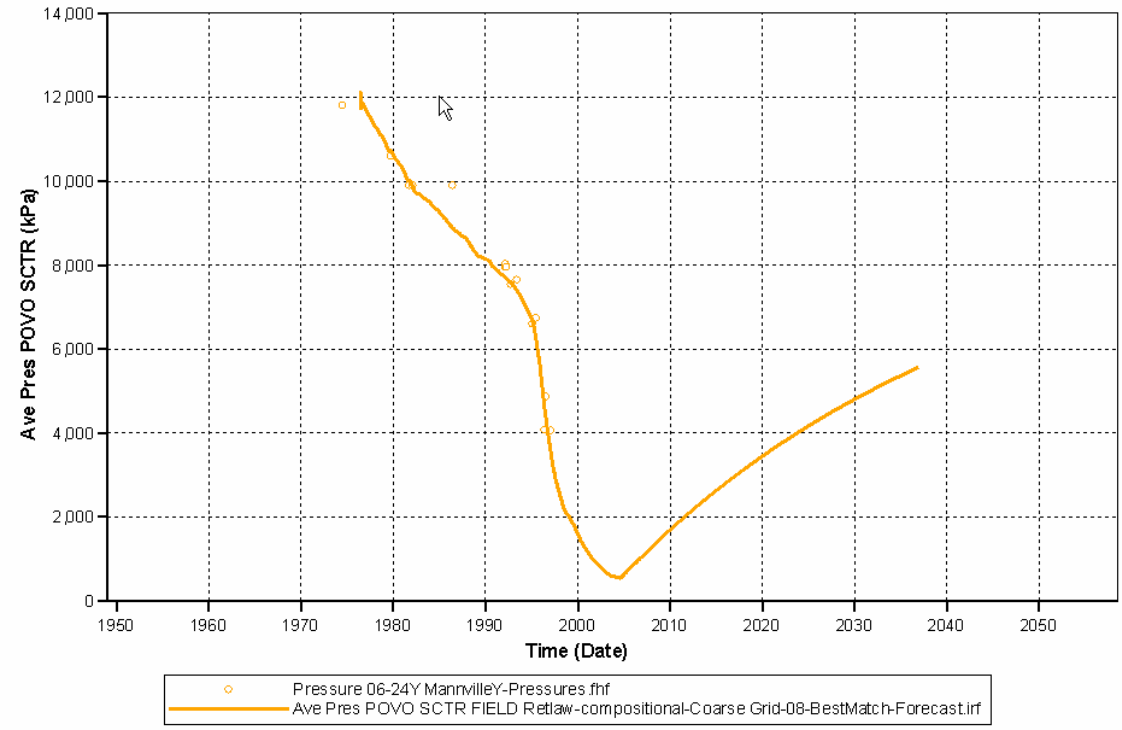

Figure 4.16: History matching and forecast of the Retlaw Mannville Y pool pressure assuming current operations (December 2006) are maintained.

Observations with respect to breakthrough of the acid gas in the producing wells in the model as compared with the historical observations are summarized below:

- Figures 4.17 to 4.20 show the history match of CO_2 and H_2S breakthroughs in wells 06-24 and 14-13. Simulated breakthroughs at the 14-13 and 06-24 wells occur somewhat later than historically observed. The CO_2 breakthrough time simulated for well 14-13 occurs in August 2005 instead of April 2005. The CO_2 breakthrough time simulated for well 06-24 occurs in June 2005 instead of February 2005. This discrepancy is believed to be due to the inaccuracy in geological interpretation made between the injector and the producing wells. Lack of well data between the injector and the producer does not allow accurate capturing of the heterogeneity that affects fluid displacement. In particular, it is expected that the level of heterogeneity in the reservoir is more than that captured with the average properties (porosity and permeability) in the model. A model that is more homogeneous as compared with the actual reservoir leads to delayed breakthrough;
- As of December 2006, an equivalent of 6% of the OGIP has been injected into the Retlaw Mannville Y pool: as the gas composition in both 14-13 and 06-24 indicate, a large portion of the gas cap is contaminated by the injected gas. This is because the reservoir pressure at the time of gas injection is significantly lower than the initial pressure, allowing the injected gas to take up a large reservoir volume. This confirms the findings summarized in the previous report (Pooladi-Darvish et al., 2008);
- The breakthrough of CO_2 occurred before that of H_2S, as a result of low H_2S concentration in the injected gas and its preferential solubility, as seen in the observed gas concentrations at producing wells. As shown in the next section, the simulation results indicate a difference between the spread areas of the CO_2 and H_2S. However, due to numerical dispersion the difference in breakthrough times predicted in the simulator is not as large as that seen in the measurements.

4.3.3 Forecast

The following section summarizes the forecasts of different scenarios applied to the Retlaw Mannville Y pool:

1) forecast of gas production based on current operating conditions;
2) forecast of gas production without acid gas injection;
3) forecast of pressure increase if all producers are shut-in.

Forecast of gas production based on current operating conditions

Figures 4.15 to 4.22 present the history matching and 20 years forecast of gas production, reservoir pressure, produced gas CO_2 and H_2S concentrations assuming that all current operating conditions are maintained; specifically the only producing well (14-13) continues producing at a constant rate of 18,000 m^3/d. Furthermore, a constant acid gas injection rate of 66,000 m^3/d is used. Therefore, the cumulative acid gas injected over 20 years is estimated to be 0.47×10^9 Sm^3. The following comments can be made based on the results presented in Figures 4.15 to 4.22:

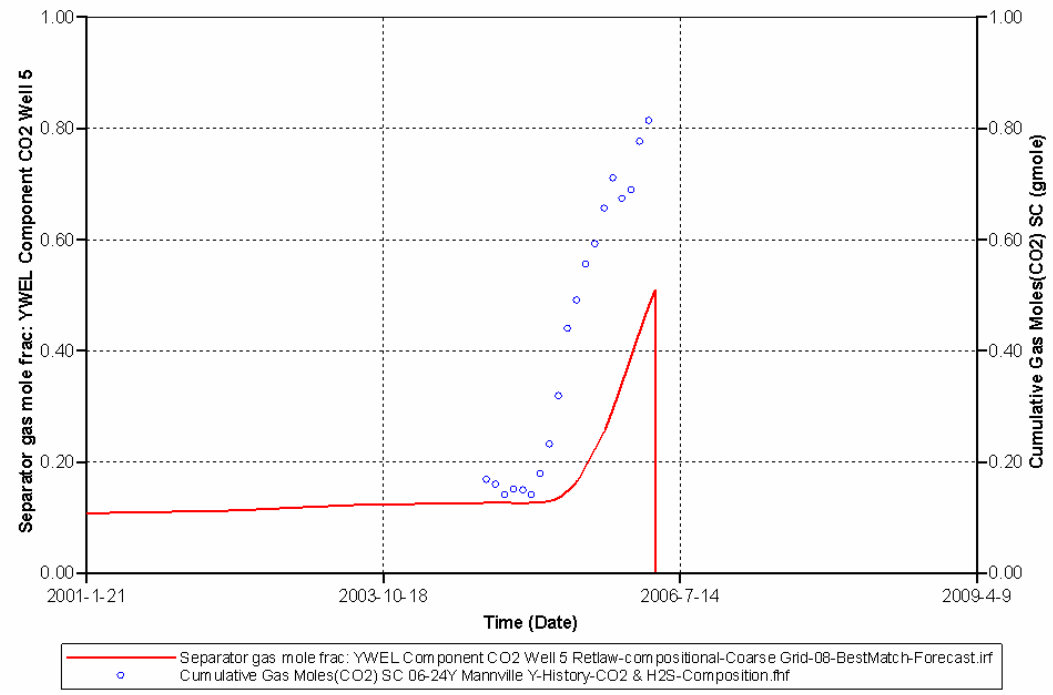

Figure 4.17: History matching and forecast of CO_2 concentration in produced gas in well 06-24 of the Retlaw Mannville Y pool assuming current operations (December 2006 – the well is shut-in) are maintained – Verification of history matching.

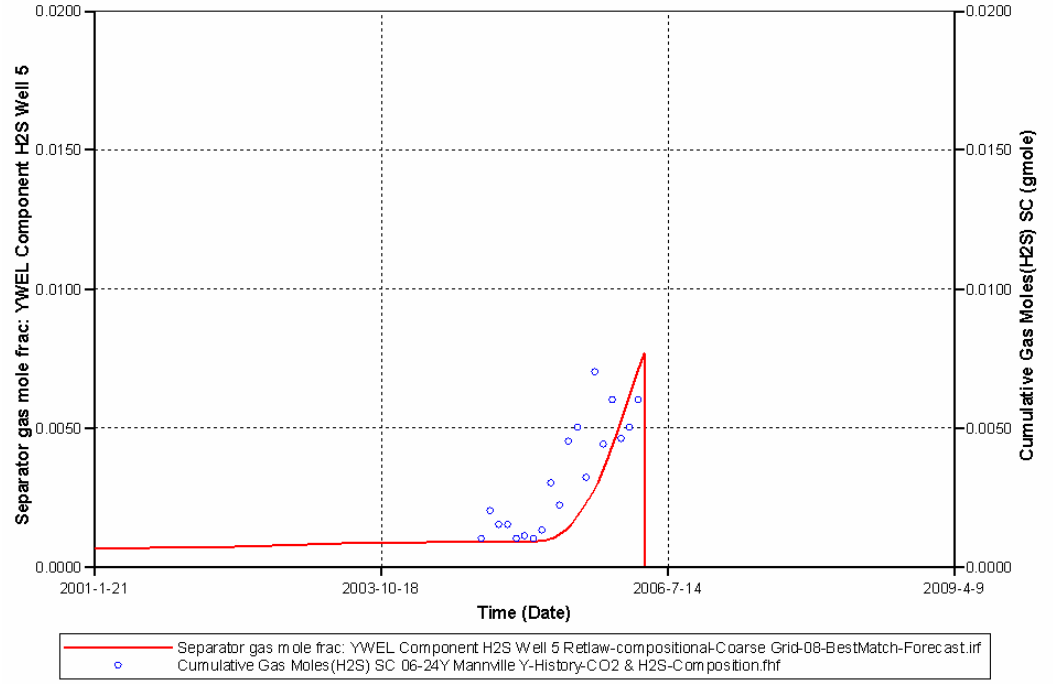

Figure 4.18: History matching and forecast of H_2S concentration in the produced gas in well 06-24 of the Retlaw Mannville Y pool assuming current operations (December 2006 – the well is shut-in) are maintained – Verification of history matching.

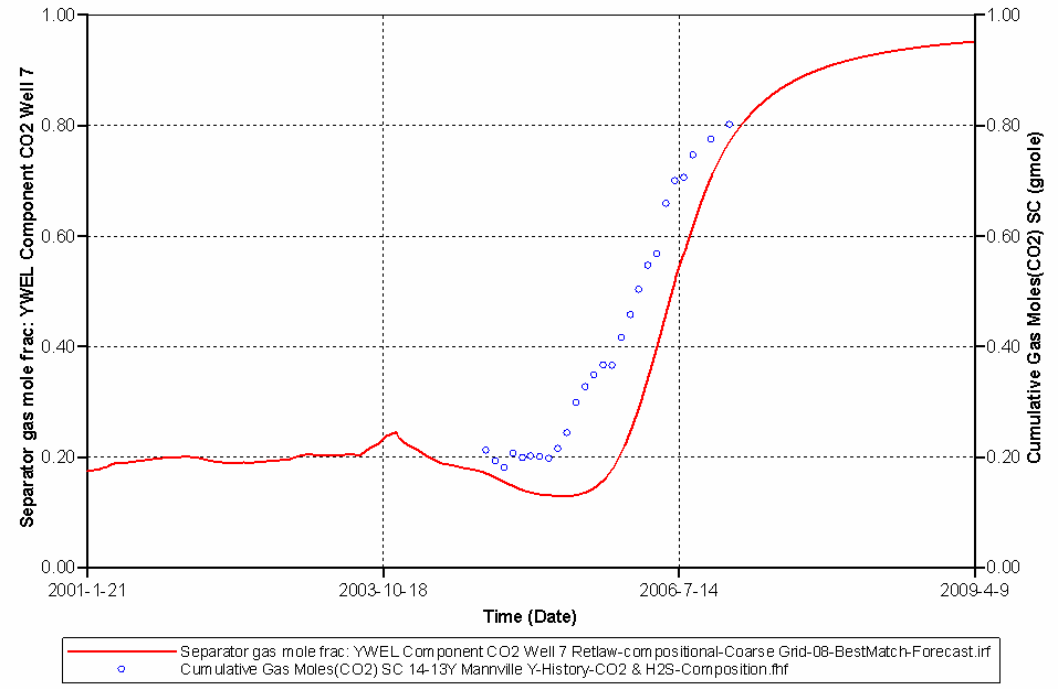

Figure 4.19: History matching and forecast of CO_2 concentration in the produced gas in well 14-13 of the Retlaw Mannville Y pool assuming current operations (December 2006 – the well is shut-in) are maintained.

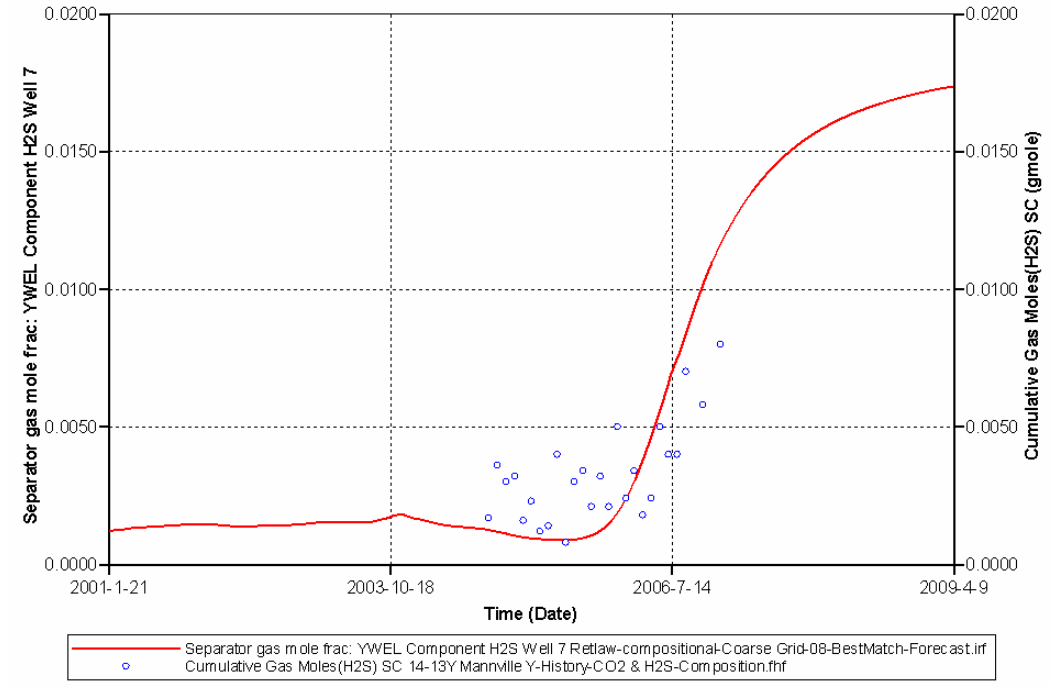

Figure 4.20: History matching and forecast of H_2S concentration in the produced gas in well 14-13 of the Retlaw Mannville Y pool assuming current operations (December 2006 – the well is shut-in) are maintained.

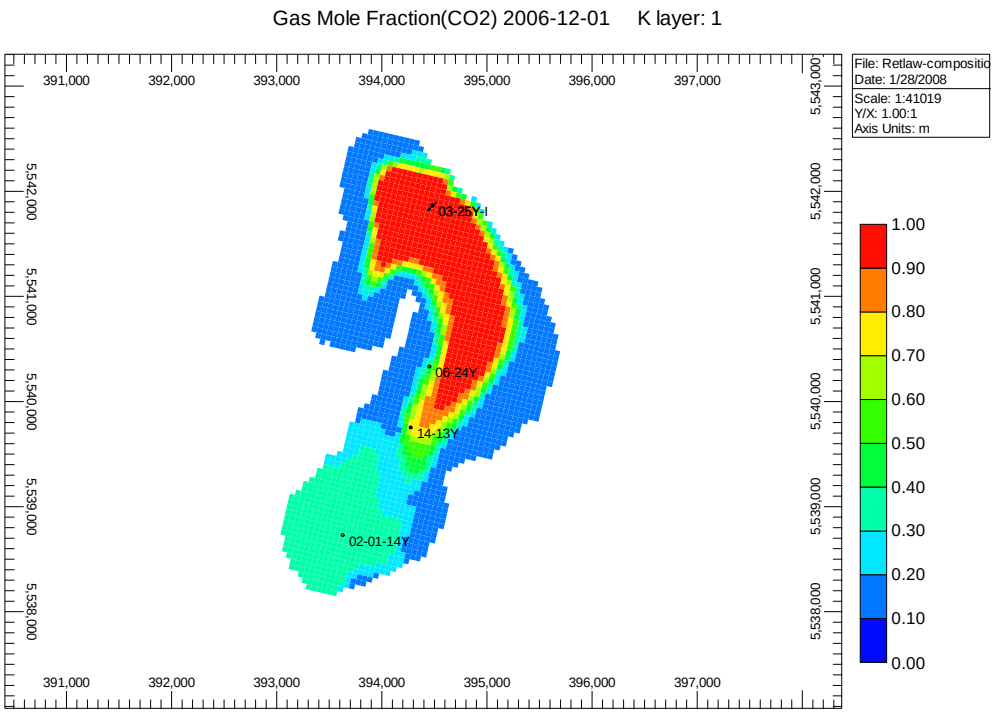

Figure 4.21: Simulated distribution of CO_2 in the Retlaw Mannville Y pool on 1st of December 2006, assuming current operations.

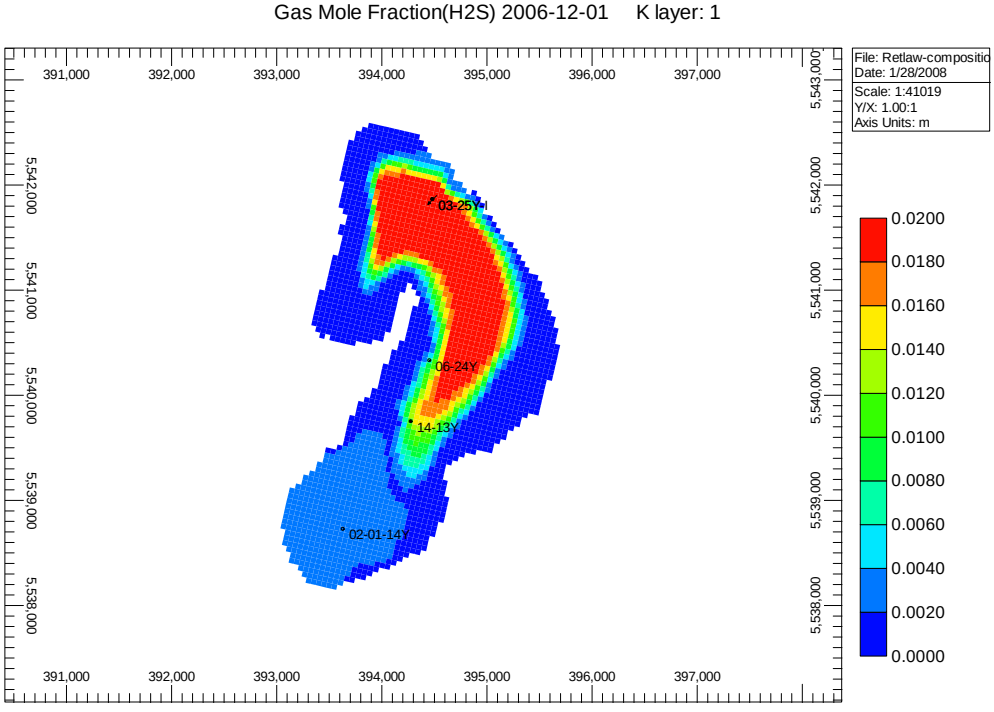

Figure 4.22: Simulated distribution of H_2S in the Retlaw Mannville Y pool on 1st of December 2006, assuming current operations.

- Cumulative gas production will increase to approximately 1.2 $\times 10^9$ Sm^3 (Figure 4.15), that is an additional 0.2 $\times 10^9$ Sm^3 of gas produced. More than 90% of this is the injected acid gas, as the concentration plots in Figure 4.19 and 4.20 show;
- The pressure is calculated to be 1050 kPa in November 2006. Taylor Management estimated the reservoir pressure to be 2550 kPa but no actual measurement of reservoir pressure is available since 1998. Upon continued injection in the model, the pressure increases steadily to 5700 kPa in 2038 (Figure 4.16), almost half of the initial reservoir pressure. This allows for more acid gas injection, under the condition that all producing wells be shut-in to avoid the acid gas to cycle back to surface;
- Figures 4.21 and 4.22 represent the distribution of CO_2 and H_2S respectively, as of December 1st, 2006. These figures show that by this time the acid gas has spread throughout the gas cap leading to breakthrough in wells 06-24 and 14-13. A careful comparison of the two figures also shows that the area over which the CO_2 spread is somewhat larger than that of H_2S. As studies in detail by Bachu et al (2007) and Pooladi-Darvish et al. (2008) show, this is attributed to the preferential solubility of H_2S in the formation water.

Forecast of gas production without acid gas injection

Figures 4.23 and 4.24 present the 20 years forecast of gas production and reservoir pressure, assuming that no acid gas injection has ever occurred in the Retlaw Mannville Y pool. That is, the gas production since December 2003 is still under primary production. The operation of the producing wells however follows the conditions actually dictated since December 2003. As such, the forecast assumes that only well 14-13 is producing. The simulated production and pressure is compared with the measured production and pressure. The following comments can be made:

- The cumulative gas production is 1 $\times 10^9$ Sm^3 and the reservoir pressure will continue dropping from the estimated 470 kPa in August 2004 to 380 kPa in 2038;
- Although the acid gas injection increases the reservoir pressure and could – in that sense – help maintain gas production, this simulation confirms that most of the in-situ gas had been produced by the time well 03-25 was put on injection; the acid gas injected is the main contributor of the gas production since December 2003.

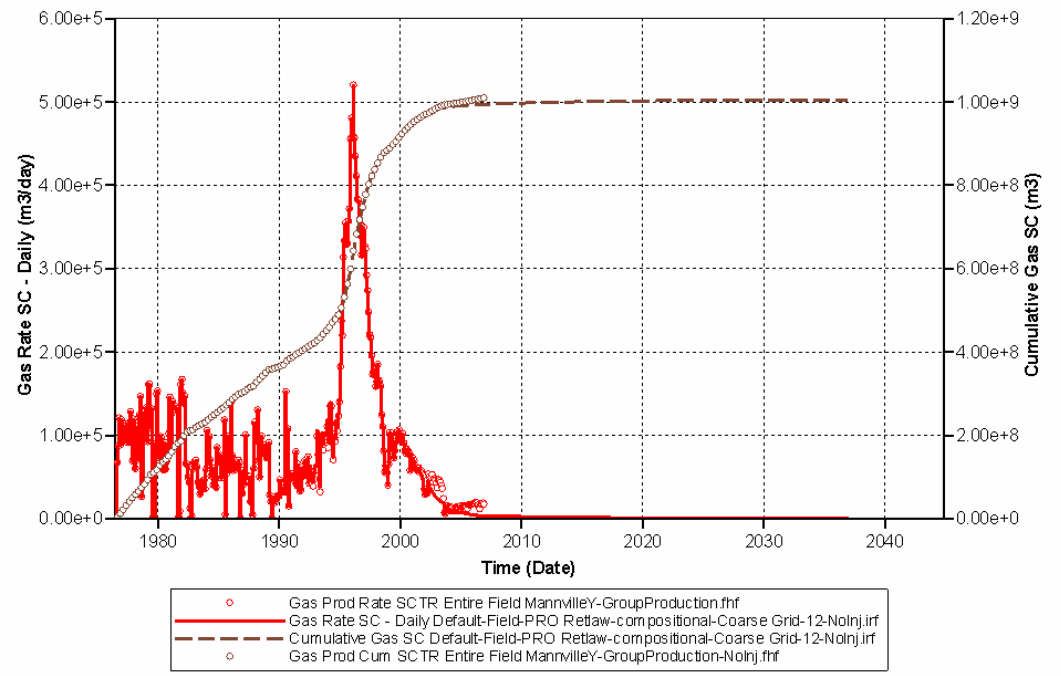

Figure 4.23: Forecast of the Retlaw Mannville Y pool gas production assuming acid gas injection never took place.

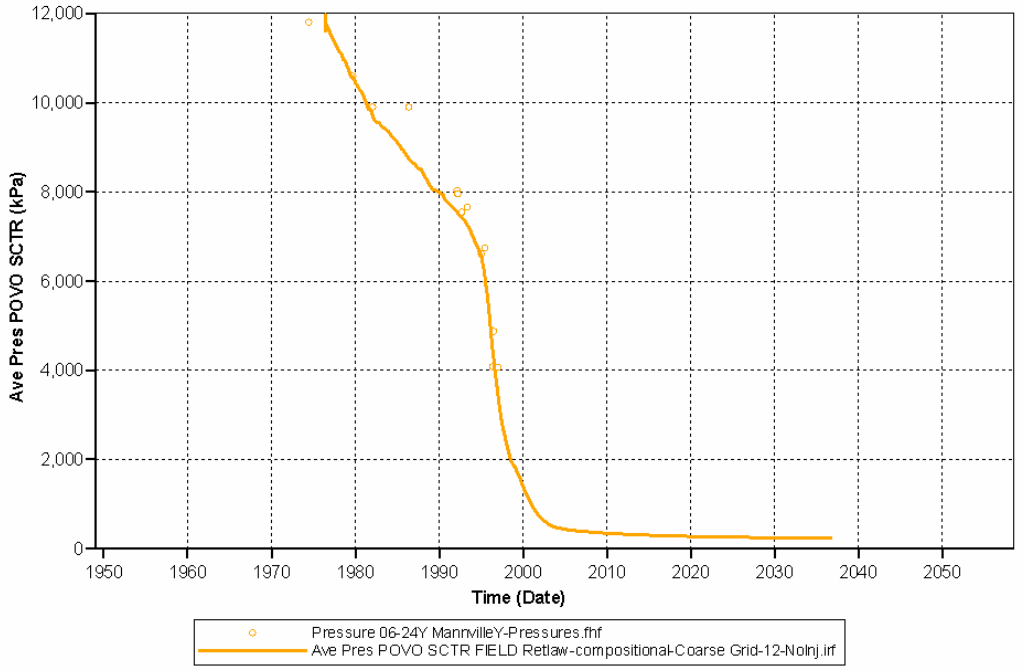

Figure 4.24: Forecast of the Retlaw Mannville Y pool pressure assuming acid gas injection never took place.

Forecast of pressure increase if all producers are shut-in

Figures 4.25 and 4.26 present the 15 years forecast of gas production and reservoir pressure, assuming that all producers are shut-in starting January 2008,i.e., four years after the start of acid gas injection. The following comments can be made:

- The increment in gas production is obviously null, since all producers are shut-in;
- The reservoir pressure increases to 4000 kPa in 2020. Note that the reservoir pressure would be 3800 kPa in 2020 if current operating conditions are maintained (Figure 4.16), which is a small difference.

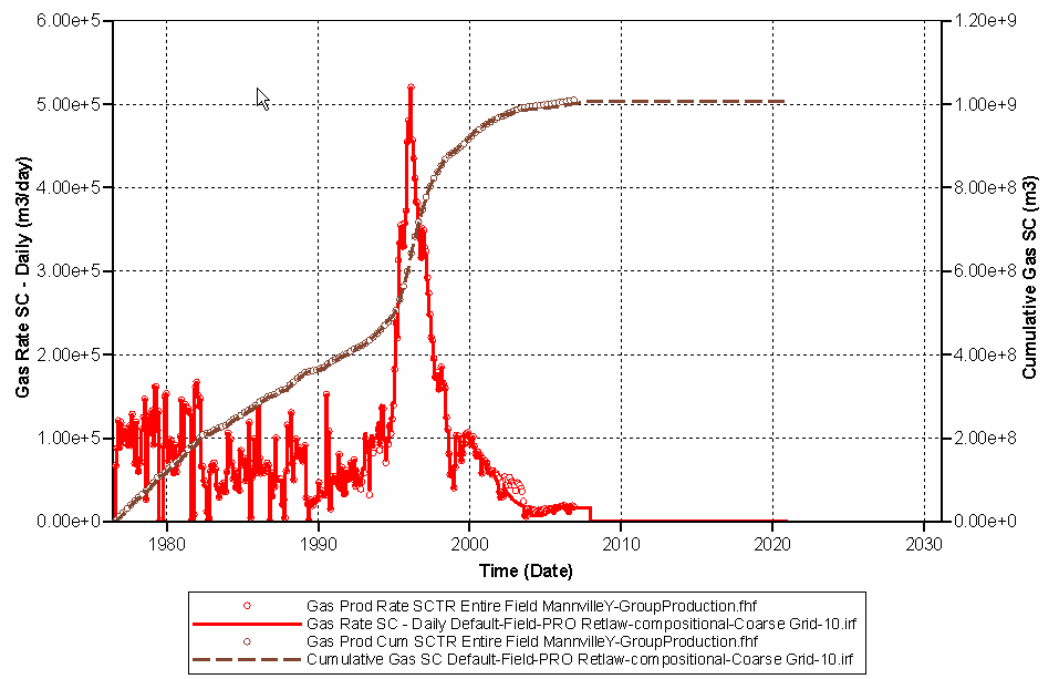

Figure 4.25: Forecast of the Retlaw Mannville Y pool gas production (none after 2008) assuming acid gas injection is maintained but all producing wells are shut-in starting January 2008.

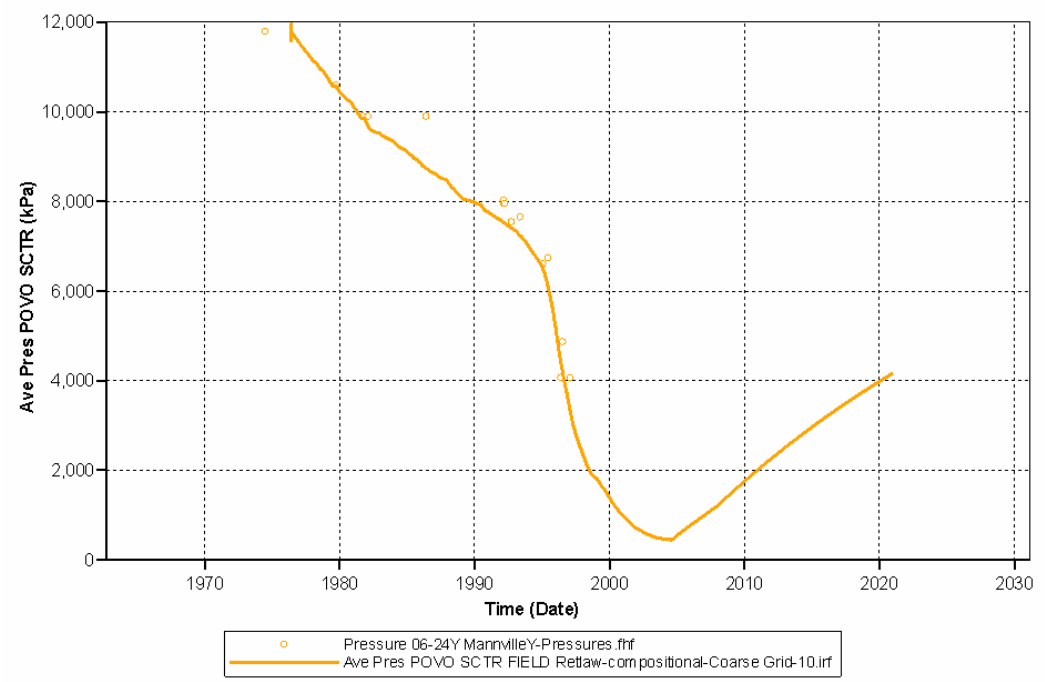

Figure 4.26: Forecast of the Retlaw Mannville Y pool pressure assuming acid gas injection is maintained but all producing wells are shut-in starting January 2008.

4.3.3 Calculation of Gas in Place

Table 4.8 compares the OGIPs provided by the ERCB (calculations based on volumetric calculations) and the OGIPs using the different maps included in the reservoir simulation models.

Table 4.8: Summary of results for estimates of original gas in place (Sm^3).

Source of Estimate	**OGIP**
ERCB original volumetric	1.208×10^9
ERCB updated volumetric	-
Material balance analysis	1.067×10^9
Production decline analysis	1.027×10^9
ERCBB initial mapping – Black Oil simulation	0.975×10^9
2^{nd} Mapping – Black Oil simulation	1.090×10^9
2^{nd} Mapping – Compositional simulation	1.015×10^9

The cumulative gas produced of 1.009×10^9 Sm^3 represents a recovery factor of approximately 92% of the OGIP as estimated using the revised mapping and the black oil model.

5. Summary and Conclusions

Carbon dioxide capture and storage in geological media is emerging as a climate-change mitigation strategy that could contribute significantly to the reduction of anthropogenic CO_2 emissions into the atmosphere in the short-to-medium term. There is already significant technological experience and know-how with analogues of CO_2 geological storage such as natural gas storage, CO_2 enhanced oil recovery and acid gas disposal. In regards to the latter, Canada is a world leader, with close to 50 operations active in Alberta and British Columbia. These operations have been studied and characterized extensively, proving that geological storage of gases such as CO_2 and H_2S is a safe operation if sites are properly selected, characterized and monitored. In a few instances of acid gas disposal in gas and oil reservoirs in Alberta acid gas broke through at producing wells. A detailed study of these sites was undertaken to understand better the behavior of acid gas injected in depleted oil and gas reservoirs that are, nevertheless, still producing. One of the cases of acid gas breakthrough is the Retlaw Mannville Y Pool in southern Alberta operated by Taylor Management Company Inc.

At peak production, Retlaw Manville Y pool comprised four gas-producing and one oil-producing wells. The peak gas and oil production rate were 0.5×10^6 Sm^3/day and 20 Sm^3/day, respectively. The cumulative gas and oil production to date (November 2006) are $\sim1\times10^9$ Sm^3 and 6,610 Sm^3, respectively. As of November 2006, one well continues to produce gas at a rate of 19,000 Sm^3/day. In 2004, when the pool had a cumulative gas production of 0.992×10^9 Sm^3, Taylor Management Company Inc. applied for use of the Retlaw Manville Y pool for acid gas disposal. The company argued that "The recovery from the pool is 85% of the OGIP", which was in total agreement with the 85% recovery factor assigned by ERCB 2002 Reserve Report (based on an estimated original-gas-in-place of 1.167×10^9 Sm^3). It further argued that: "The acid gas will be at least twice the density of the natural gas within the Manville Y Pool" and considering the fact that the planned injector is completed structurally low, "The acid gas should fill from the bottom up and will remain low providing the pressure gradient between the wells is low".

At the start of acid gas injection (August 2004) two gas wells were still producing at an approximate distance of about 1500 and 2100 m from the injection well, respectively. In March 2005, the closest well showed an increase in CO_2 concentration. This increase continued to March 2006, when the well was shut-in because of high CO_2 concentrations (more than 80%). Breakthrough of CO_2 into the second well was observed in May 2005. Acid gas concentration in this well was at 80% as of December 2006. By this time the rate of recycling was about 11% of the injected rate. The objective of this study was to study the acid gas injection and its breakthrough in the producing wells using numerical simulations based on history matching.

Conventional pressure decline curve analysis was used to estimate the remaining recoverable reserve of the two remaining producing wells at the time of acid gas injection, with what they actually produced prior to them being shut-in. Decline analysis on gas production rate from the field suggests an expected ultimate recovery (EUR) of 1.027×10^9 Sm^3. The actual volume of hydrocarbon gas recovery by the time that the wells were shut-in was estimated by adding the cumulative gas production of the three gas producing wells in the field that were shut-in prior to the start of acid gas injection to that of the two wells that continued gas production after the start

of acid gas injection and up to the time that CO_2 concentration reached 50%. As such the cumulative hydrocarbon gas produced from this reservoir was estimated at 1.004×10^9 Sm^3, suggesting that acid gas injection might have actually resulted in a reduction in the volume of gas production by 23×10^6 Sm^3.

Initially, history-matching of the Retlaw Mannville Y Pool was not possible because of a mismatch between the volumes of initial gas in place as determined from geology and rock properties, and produced gas to date (up to November 2006). The volumetric estimate of the original gas in place was significantly less than the historical cumulative gas produced and the OGIP estimates by material balance calculations, or than the OGIP booked by ERCB. History matching and forecast were obtained after ERCB revised the geological maps of the Retlaw Mannville Y pool. Both black oil and compositional models were created to first history match the total gas and oil produced and then forecast gas production and reservoir pressure based on 3 scenarios: (i) forecast assuming all operating conditions as of December 2006 to be maintained until 2038, (ii) forecast assuming that no acid gas injection ever occurred, and (iii) forecast assuming that all producers are shut-in in January 2008 while acid gas injection is maintained at its same operating conditions.

One objective of the simulation study was to examine the mechanism of displacement of the in-situ-gas by the acid gas and their mixing. The authors believe that there is a conception in industry regarding the behavior of the acid gas that is not necessarily true in all cases, and its validity needs be studied on a case-by case basis. Acid gas (both CO_2 and H_2S) is heavier than natural gas. At in-situ initial reservoir conditions, the injected acid gas would be generally in dense, supercritical phase, while natural gas is in gaseous phase (see Figures 5.1 and 5.2). Thus, it has been expressed by some that the heavier acid gas, if injected at the bottom of the dipping structure that forms a reservoir, will accumulate there and will not mix with the natural gas still present in the reservoir. Furthermore, it has been suggested that the acid gas accumulating at the bottom of the reservoir will push natural gas towards the top of the reservoir and towards the updip producing wells, thus enhancing gas recovery. This study showed that, in depleted reservoirs, acid gas is typically in gaseous phase, with a small density difference with the is-situ gas (see Figures 5.1 and 5.2). Furthermore, the spread of the acid gas in the reservoir and its breakthrough at producing wells is enhanced by the hydrodynamic forces between injection and production wells that create preferential flow paths. Finally, even at supercritical conditions where the acid gas has a density approaching that of liquids, it still has mixing properties characteristic of gases, namely that it fills all the available volume and that it mixes with other gases according to gas mixing laws. Thus, rather than accumulating at the bottom of the reservoir, the injected acid gas will spread and mix with the resident natural gas, ultimately being produced at producing wells. Figures 5.1 and 5.2 below illustrate these points by showing the density variation with pressure for acid gas and natural gas for the Retlaw Mannville Y pool, and the position in the P-T space of acid gas at initial and injection-start conditions, respectively.

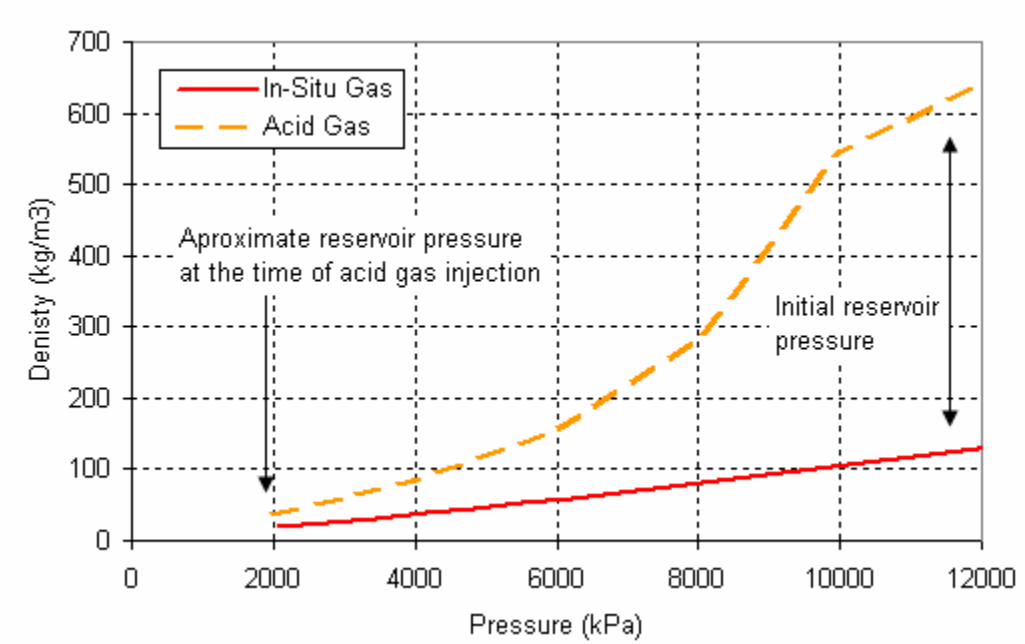

Figure 5.1: Variation with pressure at reservoir temperature of the density of the injected acid gas and of the reservoir natural gas in the Retlaw Mannville Y pool.

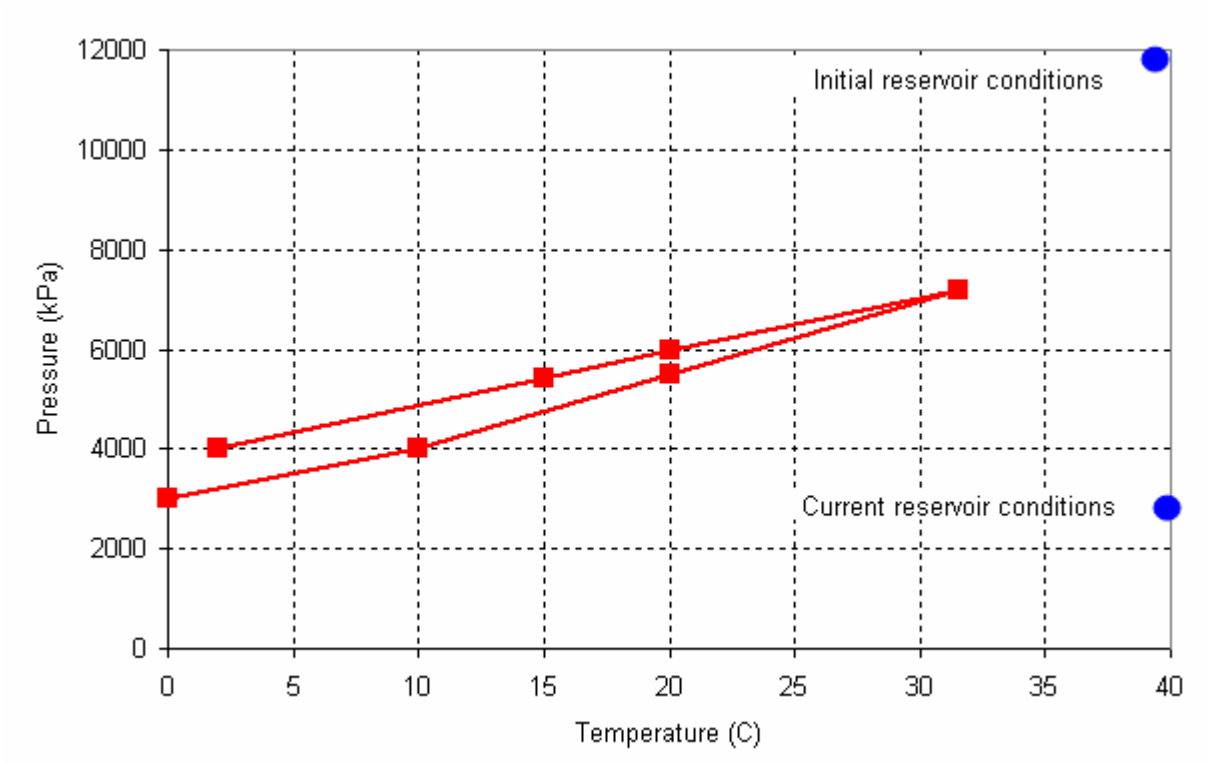

Figure 5.2: Initial and current reservoir conditions in relation to the phase envelope of the injected acid gas in the Retlaw Mannville Y pool.

The cumulative gas produced as of December 2006 represents approximately 99% of the total gas in place. As such, any additional gas produced from the Retlaw Mannville Y pool will be mostly acid gas, as confirmed by the CO_2 and H_2S concentrations simulated, as well as scenario (ii) which simulates the gas production of the pool without acid gas injection occurring. Estimated pressures in all scenarios are well below the initial reservoir pressure. The Retlaw Mannville Y reservoir can be used for storage of the acid gas.

References

Broger, E.J., Syhlonyk, G.E., and Zaitlin, B.A. (1997): Glauconite sandstone exploration: A case study from the Lake Newell project, southern Alberta; *in* Petroleum Geology of the Cretaceous Mannville Group, Western Canada, S.G. Pemberton and D.P. James (eds.), Canadian Society of Petroleum Geologists, Memoir 18, p. 140-168.

Craft, B.C., and Hawkins, M.F. (1959): Applied Petroleum Reservoir Engineering, Prentice-Hall, Englewood Cliffs, NJ, 437 p.

CMG - Computer Modelling Group Ltd (2005a). User's Guide – IMEX: Advanced Oil/Gas Reservoir Simulator, Computer Modelling Group Ltd., Version 2005, Calgary, AB.

CMG - Computer Modelling Group Ltd (2005b). User's Guide – GEM: Advanced Compositional Reservoir Simulator, Computer Modelling Group Ltd., Version 2005, Calgary, AB.

Farshori, M.Z. and Hopkins, J.C. (1989): Sedimentology and petroleum geology of fluvial and shoreline deposits of the Lower Cretaceous Sunburst Sandstone Member, Mannville Group, southern Alberta; Bulletin of Canadian Petroleum Geology, v. 37, no. 4, p. 371-388.

Hayes, B.J.R. (1986): Stratigraphy of the basal Cretaceous Lower Mannville Formation, southern Alberta and north-central Montana; Bulletin of Canadian Petroleum Geology, v. 34, no. 1, p. 30-48.

Hayes, B.J.R., Christopher, J.E., Rosenthal, L., Los, G., McKercher, B., Minken, D., Tremblay, Y.M., and Fennel, J. (1994): Cretaceous Mannville Group of the Western Canada Sedimentary Basin; *in* Geological Atlas of the Western Canada Sedimentary Basin, G.D. Mossop and I. Shetson (comp.), Canadian Society of Petroleum Geologists and Alberta Research Council, Calgary, Alberta, p. 317-334.

Leckie, D.A., Bhattacharya, J.P., Bloch, J., Gilboy, C.F., and Norris, B. (1994) Cretaceous Colorado/Alberta Group of the Western Canada Sedimentary Basin; *in* Geological Atlas of the Western Canada Sedimentary Basin, G.D. Mossop and I. Shetson (comp.), Canadian Society of Petroleum Geologists and Alberta Research Council, Calgary, Alberta, p. 335-352.

Lee, B.I., and Kesler, M.G. (1975): A generalized thermodynamic correlation based on three-parameter corresponding states. AIChE Journal., v. 21, May 1975, p. 510-527.

McLean, J.R. and Wall, J.H. (1981): The Early Cretaceous Moosebar Sea in Alberta; Bulletin of Canadian Petroleum Geology, v. 29, p. 334-377.

Pooladi-Darvish, M., Hong, H., and Bachu, S. (2008): Differential spread of CO_2 and H_2S injected in the Long Coulee Glauconite F pool. Report to Natural Resources Canada, 67 p.

Porter, I.W., Price, R.A., and McCrossan, R.G. (1982): The Western Canada sedimentary basin. Philosophical Transactions of Royal Society of London, Series A, v. 305, p. 169-182.

Poulton, T.P., Christopher, J.E., Hayes, B.J.R., Losert, J., Tittemore, J., and Gilchrist, R.D. (1994): Jurassic and Lowermost Cretaceous Strata of the Western Canada Sedimentary Basin; *in* Geological Atlas of the Western Canada Sedimentary Basin, G.D. Mossop and I. Shetson (comp.), Canadian Society of Petroleum Geologists and Alberta Research Council, Calgary, Alberta, p. 297-316.

Twu, C.H. (1984): An internally consistent correlation for predicting the critical properties and molecular weights of petroleum and coal-tar liquids. Fluid Phase Equil., v. 16, p.137-150.

Zaitlin, B.A., Warren, M.J., Potocki, D., Rosenthal, L., and Boyd, R. (2002): Depositional styles in a low accommodation foreland basin setting: an example from the Basal Quartz (Lower Cretaceous), southern Alberta; Bulletin of Canadian Petroleum Geology, v. 50, no. 1, p. 31-72.